Identification of new Ca^{2+}-regulated proteins in endothelial cell signal transduction

Markus WALDECK-WEIERMAIR

Institut für Molekularbiologie und Biochemie
Zentrum für Molekulare Medizin
Medizinische Universität Graz

Dissertation

submitted to the Medical University of Graz
in fulfilment of the academic degree of
a doctor of medical sciences

Publication

WALDECK-WEIERMAIR M., ZORATTI C., OSIBOW K., BALENGA N., GOESSNITZER E., WALDHOER M., MALLI R., GRAIER WF.: Intergrin clustering enables anandamide-induced Ca^{2+} signaling in endothelial cells via GPR55 by protection against CB_1-receptor-triggered repression. *Journal of Cell Science* **121**: 1704-1717, 2008.

Acknowledgements

I would like to thank my supervisor Prof. Dr. Wolfgang Graier for his continual support during this work, for his guidance and enthusiasm for research, thoughtful insight, and support over the past years.

I gratefully acknowledge my colleagues Dr. Roland Malli, Dr. Michael Trenker, Ismene Fertschai, Karin Osibow, Ingund Anderl, Beatrix Petschar and Anna Schreilechner for useful discussion, great assistance in work and time we shared in the lab.

Special thanks to Helga Reicher and Prof. Dr. Wolfgang Sattler, who were a great help in my proteomic approach.

Last but not least, I want to thank my beloved wife Nina, for her support, love and patience.

Table of contents

Index of Tables

Index of Figures

Abbreviations

aa	amino acid
Ab	antibody
ACN	acetonitrile
ACPA	N-cyclopropyl-5Z,8Z,11Z,14Z-eicosatetraenamide, arachidonoyl cyclopropylamide
ACTH	adrenocorticotropic hormone
AEA, Anandamide	N-(2-hydroxyethyl)-5Z,8Z,11Z,14Zeicosatetraenamide, arachidonoylethaolamide
Amp	ampicillin
ADP	adenosine-5-diphosphate
ATP	adenosine-5-triphosphate
AM251	1-(2,4-dichlorophenyl)-5-(4-iodophenyl)-4-methyl-N-1-piperidyl-1H-pyrazole-3-carboxamide
ß-ME	beta-mercaptoehtanol
bp	base pair
BPB	bromophenol blue
BHQ	2,5-di-*tert*-butylhydroquinone
BK_{Ca}	large conductance Ca^{2+}-activated K^+ channels
BSA	bovine serum albumin
$[Ca^{2+}]$	calcium concentration
$[Ca^{2+}]_{c(yto)}$	free cytosolic Ca^{2+} concentration
$[Ca^{2+}]_{er}$	free endoplasmatic reticulum Ca^{2+} concentration
$[Ca^{2+}]_{mito}$	free mitochondrial Ca^{2+} concentration
CaM	calmodulin
CCE	capacitative Ca^{2+} entry
cDNA	complementary DNA
CGP 37157	7-chloro-5-(2-chlorophenyl)-1,5-dihydro-4,1-benzothiazepin-2(3H)-one
CF_3COOH	trifluoracetic acid
CHCA	α-cyano-4-hydroxycinnamic acid
$CHCl_3$	chloroform
CH_3COOCH_3	methyl acetate
CICR	calcium-induced calcium release

CNS	central nervous system
DAG	diacylglycerol
ddH_2O	double destilled water
DMEM	Dulbecco's modified Eagles medium
DMSO	dimethylsulfoxide
DNA	desoxyribonucleic acid
DNase	desoxyribonuclease
dNTP	didesoxyribobucleotide: dATP, dCTP, dGTP, dTTP
DTT	1,4-dithiothreitol
EC	endothelial cell(s)
ECL	Enhanced ChemiLuminescent
ED	endothelial dysfunction(s)
EDTA	ethylen diamine bis(2-aminoethylether)-N,N,N´,N´-tetraacetic acid
EGTA	ethylen glycol bis(2-aminoethylether)-N,N,N´,N´-tetraacetic acid
ER	endoplasmatic reticulum
EtOH	ethanol
FCCP	carbonyl cyanide-(4-trifluoromethoxy)phenylhydrazone
FCS	Fetal Calf Serum
FP	fluorescent protein
g	gram or gravitation constant
Gaf1	gamma- (γ-) SNAP associated factor 1
GFP	green fluorescent protein
GPCR	G-protein –coupled receptor
h	hour(s)
HBSS	Hanks buffered salt solution
HCl	hydrochloric acid or hydochloride
HEPES	N-2-hydroxyethylpiperazine-N´-2-ethasulfonic acid
HRP	horseradish peroxidase
Kan	kanamycin
kDa	kilo Dalton
IMM	inner mitochondrial membrane
IP_3	inositol-1,4,5-triphosphate
l	liter
LFM-A13	α-cyano-β-hydroxy-β-methyl-N-(2,5-dibromophenyl)propenamide
LPI	L-α-Lysophosphatidylinositol (sodium salt from soybean)

µ	micro (10^{-6})
m	milli (10^{-3})
MALDI–TOF	Matrix assisted laser desorption / ionization–Time of Flight
MAPK	mitogen-activated protein kinase
max.	maximum
MCS	multiple cloning site, polylinker
MCU	mitochondrial calcium uniporter
MeOH	methanol
min	minute(s)
min.	minimum
mRNA	messenger RNA
MT	microtubule(s)
mtDSRed	mitochondria-targeted DSRed
mtRP	mitochondria-targeted ratiometric pericam
MW	molecular weight
NaOH	natrium hydroxide
NCX_{PM}	plasma membrane Na^+/Ca^{2+} exchanger
NCX_{Mito}	mitochondrial Na^+/Ca^{2+} exchanger
NFDM	non fat dry milk
NH_4HCO_3	ammonium bicarbonate
nt	nucleotide
O-1602	5-methyl-4-[(1R,6R)-3-methyl-6-(1-methylethenyl)-2-cyclohexen-1yl] -1,3-benzendiol
OD	optical density
OMM	outer mitochondrial membrane
ORF	open reading frame
PAGE	polyacrylamide gel electropphoresis
PCR	polymerase chain reaction
pI	isoelectric point
PIP_2	phosphatidylinositol-4,5-biphosphate
PKCα	Protein Kinase C isoform alpha
PLC	phospholipase C
PM	plasma membrane
pos.	Position
Prdx1	Peroxiredoxin 1

PVDF	polyvinylidene fluoride
REST	Relative Expression Software Tool
RaM	Rapid Uptake Mode
ROC	Receptor-operated channels
ROS	Reactive oxygen species
RNA	ribonucleic acid
RNAi	RNA interference
RNase	ribonuclease
rpm	revolutions per minute
RPmt	mitochondria-targeted ratiometric pericam
SCCU	subplasmamembrane Ca^{2+} control units
SDS	sodium dodecyl sulfate
SDS-PAGE	SDS-Polyacrylamide Gel Electrophoresis
sec	second(s)
SERCA	sarco/endoplasmic reticulum Ca^{2+} ATPase
shRNA	short hairpin RNA
siRNA	small interfering RNA
SMOC	Second messenger-operated channels
SOC	store-operated channel
TEMED	N,N,N´,N´,-tetramethyl-ethylendiamine
TFA	trifluoroacetic acid
TG	thapsigargin
Tris	Tris-hydroxymethyl-aminomethane
tVh	total Volt hour(s)
U	Unit(s)
UCP	uncoupling protein(s)
V	Volt(s)
VCP	Valosin containing protein
Vh	Volt hour(s)
VOC	Voltage-operated channels
vol	volume

Summary

Twofold positive charged calcium ions (Ca^{2+}) serve as ubiquitous second messengers for communication within cells. Depending on the appearance of different spatio-temporal Ca^{2+} signals, Ca^{2+} is able to activate or inhibit various Ca^{2+} dependent proteins. Some of these Ca^{2+}-sensitive protein molecules work as so called scaffold proteins that act as platforms for interaction proteins. Thereby Ca^{2+}-regultated translocations may occur resulting in an amplification, activation or inhibition of distinct signaling pathways.

In the present study, it was intended to identify new, yet unknown Ca^{2+} dependent scaffold proteins or their interaction partners in endothelial cells by the use of two different independent approaches. In the first proteomic approach protein extracts of various cell compartments were visualized using 2D-gel electrophoresis before or after a cell stimulation with histamine. The histamine-induced cellular Ca^{2+} elevation resulted in the translocations of Valosin containing protein from the nucleus to the cytosol and Peroxiredoxin 1 towards cellular membranes. Further experiments are necessary to understand these still unknown Ca^{2+} dependent effects.

In the second bioinformatic approach Gaf1, γ-SNAP associated factor 1, was identified to serve as a putative Ca^{2+} regulated scaffold protein. Using several biochemical strategies such as protein overexpression, gene silencing via siRNA or mutagenesis, the functional role of Gaf1 was tested. Thereby it was observed that Gaf1 is involved in the regulation of Ca^{2+} entry form the plasma membrane into the mitochondria and further into the cytosol as well as into the endoplasmic reticulum (ER). The Ca^{2+} release from the ER and the direct Ca^{2+} refilling of this Ca^{2+} store was not under the control of Gaf1. These results indicate that Gaf1 is involved in the selective transfer of extracellular Ca^{2+} into the mitochondrial matrix during cell stimulation. Therfore Gaf1 may act as a linking protein between a plasma membrane Ca^{2+} channel and the mitochondria. Moreover further observations confirmed this hypothesis as the inhibition of mitochondrial motility by Ca^{2+} in single cells during histamine stimulation was found to be Gaf1 dependent and Gaf1-Citrine was mainly observed to be localized at sites of the plasma membrane.

1 Introduction

1.1 Endothelial Cells (EC)

The term endothelium was coined by the swiss anatomist Wilhelm His in 1865, to differentiate the inner lining of body cavities from epithelium. The original definition included the cell lining of blood vessels, lymphatics, and mesothelial-lined cavities and was later narrowed to include only the inner cell layer of blood vessels and lymphatics (Aird WC., *Circulation Research* **100**: 158-173, 2007). Since that time the structural composition of blood vessels were of special interest in the scientific field and in the early 1970s endothelial cells were first isolated and cultivated (Jaffe EA. et al., *J. Clin. Invest.* **52**: 2745-2756, 1973). This was the crucial step for the understanding of endothelial function, as it offered the possibility to observe them independently of being influenced by neighbored tissue.

According to the diversity and complexity of their functions (1.1.1) and their total weight of about one kilogram in a human body, today endothelial cells are mostly interpreted as a whole organ, the endothelium (Just H., *Biotechnology in Drug Research* **44**: 382-384, 1994).

In most of the endothelial functions (1.1.1) and dysfunctions (1.1.2) calcium plays a major role (1.4). Additionally, this can induce a change in the protein composition of cell compartments like plasma membrane, mitochondria, ER or nuclei. Such changes may play a key role in the regulation of various endothelial cell functions and might be also related to the development of human disease. However, the flexibility of protein composition in response to different stimuli in a large scale approach has not been performed so far.

1.1.1 Endothelial Functions

For a long time endothelial cells were restricted to be a non-reactive barrier between blood and tissue acting as a non-thrombogenic surface for blood flow and guarding against pro-inflammatory insults. However, the discovery of the multiple functions of EC began in the early 1980s and lasts until now. Accordingly, it was found out that EC are essential for the regulation of the vascular tone, as it was observed by Furchtgott and Zawadsky that EC are essential for the relaxation of vessels (Furchtgott RF. et al., *Nature* **288**: 373-376, 1980). Furthermore it was found that EC mediate immune

reactions (Cotran RS., *Am. J. Pathol.* **129**: 407-413, 1987), participate in hemostasis (Nawroth P. et al., *Clin. Haematol.* **14(2)**: 531-546, 1985) and are involved in angiogenesis (Jaffe EA., *Ann N Y Acad Sci.* **454**: 279-291, 1985). Moreover it senses mechanical stimuli, like shear stress or blood pressure, and hormonal stimuli like vasoactive substances and therefore response in a release of agents (mediators) to regulate vasomotor function, trigger inflammatory processes, and affect hemostasis. Accordingly these cells both produce and react to a wide variety of mediators including cytokines, growth factors, adhesion molecules, vasoactive substances and chemokines, with effects on many different cells. A detailed list of so far known most important functions and its mediators of EC is presented in Figure 1.

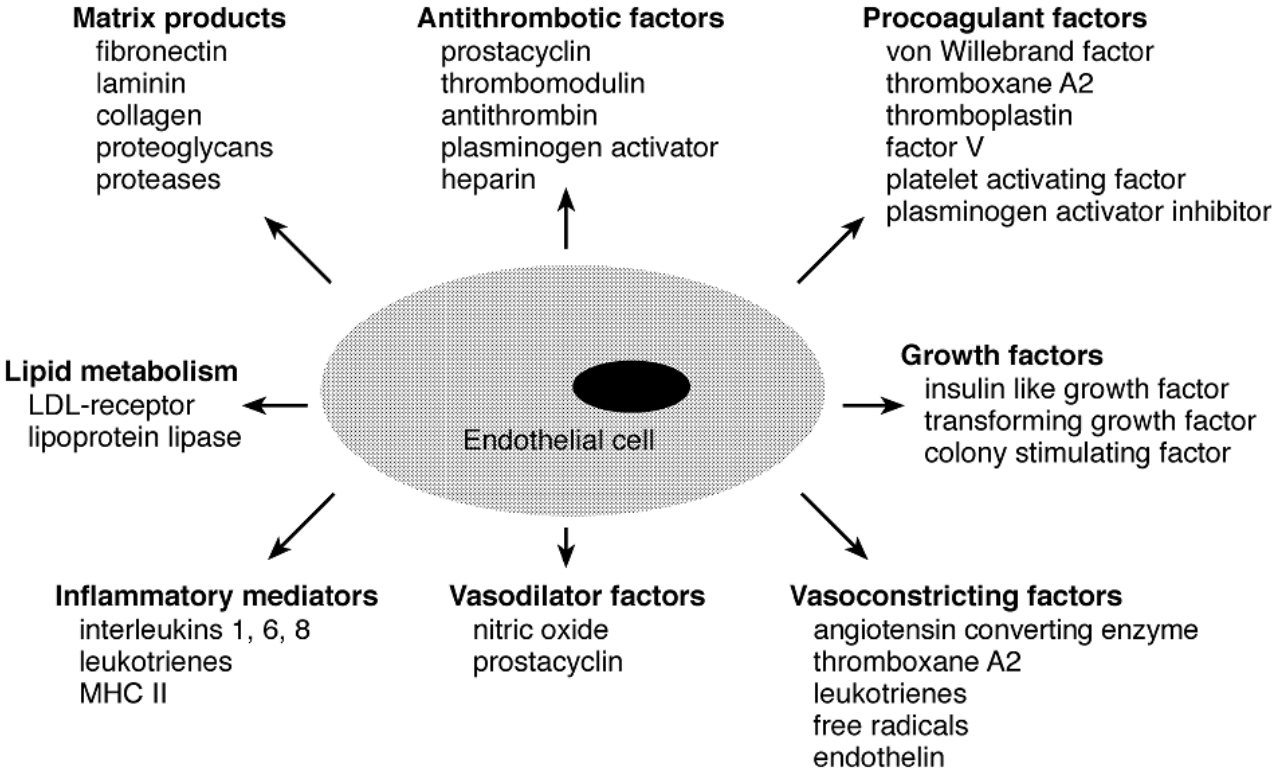

Figure 1: Endothelial Cell Functions
Endothelial cells have both metabolic and synthetic functions. Through the secretion of a large variety of mediators they are able to influence cellular function throughout the body (Galley HF. et al., *British Journal of Anaesthesia* **93.1**: 105-113, 2004)

1.1.2 Endothelial Dysfunction

According to the multiple functions (1.1.1) the endothelium is involved in a network of interactions between cells, cellular factors, humoral factors and matrix components, and endothelial malfunctions are the cause of a great variety of pathophysiological states. Endothelial Dysfunction (ED) is characterized in a malfunction of endothelial actions: (1). Reduced nitric oxide generation, oxidative stress or reduced production of

hyperpolarizing factor are leading to a reduced vasodilation. (2) Upregulation of adhesion molecules or generation of chemokines results in an inflammatory response and contribute to a prothrombic state. Thus, ED is associated with most forms of cardiovascular disease, like atherosclerosis, vasospasm, hypertension, coronary heart disease, chronic heart failure, peripheral artery disease, diabetes, and chronic renal failure (ED in detail shown in Figure 2, Endemann DH. et al., *Am Soc Nephrol* **15**:1983-1992, 2004), but also in inflammation, cancer, insulin resistance or metabolism.
Therefore, there is a great demand of in vitro models for the study of various diseases on a cellular basis provided by endothelial cell cultures.

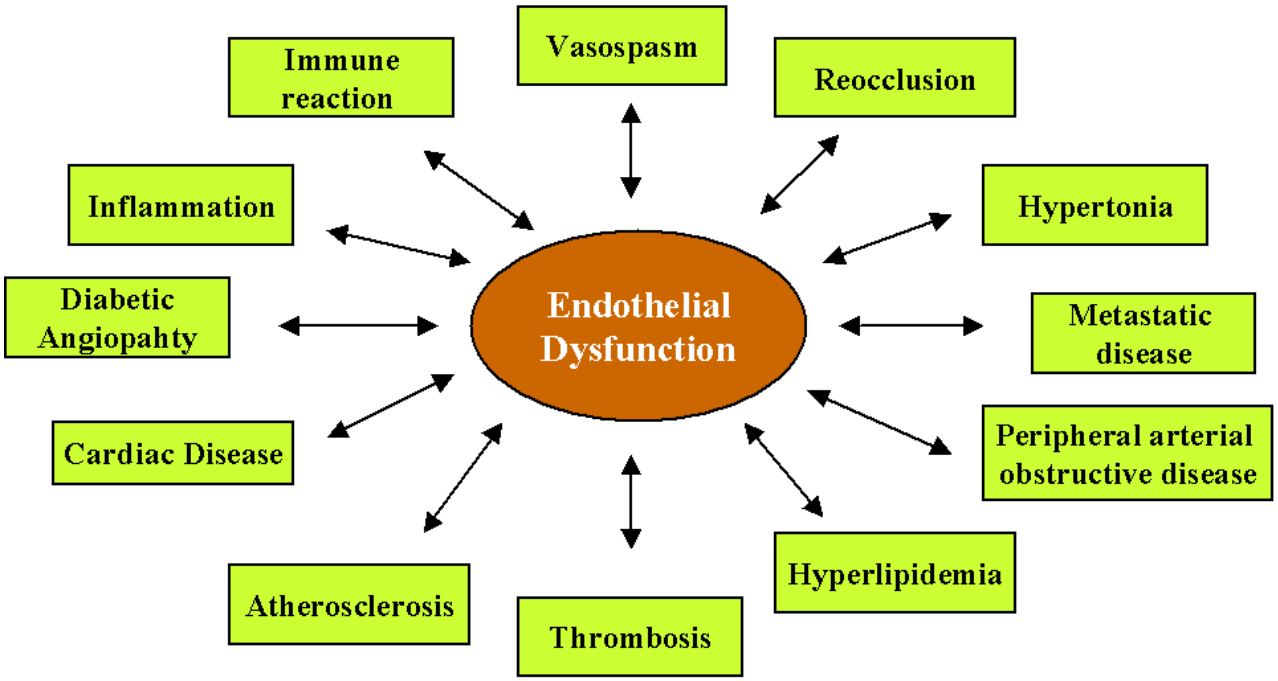

Figure 2: Endothelial Cell Dysfunctions

1.2 Mitochondria: Structure and Function

In electromicroscopy images mitochondria are ~ 1-2 µm long organelles that are typically present in a high number up to 2,000 of nearly all eucaryotic cells. This image has been dramatically changed by the introduction of high resolution live cell imaging techniques (e.g. confocal laser scanning microscopy) that revealed mitochondria to be highly dynamic organelles that undergo continuous fission and fusion processes. They are boarded by two membranes, a smooth outer mitochondrial membrane (OMM) and a tubular folded (cristae) inner mitochondrial membrane (IMM) with a large surface enclosing the mitochondrial matrix. According to the endosymbiont theory that mitochondria originally derived from anaerob bacteria they possess their own circular

DNA (4 molecules per mitochondrion) and their own ribosomes. In human the mitochondrial genome consists of 16569 base pairs that encode 13 proteins (most are subunits of complexes from the respiratory chain) and t-RNAs for the organelle's own protein synthesis. Only these proteins are synthesized by the mitochondrion itself, while all the other mitochondrial proteins are encoded in the nuclear genome and have to be imported after the translation from the cytoplasm (Neupert W., *Annu. Rev. Biochem.* **66**: 863-917, 1997). The OMM consists of pores for the passage of molecules smaller than 10 kDa, whereas the IMM is highly impermeable (except water, O_2, CO_2, and NH_3 can pass), while all other substrates for the mitochondrial metabolism as well as its products have to be active transported by specific transport systems. As the IMM is also impermeable for protons (H^+) and the complexes I, III and IV of the respiratory chain pump H^+ from the matrix into the intermembrane space a proton gradient is generated that may conserve chemical energy. An IMM associated enzyme, the ATP-synthase, uses this energy for the production of ATP from ADP and anorganic phosphor (Oxidative Phosphorylation), which is the energy source of a cell. In addition to that, mitochondria like the ER act as intracellular calcium stores (Dhalla NS., *Arch. Int. Physiol. Biochim.* **77**: 916-934, 1969; Rizzuto R. et al., *Science* **280**: 1763-1766, 1998). Furthermore they play an important role in apoptosis (Er E. et al., *Biochim. Biophys. Acta* **1757**: 1301-1311, 2006; Schwarz M. et al., *Apoptosis* **12**: 869-876, 2007), moreover it was convincingly reported that mitochondrial Ca^{2+} is interrelated to apoptosis (Demaurex N. et al., *Science* **300**: 65-67, 2004; Scorrano L. et al., *Science* **300**: 135-139, 2003; for reviews see: Hajnoczky G. et al., *Cell Calcium* **40**: 553-560, 2006; Armstrong JS., *Mitochondrion* **6**: 225-234, 2006; Chan DC., *Cell* **125**: 1241-1252, 2006).

However, these are well accepted functions of mitochondria, today they become more and more important as it was recently reported that they may act as essential intracellular communicators, which are virtually involved in every signaling cascade and metabolic process (Graier WF. et al., *Pflugers Arch. Eur. J. Phys*. **455.3**: 375-396, 2007). Therefore mitochondrial dysfunction associates with a number of diseases like atherosclerosis, diabetes, neurological disorder, cancer or aging processes that have their origin in a variety of pathogenetic mutations of either mitochondrial or nuclear DNA.

Accordingly, beside the fundamental role of mitochondria to supply energy that is well understood over the last 2 decades, mitochondria received more into focus to regulate

intracellular signaling events. Thus, two phenomena of mitochondrial functions are believed to accomplish these:

The complex processes that occur in mitochondrial motility (1.3)

The regulation of cellular calcium by mitochondria (1.4, 1.5, 1.6).

1.3 Mitochondrial Motility

The phenomenon of mitochondrial motility was first documented in 1915 (Lewis, MR. et al., *Am. J. Anat.* **17**: 339–401, 1915) and for a long time had been elusive until it was found to be driven by a cytoskeleton-based transportation system. Accordingly they were visualized by Malli R. (Figure 3) and others in various cell types to be in association with microtubles (Ball EH. et al., *PNAS* **79**: 123-126, 1982), microfilaments (Drubin DG. et al., *Mol. Biol. Cell.* **4**: 1277-1294, 1993; Morris RL. et al., *J. Cell Biol.* **131**: 1315-1326, 1995), and intermediate filaments (Summerhayes IC. et al., *J. Cell Sci.* **61**: 87-105, 1983; Stromer MH. et al., *Cell Motil. Cytoskeleton* **17**: 11-18, 1990). In order that these cytoskelatal elements are hardly moveable they are acting as a fixed framework for mitochondrial motility. Accordingly it was found out that a synchronized interplay of several proteins are necessary to move mitochondria along these cytoskeletal elements: (1.) docking or adaptor proteins that link and anchor mitochondria to cytoskeletal fibres; (2.) motor proteins that are responsible for the driving force of and (3.) receptor proteins that allow mitochondria to move in a directed and regulated way to signaling events. Some motor proteins have been already identified e.g. dynactin for the microtubular motor protein (Habermann A. et al., *J. Cell Sci.* **114**: 229-240, 2001), dynein (Varadi A. et al., *J. Cell Sci.* **117**: 4389-4400, 2004) or both dynein and kinesin (Deacon SW. et al., *J. Cell Biol.* **160**: 297-301, 2003). Movements of mitochondria towards the plus end are established by kinesin motors, while those to the minus end are done by dynein motor proteins (Tanaka Y. et al., *Cell* **93**: 1147-1158, 1998). Adaptor proteins are still under debate, but mainly seem to belong to the complex superfamily of Ras GTP-ase (Szabadkai G. et al., *Biochim. Biophys Acta* **1763**: 442-449, 2006), now consisting of at least seven families of proteins (Sar1, Arf, SRb, Rab, Ran, Ras, Rho; Leipe DD. et al., *J. Mol. Biol.* **317.1**:41-72, 2002). However, some of them have already been identified (for reviews see Frederick RL. et al., *Traffic* **8**: 1668-1675, 2007; Boldogh IR. et al., *Trends in Cell Biol.* **17.10**: 502-510, 2007; Pfeffer SR., *Trends in Cell Biol.* **11.12**: 487-491, 2001) , e.g. Rab32 (Alto NM. et al., *J. Cell Biol.* **158**: 659-668, 2002) or Miro (Fransson A. et al., *J. Biol. Chem.* **278**:

6495-6502, 2003). Thus, mitochondria are highly dynamic organelles and can be defined into two main kinds of movements, long-distance travel and complex local actions (for review see Yaffe MP., *Nat. Cell Biol.* **1**: E149-E150, 1999). The control of mitochondrial motility by signaling mechanisms and the significance of rapid changes in motility remains elusive and it is still unclear, how and why mitochondria are moving, but several functions are postulated for these actions. Movements may rearrange the spacial pattern of ATP production, Ca^{2+} buffering, increase the change of dynamic interactions between discrete organelles or aid in the transport of molecules between the cytoplasm and mitochondria.

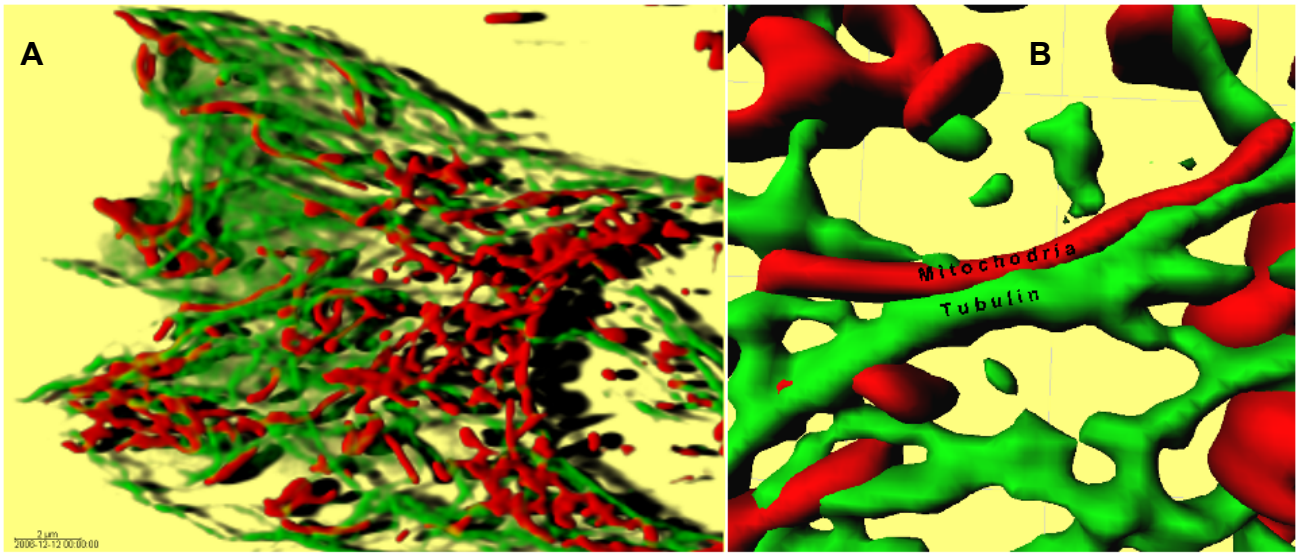

Figure 3: Colocalization of mitochondria with microtubules (MT)
Ea.hy926 cells co-transfected with mtDSRed and tubulin-pEYFP. Z-scans were performed on an array confocal laser scanning microscope applying 514 nm excitation and measuring 570 nm emission for mtDSRed or 488 nm excitation and 535 nm emission for tubulin-pEYFP (Clontech). The MT and mitochondria z-stacks were deconvoluted using the interactive quick maximum likelihood estimation algorithm (QMLE) of huygens 2.4.1p3 (SVI, Hilversum, Netherlands). 3-D reconstruction of the mitochondrial and microtubular networks were performed with the Imaris 3.3 software (Bitplane AG, Zürich, Switzerland). **A:** Distribution of MT(green) and mitochondria(red) in an endothelial cell. **B:** Focal contacts between MT and mitochondria.

Interestingly, mitochondrial motility depends on intracellular calcium concentration $[Ca^{2+}]_c$ (Rintoul GL. et al., *J. Neuroscience* **23.21**: 7881-7888, 2003). Whenever a rise in $[Ca^{2+}]_c$ occurs by either Ca^{2+} mobilization or Ca^{2+}-entry movements decreases that may include the involvement of a distinct Ca^{2+} sensor molecule or receptor protein (Vale RD., *Cell* **112**: 467-480, 2003). As one putative candidate of such a Ca^{2+} receptor protein Myosin Va was identified, a motor protein which is able to bind CaM (Reck-Peterson SL. et al., *Biochim. Biophys. Acta* **1496**: 36-51, 2000) and display Ca^{2+}-dependent interaction with MTs (Cao TT. et al., *Mol. Biol. Cell.* **15**: 151-161, 2004) or actin-filaments (Tauhata SB., et al., *J. Biol. Chem.* **276**: 39812-39818, 2001; Krementsov DN. et al., *J. Cell Biol.* **164**: 877-886, 2004). In addition to that

mitochondrial motility is that sensitive to $[Ca^{2+}]_c$ that it can be regulated and measured by clamping cytosolic calcium $[Ca^{2+}]_c$ at various levels in the physiological range (Yi M. et al., *The Journal of Cell Biology* **167.4**: 661-672, 2004).
Accordingly, regarding mitochondrial motility, their starts, stops and redistribution can be also regulated by physiological events and intracellular signaling.

1.4 Calcium Signaling

1.4.1 Early discoveries

Calcium (Ca^{2+}) is one of the most important second messenger and ubiquitous in all life-forms. The relevancy of Ca^{2+}-ions for signal transduction and its maintenance in biological processes was first documented in 1883 with the discovery of the electromechanical coupling of muscles (Ringer S., *J. Physiol.* **4**: 29-42, 1883). Much later the 'theory of cell stimulation' was described by the observation of a dramatic elevation of intracellular calcium upon cell stimulation (Heilbrunn LV. et al., *J. Cell Comp. Physiol*. **19**: 15-32, 1947). Nevertheless even this observation passed away unnoticed until the tide began to turn in the 1960s with the finding that Ca^{2+}-uptake into sarcoplasmic reticulum vesicles is mediated by a Ca^{2+}, Mg^{2+}-ATPase (Ebashi S. et al., *Prog. Biophys. Mol. Biol.* **18**: 123-183, 1968). At the very same time it was discovered that Ca^{2+}-channels controlled by membrane voltage allow the specific regulated pathway for transmembrane Ca^{2+}-entry (Katz B. et al., *J. Physiol.* **189**: 535-544, 1967). Additionally with the technical developments of the patch-clamp technique (Neher E. et al., *Nature* **260**: 799-802, 1976) and Ca^{2+}-sensitive fluorescent dyes (Tsien RY., *Nature* **290**: 527-528, 1981) the large expansion in understanding calcium signaling was accomplished. Nowadays it is known that Ca^{2+} displays a major role in the regulation of enzyme activity, cell metabolism, intracellular communication, permeability of the cell membrane, cell division and cell death (for review see Peterson OH. et al., *Cell Calcium* **38**: 161-169, 2005).

1.4.2 Introduction to Calcium signaling

In eucaryotic cells basal intracellular $[Ca^{2+}]$ is in the range of 100-150 nM, whereas the extracellular $[Ca^{2+}]$ is much higher by a factor of 1,000-10,000, e.g. in human blood 1.5-2.5 mM. Thus, this gradient arranges the mediation of information and signals across the plasma membrane (Kirischuk S. et al., *FASEB J.* **11.7**: 566-572, 1997). During

stimulation of a cell the intracellular [Ca^{2+}] gets elevated up to more than 1 µM depending on the cell type (Bootman M. et al., *Semin. Cell Dev. Biol.* **12**: 3-10, 2001). Beside the extracellular Ca^{2+} there are intracellular Ca^{2+}-stores, like the ER or mitochondria that are able to release their Ca^{2+} upon activation of distinct signaling pathways or buffer it in order to maintain the lower $[Ca^{2+}]_{cyto}$ and refill (Putney JW. jr., *J. Physiol.* **268**: 139-149, 1977). Additionally they are able to influence Ca^{2+} signals by intercepting, prolonging or delimiting them. Mitochondria are able to attenuate Ca^{2+}-waves in the uptake of entering Ca^{2+}, which is pumped out thereafter in order to control and prolong Ca^{2+} signals (Rizzuto R. et al., *J. Physiol.* **529.1**: 37-47, 2000; Hajnoczky G. et al., *Cell Calcium* **40**: 553-560, 2006). The Ca^{2+} uptake is performed by the mitochondrial calcium uniporter (MCU) that has recently been identified to consist of members of the UCP family (Trenker M. et al., *Nat. Cell Biol.* **9**: 445-452, 2007). The active transport of Ca^{2+} into the ER is accomplished by the sarco/endoplasmic reticulum Ca^{2+} ATPase (SERCA).

Depending on the cell type different functions and processes are initiated by Ca^{2+}, e.g.: release of insulin in β cells, activation of the actin-myosin interaction in contractile muscle cells or delivery of acetylcholine in neurons. In endothelial cells the cytosolic calcium concentration, $[Ca^{2+}]_{cyto}$, is essential for the regulation of the vascular tone.

Beside these functions Ca^{2+} signals are involved in many other processes like mitosis, apoptosis or synthesis of mediators like zytokines. The versatility of this ion to act as such a multifunctional messenger is essential in cell biology and depends on the cell's potential to shape Ca^{2+} signals in space, time and amplitude.

1.4.3 Plasma Membrane Ca^{2+}-Channels

In general plasma membrane Ca^{2+}-channels can be classified into four separated groups. The opening of these channels result in a passive transport of Ca^{2+} into the cell increasing the $[Ca^{2+}]_{cyto}$:

1. Voltage operated channels (VOC): These are mainly expressed in excitable cells like muscle (L-type Ca^{2+}-channel) or nerve cells (N-type, P/Q-type and T-type Ca^{2+}-channels) and get opened upon depolarization of the cell membrane resulting in a huge$[Ca^{2+}]_{cyto}$ elevation within milliseconds (Cao YQ., *Pain* **126**: 5-9, 2006).
2. Receptor operated channels (ROC): These are mainly located in neurons, e.g. ionotropic receptors for amino acids like glutamate (NMDA-receptors; Hu B. et al. *Acta Pharmacol. Sin.* **25**: 714-720, 2004), for nucleotides (P2X-receptors; Burnstock G., *Cell. Mol. Life Sci.* **64.12**:1471-1483, 2007), the nicotinic acetylcholin-receptor (Rogers M., *J.*

Neurophysiol. **77**: 1407-1417, 1997) or receptor-activated calcium entry channels in EC (Jousset H. et al, *Cell Calcium* **43**: 83-94, 2008).

3. Second messenger-operated channels (SMOC): These are activated by intracellular second messenger. Some open in response to cyclic nucleotides like cAMP or cGMP (Lenz T. et al., *Am J Physiol Cell Physiol* **273**: C1526-C1532, 1997). Other channels react on arachidonic acid (van der Stelt M. et al. *Eur. J. Biochem.* **271**: 1827-1834, 2004; Graier WF. et al., *Journal of Physiology* **482.2**: 259-274, 1995;). Many of the SMOCs are members of the TRPC family (Vazquez G. et al., *Biochim. Biophys. Acta* **1742**: 21-36, 2004).

4. Channels that get activated upon depletion of intracellular Ca^{2+}-stores (Capacitative channels, store-operated channels, transient receptor potential channels): The capacitative Ca^{2+} entry (CCE) occurs through TRPCs in non-excitable cells (1.4.4). According to Puntney's hypothesis that intracellular increased Ca^{2+} levels cause an additional Ca^{2+}-influx, this phenomenon is also called store-operated calcium entry (Putney JW., *Cell Calcium* **7**: 1-12, 1986; Dutta D., *J. Biosci*. **25**: 397-404, 2000).

1.4.4 Ca^{2+}-channeling in non-excitable cells

Electrically non-excitable cells like firbroblasts, adipocytes or endothelial cells are not able to propagate action potentials. The main mechanism of Ca^{2+} mobilization in these cells is established through the generation of inositol-1,4,5-triphosphate (IP_3), that is initiated by the binding of a hormone/agonist to a G-protein-coupled receptor (GPCR) located in the plasma membrane. The receptor stimulation is coupled with a G-protein that in turn actives the enzyme phospholipase C (PLC) to catalyze the hydrolysis of phosphatidylinositol-4,5-biphosphate (PIP_2) resulting in the formation of IP_3 and diacylglycerol (DAG). Intracellular Ca^{2+}-stores like the sarco-/endoplasmic reticulum offer IP_3- and RyR-receptors, which act as Ca^{2+} channels(Berridge MJ. et al., *Nature* **312**: 315-321, 1984). When IP_3-receptors are activated by the generated IP_3, Ca^{2+} gets depleted from the ER (Supattapone S. et al., *J. Biol. Chem.* **263**: 1530-1534, 1988). The released Ca^{2+} into the cytosol generating complex local and global Ca^{2+} signals (1.4.5) that regulate numerous physiological processes, but is spatiotemporarily limited as it gets uptaken either through the SERCA again into the ER or through the MCU into the mitochondria (for reviews see Foskett et al., *Physiol. Rev.* **87**: 593-658, 2007; Yoshida Y. et al., *Jpn. J. Pharmacol.* **74**: 125-137, 1997).

Ca^{2+} and DAG together activate the enzyme protein kinase C (PKC) due to a phosphorylation of different proteins and therefore modulate their function (Huang KP., *Trends Neurosci.* **12**: 425-432, 1989).

Instead of VOC, non-excitable cells just express SOC that regulate the $[Ca^{2+}]_{cyto}$ upon Ca^{2+} entry and therefore is called CCE (Parekh AB. et al., *Physio. Rev.* **77**: 901-930, 1997). The CCE is initiated by an ER Ca^{2+} store depletion and occurs within seconds or minutes in opening the voltage-independent plasma membrane cation channels that are termed SOC (for reviews see Nilius B. et al., *Physiol. Rev.* **81**: 1415-1459, 2001; Putney JW. jr. et al., *J. Cell Sci.* **114**: 2223-2229, 2001; Parekh AB. et al., *Physiol. Rev.* **85**: 757–810, 2005). As SOCs are activated by emptying the ER Ca^{2+}-stores (1.6.), this happens by IP_3 produced upon either activation of G-protein-coupled or tyrosine kinase receptors. Although it is still elusive which proteins are involved in CCE, it was throughly demonstrated that CCE is inhibited if $[Ca^{2+}]_{cyto}$ is elevated at the mouth of the channels (Hoth M. et al., *J. Cell Biol.* **137**: 633-648, 1997; Parekh AB., *J. Biol. Chem.* **273**: 14925-14932*,* 1998; Gilabert JA. et al., *EMBO J.* **19**: 6401-6407, 2000; Hoth M. et al., *PNAS* **97**: 10607-10612, 2000). Furthermore it was shown in endothelial cells that superficial ER domains are able to create spatial Ca^{2+} gradients near the PM, so called subplasmamembrane Ca^{2+} control units (SCCU), activating local BK_{ca} channels (Graier WF. et al., *The Journal of Physiology* **506.1**: 109-125, 1998; Paltauf-Deburzynska J. et al., *The Journal of Physiology* **513.2**: 369-379, 1998; Frieden M. et al., *J. Physio.* **524**: 715-724, 2000). Whenever BK_{ca} channels get activated during strong cell stimulation, a strong CCE takes place even in regions far from the ER. In addition to that local buffering of the subplasmalemmal $[Ca^{2+}]$ occurs via activation of K^+ channels in parallel to a Ca^{2+}-regulated CCE (Frieden M. et al., *J. Physio.* **540**: 73-84, 2002). This local subplasmalemmal Ca^{2+} buffering is thought to get achieved by mitochondria (Hofer AM. et al., *J. Cell Biol.* **140**: 325-334, 1998; Gilabert JA. et al., *EMBO J*. **20**: 2672-2679, 2001; Malli R. et al., *J. Biol. Chem.* **278.45**: 44769-79, 2003) and therefore facilitates CCE in lowering $[Ca^{2+}]$ in regions next to the SOCs (Duchen MR., *Cell Calcium* **28**: 339-348, 2000; Malli R. et al., *J. Biol. Chem.* **278**: 10807-10815, 2003).

1.4.5 Local and Global Ca^{2+} events

Notable, Ca^{2+} elevations may occur local or global and may appear different in terms of their time-frames and amplitude (Bootman MD. et al., *J. Cell Sci.* **114**: 2213-2222, 2001). Accordingly the diversity and plasticity of Ca^{2+} are different as there are short

Ca^{2+} spikes, long lasting signals, oscillating Ca^{2+} waves or local Ca^{2+} microdomains. The latter are mainly localized next to the mouth of channels (10-100 nm) and are often initiating global Ca^{2+} transients (Canela JM. et al., *EMBO J.* **21**: 909-919, 2002). An important mechanism for the transformation of local Ca^{2+} events into global is the calcium-induced calcium release (CICR). Therfore Ca^{2+} gets depleted from the ER by the activation of either IP_3- or RyR-receptors. For the IP_3-receptor it was demonstrated that low $[Ca^{2+}]_{cyto}$ acts as a stimulant, whereas $[Ca^{2+}]_{cyto}$ higher than 300 nM work against the opening of this ion channel (Taylor CW. et al., *Cell Calcium* **32**: 321-334, 2002; Bezprozvanny I. et al., *Nature* **351**: 751-754, 1991). The stimulatory effect is of main importance for coordinating the elementary Ca^{2+} release events into spikes or waves. RyR-receptors behave similar as they are just activated at low µM $Ca^{2+}]_{cyto}$, but inhibited in the presence of nM or mM $[Ca^{2+}]_{cyto}$ (Verkhratsky A. et al., *Cell Calcium* **19**: 1-14, 1996). Like the IP_3-receptor is additionally opened by IP_3 even at higher $[Ca^{2+}]_{cyto}$ (1.4.4) the RyR-receptor gets activated upon stimulation with cADPR or caffeine (Gallant EM. et al., *Am. J. Physiol. Cell Physiol.* **286**: C821-830, 2004).

Due to this complex temporal and spatial arrangement of Ca^{2+} offers a large variety of responses for the cell. Each cell expresses a precisely defined composition of proteins, which are able to mediate or participate in distinct Ca^{2+} activated signal transduction pathways (Berridge MJ. et al. *Nat. Rev. Mol. Cell Biol.* **1**: 11-21, 2000; da Silva CP. et al., *Biochim. Biophys. Acta* **1498**: 122-133, 2000). Thus, different signals can be induced by just one ion, Ca^{2+} (Berridge MJ. et al., *Nat. Rev. Mol. Cell Biol.* **4**: 517-529, 2003).

1.5 Regulation of Ca^{2+} influx by mitochondria

During the last 15 years it was observed that mitochondria are in focal contacts with sites of the plasma membrane (PM) maintaining a direct Ca^{2+}-entry from a selective plasma membrane Ca^{2+}-channel through the MCU into the mitochondrial matrix (Rizzuto R. et al., *Science* **262**: 744-747, 1993; for reviews see Duchen MR., *Cell Calcium* **28**: 339-348, 2000; Parekh AB. and Putney JW.jr., *Physiol. Rev.* **85**: 757–810, 2005). Several examples regarding this transaction were reported by a number of scientists in various cell lines using different techniques:

In ECV304 cells, < 4 % of mitochondria are within 700 nm of the ER (65 % in HeLa), whereas 14 % are within 700 nm of the inner surface of the PM (< 6 % in HeLa). Following readdition of extracellular Ca^{2+} after Ca^{2+} depletion upon ATP stimulation an

increase in $[Ca^{2+}]_{mito}$ was evoked but not in $[Ca^{2+}]_{cyto}$. This result may indicate that in ECV304 cells microdomains of high $[Ca^{2+}]_{cyto}$ may occur beneath the PM resulting in the preferential elevation of mitochondrial Ca^{2+} located in this region during Ca^{2+} readdition (Lawrie AM. et al., *J. of Biol. Chem.* **271.18**: 10753-10759, 1996).

In parenteral T-Jurkat cells it was observed that mitochondria do not just act to buffer intracellular Ca^{2+}, but are also able to regulate the CCE. This was demonstrated by depletion of the ER Ca^{2+} store using the SERCA inhibitor thapsigargin (TG) that in turn activates the Ca^{2+} release-activated Ca^{2+} (CRAC) -channels, and the ensuing influx of Ca^{2+} loads a TG-insensitive intracellular store, the mitochondria. This Ca^{2+} uptake by the mitochondrial store is sensitive to different extracellular $[Ca^{2+}]$ (Hoth M. et al., *J. Cell Biol.* **137.3**: 633-648, 1997).

In chromaffin cells it was found that stimulation generates localized Ca^{2+} transients, with $[Ca^{2+}]_{cyto}$ of above 20-40 µM (Ca^{2+} hotspots) and mitochondria that are strategically near these Ca^{2+} hotspots may absorb Ca^{2+} resulting in a large mitochondrial Ca^{2+} uptake. Accordingly $[Ca^{2+}]_{mito}$ can reach the millimolar range in these cells. Moreover it was concluded that about 30 % of mitochondria co-localized with both plasma-membrane Ca^{2+} channels and ryanodine receptors, 20 % of mitochondria just co-localize with the PM and the remaining 50 % of mitochondria were located far away from these Ca^{2+} hotspots (Montero M. et al., *Nat. Cell Biology* **2**: 57-61, 2000).

Finally it was shown in Ea.hy926, a human umbilical vein endothelial cell derived line, cells using the patch clamp technique that mitochondria located just below the PM prevented subplasmalemmal $[Ca^{2+}]$ from rising high enough to open Ca^{2+}-dependent K^+-channels following histamine stimulation. Through maintaining a low Ca^{2+} concentration at these sites, it was suggested that mitochondria sustain store-operated Ca^{2+} entry by preventing Ca^{2+}-dependent inactivation of the Ca^{2+} entry channels. Indeed, mitochondrial depolarization with a protonophore or antimycin substantially reduced the size of the cytoplasmic Ca^{2+}-signal following Ca^{2+} readdition to cells treated with histamine or BHQ (Malli R. et al., *J. Biol. Chem.* **12.21**: 10807-10815, 2003). Remarkably, inhibition of mitochondrial Ca^{2+}-release by blocking the Na^+/Ca^{2+}-exchanger located on the inner mitochondrial membrane also impaired Ca^{2+}-influx, suggesting that trans-mitochondrial flux is essential for maintaining store-operated entry (Figure 4; Malli R. et al., *J. Biol. Chem.* **278.45**: 44769–44779, 2003; Malli R. et al., *J. Biol. Chem.* **280.13**: 12114-12122, 2005).

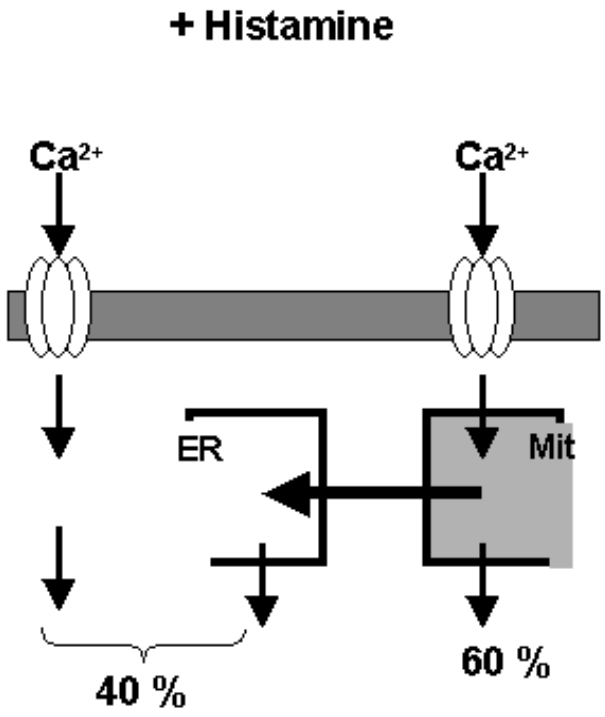

Figure 4: Schematic illustration of the Ca^{2+} fluxes
In case of non-excitable cells, upon histamine stimulation following Ca^{2+} readdition most Ca^{2+} that enters the cell to elevate cytosolic Ca^{2+} passes the mitochondria (60 %) and gets distributed towards the ER and the cytosol thereafter, whereas the remaining 40 % of Ca^{2+} entry goes the direct way into the cytosol or the ER (Scheme taken from Malli R. et al., *J. Biol. Chem.* **280.13**: 12114-12122, 2005).

In addition to the MCU there is another alternative route for mitochondrial Ca^{2+}-uptake described as Rapid Uptake Mode (RaM). RaM was observed in isolated liver mitochondria exposed to short pulses of $[Ca^{2+}]$ changes resulting in very high rates of Ca^{2+}-uptake that was quickly inhibited according to the high $[Ca^{2+}]_{mito}$ (Sparagna GC. et al., *J. Biol.Chem.* **270**: 27510-27515, 1995).
However, regarding these studies it is still unclear which proteins are involved to link mitochondria next to the plasma membrane and/or to facilitate the mitochondrial Ca^{2+} uptake of entering Ca^{2+}.

1.6 Regulation of ER Ca^{2+}-Refilling by mitochondria

A close association between subdomains of the ER and mitochondrial surface (Figure 5, imaged by Malli R.) appears to be necessary for the propagation of ER Ca^{2+} release to the mitochondria (for review see Rizzuto R. et al., *Cell Calcium* **26.5**: 193-199, 1999).
In Ea.hy926 cells it was shown that the mechanisms of ER Ca^{2+} refilling are multiple. It was shown that in the presence of histamine, ER Ca^{2+} refilling requires trans-mitochondrial Ca^{2+} flux, whereas in the absence of the agonist, the ER refills independently of mitochondria (Malli R. et al., *The Journal of Biological Chemistry* **288.13**: 12114-12122, 2005). Furthermore it was demonstrated that a Ca^{2+} flux from the extracellular area through mitochondria is essential to maintain mitochondrial Ca^{2+}

buffering, store operated Ca^{2+} entry (1.4.4) and Ca^{2+} filling of the ER during cell stimulation (Malli R. et al., *Cell Calcium* **41**: 63-76, 2007).

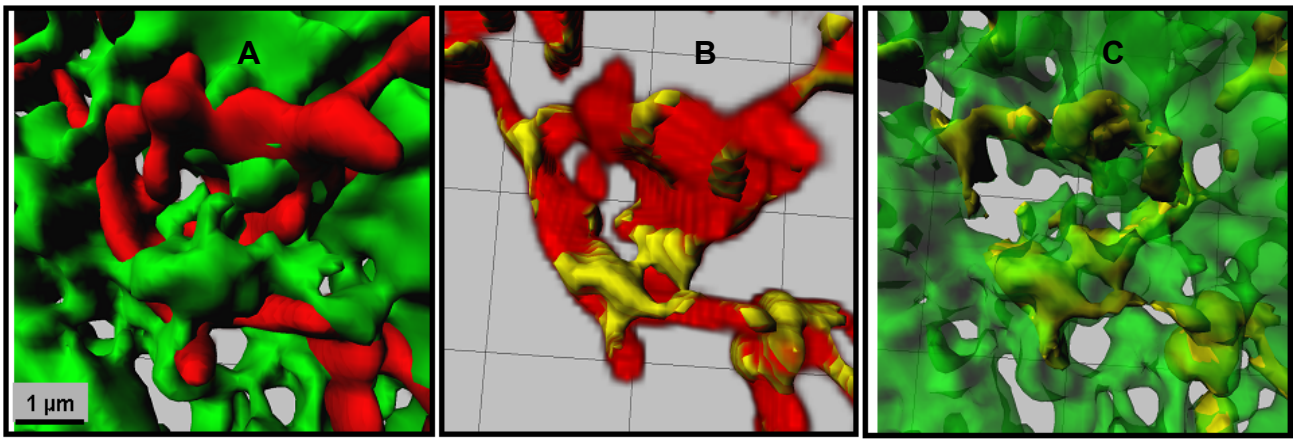

Figure 5: Colocalization of mitochondria and ER
Ea.hy926 cells co-transfected with mtDSRed and YC4-er (Miyawaki A. et al., *Nature* **388**: 882-887, 1997). Z-scans were performed on an array confocal laser scanning microscope applying 514 nm excitation and measuring 570 nm emission for mtDSRed or 488 nm excitation and 535 nm emission for YC4-er. ER and mitochondria z-stacks were deconvoluted and 3-D reconstructed as previously described (Figure 3). **A:** Distribution of ER (green) and mitochondria(red) **B and C:** Focal contacts (yellow) between ER and mitochondria.

1.7 Scaffold Functions and Characteristics

Today, the term scaffold is very often used to describe proteins that regulate signal transduction processes, a usage first employed in the early 1990 to characterize mitogen-activated protein kinase (MAPK) signaling (for reviews see Pawson T. et al, *Science* **278**: 2075-2080, 1997; Pullikuth AK. et al., *Cellular Signalling* **19**: 1621–1632, 2007). Scaffold proteins coordinate signal transduction pathways by tethering molecules together and serving as molecular backbones for signaling complex assembly: they anchor proteins to given subcellular targets and serve as backbones for the assembly of multiprotein complexes (for review see Ferrell JE. jr., *Sci STKE* **52**: PE1, 2000; Weston CR. et al., *Science* **292.5526**: 2439-2440, 2001). Sufficient criteria for a protein to act as a scaffold involves facilitating protein interactions without enzymatic activity. It is a well-accepted principle in signal transduction that post-transcriptional modification, for example resulting from the enzymatic activity of a kinase, can facilitate interactions of the targeted molecule(s) with other proteins. These interactions would not overtly be considered scaffolding unless they fulfill the second criteria that is the ability to simultaneously localize two or more other protein interaction domains that recruit specific molecules into multiprotein complexes (Vondriska TM. et al., *J. of Mol. and Cell. Cardiology* **37**: 391-397, 2004). The targeting functions of scaffolds facilitate the

regulated or constitutive movement of signaling proteins to specific subcellular compartments during signaling events (Burack WR. et al., *Current Opinion in Immunology* **14**: 312–316, 2002), whereas the catalytic scaffold functions would enhance the interaction of various members of the same signal transduction pathway (Burack WR. et al., *Curr. Opin. Cell Biol*. **12**: 211-216, 2000; Lester LB. et al., *Recent. Prog. Horm. Res.* **52**: 409-429, 1997).

However, signaling events upon scaffolding just happen if the concentrations of a scaffold and its client proteins are ideal. This is illustrated in Figure 6 for the well characterized MAPK cascade in the budding yeast (Ferrell JE. jr., *Sci STKE* **52**: PE1, 2000):

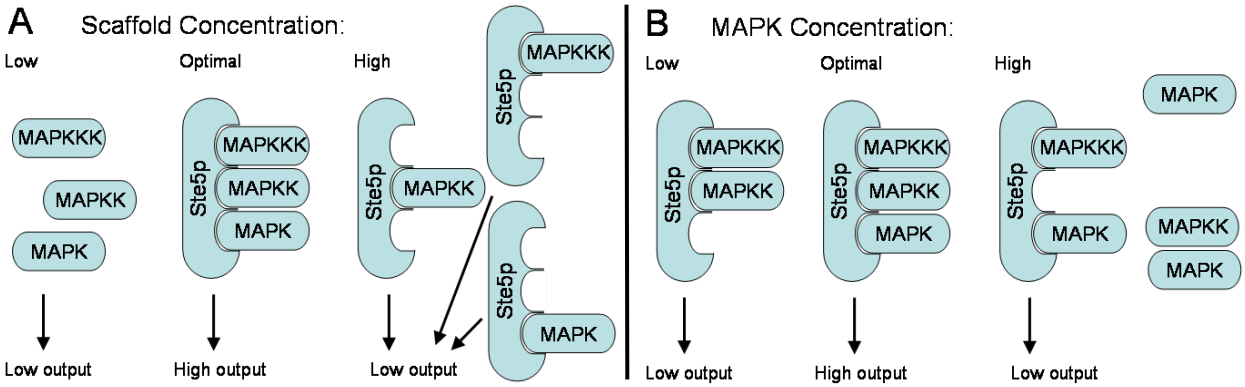

Figure 6: Schematic of the scaffolded MAPK cascade
A: Signaling down a scaffolded protein kinase cascade is a question of balance. If there is low scaffold (in this case Ste5p), signalling is low (left). At an intermediate concentration of scaffold, signalling will be high (center). Once the concentration of the scaffold exceeds that of the kinases, the signalling begins to decrease (right) (Schemes A, B taken from Ferrell JE. jr., *Sci STKE* **52**: PE1, 2000).
B: Out of balance again: Adding too much kinase can decrease the output of a scaffolded cascade.

Notably, an overexpression or downregulation of one distinct interaction partner of the MAPK signaling cascade will reduce the effect.

Accordingly a signal transduction pathway is activated by a certain stimulus to optimize the conditions for the scaffold function in distinct regions within a cell. That, in turn, may initiate the translocation of the multiprotein complex to mediate the signal to the target region. Just to give an example, the cytosolic Protein Kinase C isoform alpha (PKCα) is throughly shown to translocate to the plasma or internal membranes by the formation of such a multiprotein complex or signalplex (Baldassare JJ. et al., *J. Biol. Chem.* **267.22**: 15585-15590, 1992; Malolanarasimhan K. et al., *J. Med. Chem.* **50.5**: 962-978, 2007). As previously mentioned PKC proteins get concertedly activated via DAG and Ca^{2+}. Therefore the isoform PKCα consists of two C1 domains for the binding of DAG (Colón-González F. et al., *Biochim. Biophys. Acta* **1761.8**: 827-837, 2006) and one C2 domain

for the binding of Ca^{2+} (Rizo J. et al., *J. Biol. Chem.* **273.26**: 15879-15882, 1998). In response to this bondage PKCα and other proteins may be linked to a yet unknown scaffold protein that transports the proteins to their distinct targets. Although the formation of the signalplex is still not fully declared, the dramatic impact of Ca^{2+} and DAG to initiate the translocation of PKCα are shown below (Figure 7) (Oancea E. et al., *Cell* **95.3**: 307-318, 1998).

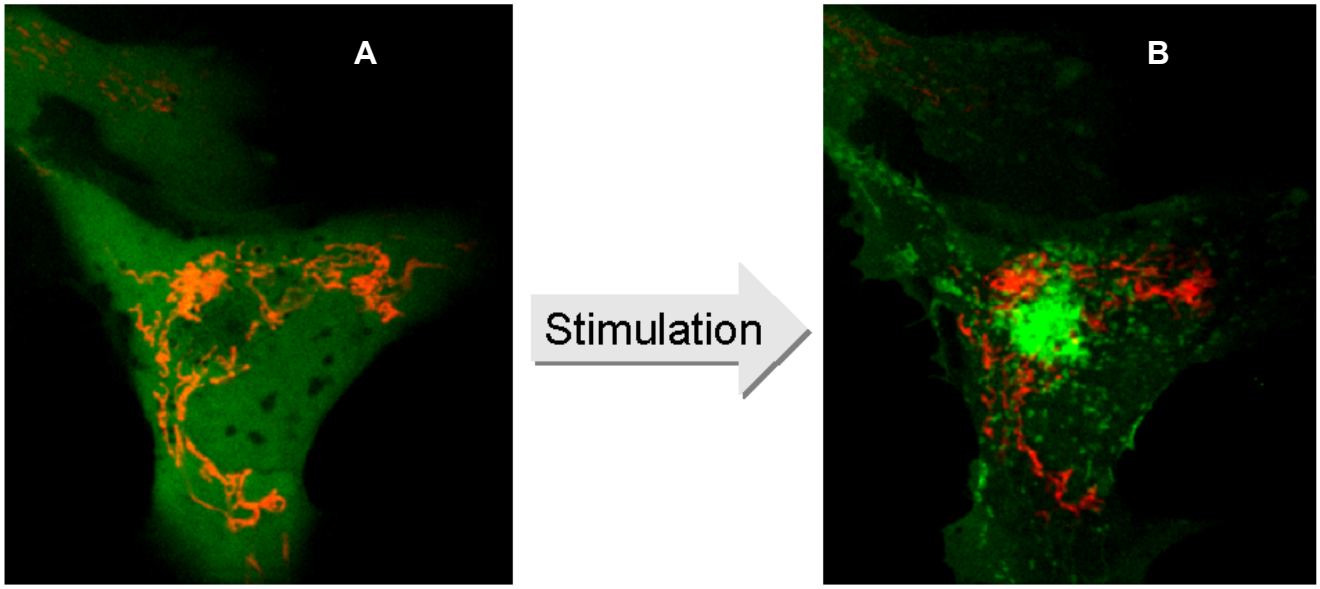

Figure 7: Translocation of PKCα
Ea.hy926 cell transfected with a PKCα-YFP plasmid before (**A**) and after stimulation (**B**) with 100 µM Histamine, 15 µM BHQ and 3 µM ionomycin.

For the identification of new putative Ca^{2+}-activated scaffold proteins two strategic plans were performed (1.8; 1.9, excerpted from a grant application by Graier WF.).

1.8 Strategic Plan of the Proteomic Approach

Based on the assumption that Ca^{2+}-activated scaffolds may translocate from a distinct cell compartment to another in order to assemble distinct signalplexes, the pattern of associated proteins upon a specific Ca^{2+} signaling patterns (e.g. histamine stimulation) were assessed and correlated with that under resting condition using 2D-DIGE. Subsequently, proteins that accumulate at the plasma membrane, membrane or nucleus in response to a Ca^{2+} stimulus were subjected to tryptic in gel digestion and peptide mass fingerprinting by MALDI-TOF.

1.8.1 A scaffold finds its client

Proteins of interest were further investigated based on their properties to bind to other proteins upon Ca^{2+} elevation in order to identify their binding partners. Thus, on the one hand proteins of interest will be fused with a GFP to visualize their translocation. On the other hand they will be fused with a His-tag to and transiently expressed under the control of a strong (CMV-) promotor. Defined Ca^{2+} signals will be generated and proteins will be reversibly cross-linked. Subsequently, signalplexes that contain the respective protein of interest will be separated by means of their His-tag using affinity columns, rinsed and liberated. Subsequent to reversal of cross-linking, signalplexes will be analyzed using 1D/2D-electrophoresis and analyzed by MALDI-TOF. As a result, the composition of signalplexes that contain the protein of interest will be revealed and contribution of this respective signalplex will be further analyzed as described above. Notably, the knowledge of specific sequences and structures of these newly verified scaffolds will be further incorporated in our in silico analyses for the search of putative Ca^{2+}-regulated scaffolds.

1.8.2 A client finds its scaffold

Another strategy to discover new Ca^{2+}-regulated scaffolds will embark the isolation and subsequent characterization of signalplexes that contain presumable client proteins (e.g. PKC isoforms, calmodulin, calcineurin) to yet unknown scaffolds and are assembled upon certain Ca^{2+} signals. Accordingly, client proteins will be fused to FP/His-tags and the composition of signalplexes assembled in response to specific Ca^{2+} signals will be assessed as described above.

1.9 Strategic Plan of the Bioinformtic Approach: *in silico analyses*

1.9.1 Sequence-based annotation of putative Ca^{2+}-activated scaffolds

As perequisite of the bioinformatical identification of new scaffolds, known scaffolds will be analyzed regarding their domain architecture, sequence features primary sequence and experimentally resolved 3D-structures of important domains (e.g. PDZ domain). This will define the general requirements of a protein to act as a scaffold. Additionally new specific sequences will be introduced for annotation based on the analysis of a protein of interest as described (1.8.1). This knowledge will be conferred to the human proteome by either locally applied assignment methods or by importing from public

annotation databases. Furthermore, prediction methods for special sequence features such as signal peptides will be applied (Prlic A. et al., *Bioinformatics* **20**: 127-28, 2004). Subsequently, the annotation data will be stored in a relation database that will be the basis for the combinatorial search for scaffold features within the annotated human sequences.

1.9.2 Structure-based annotation of putative Ca^{2+}-activated scaffolds

The structure-based approach will be used to scan the human proteome for sequences, which might fold into a given query structure. The PDZ domain, for example is rather unique in its 3D-structure and sequences identified to contain such domain will be further evaluated on other characteristic structures. To go beyond the limitation of a sequence signal, fold recognition procedures based on statistical potentials are the methods of choice. Since such methods are computational expansive, a pre-selection of the human protein sequences will be required and, thus, the annotation database constructed in the previous step will be used to exclude sequences, which are apparently not scaffolds.

An extension of the structure-based approach is the investigation of structural motifs (Sippl MJ. et al., *Protein Science* **1**: 625-640, 1992). Rather than asking the question, “does a given sequence fit to a given fold” we will ask, “if a sequence fragment may adopt a certain, characteristic structure”, such as e.g. the EF-hand motif in calmodulin. In conjunction with the methods described above, this can be indicative for the scaffold proteins.

1.10 Structural and functional characteristics of Valosin containing protein

Valosin is a 25 aa long peptide that was first detected in protein extracts of various pig tissues using immunoreactive antibodies against valosin. Interestingly the identified protein was much larger than valosin and thus, it was called Valosin-containing protein (Koller JK. et al., *Nature* **325**: 542-545, 1987). Additionally VCP was found to be the human homologue to the yeast CDC48 protein (Fröhlich KU. et al., *J. Cell Biol.* **114.3**: 443-453, 1991) and that it is a member of a larger gene family that includes putative ATP-binding proteins involved in vesicle transport and fusion (Wilson DW. et al., *Nature* **339**: 355-359, 1989), 26S proteasome function (Dubiel W. et al., *J. Biol Chem.* **267.32**:

22699-22702, 1992), regulation of the expression of human immunodeficiency virus Shibuya H. et al., *Nature* **357**: 700-702, 1992), assembly of peroxisomes (Erdmann R. et al., *Cell* **64.3**: 499-510, 1991) and degradation of proteins by the ubiquitin proteasome system (Halawani D. et al., *Mol. Cell* **22**: 713-717, 2006). Accordingly VCP interacts with at least 30 different cellular proteins, some of which may differentially mediate its functions. The most important seems to be the interaction with Ufd1 (required for ubiquitin-dependent protein degradation) and Npl4 (implicated in nuclear transport) forming a multiprotein complex that is essential for endoplasmic reticulum-associated degradation (ERAD) via the ubiquitin–proteasome system (UPS) (Woodman PG.: *J. Cell Sci.* **116**: 4283–4290, 2003; Wójcik C. et al., *Mol. Biol. Cell* **17**: 4606-4618, 2006; for review see Wang Q. et al., *J. Struct. Biol.* **146**: 44-57, 2004).

However, mutations of VCP lead to CNS, muscle and bone disease by yet unknown mechanisms (for reviews see Guinto JB. et al., *Acta Neuropathol.* **114**: 55-61, 2007; Talbot K. et al., *Hum. Mol. Genet.* **15.2**: R182-R187, 2006).

The localization of VCP will be further discussed in 4.1.9 and 5.1.2.

1.11 Structural and functional characteristics of Peroxiredoxin 1

The existence of a protective thiol-specific antioxidant compound was first observed in the yeast and led to the discovery of an enzyme that protects against oxidation in a thiol-containing system (Kim K. et al., *J. Biol. Chem.* **260.29**: 15394-15397, 1985). In mammalian cells several thiol-specific antioxidants were identified with high similarities to that of the yeast and were later termed peroxiredoxins (Prdx) (Chae HZ. et al., *PNAS* **91.15**: 7017-7021, 1994). Mammalian cells express six Prdx isoforms (Prdx I–VI) that all share the same basic catalytic mechanism, in which an active site cysteine is oxidized to a sulfenic acid by the peroxide substrate (Seo MS. et al., *J. Biol. Chem.* **275.27**: 20346-20354, 2000) exerting their protective antioxidant role in cells through their peroxidase activity ($ROOH + 2\ e^- \rightarrow ROH + H_2O$) (for reviews see Wood ZA. et al., *Trends Biochem. Sci.* **28.1**: 32-40, 2003; Rhee SG. et al., *Free Radical Biology & Medicine* **38**: 1543– 1552, 2005).

Reactive oxygen species (ROS) are involved in many cellular metabolic and signaling processes (Finkel T., *Curr. Opin. Cell Biol.* **10.2**: 248-253,1998) and are thought to have a role in disease, particularly in carcinogenesis and aging (Finkel T. et al., *Nature* **408.6809**: 239-247, 2000). As a member of the redox-regulating protein family, Prdx1 (Figure 9) serves as an important defense against oxidants. Accordingly it was

demonstrated that Prdx1-deficient fibroblasts showed a decreased proliferation and an increased sensitivity to oxidative DNA damage. Moreover Prdx1-null mice had abnormalities in numbers, phenotype and function of natural killer cells (Neumann CA. et al., *Nature* **424**: 561-565, 2003).

The localization of Prdx1 will be further discussed in 4.1.9 and 5.1.3.

1.12 Structural and functional characteristics of Gaf1

The Rab11 protein is a small GTPase belonging to the superfamily of Ras GTPases. Rab11 plays an important role in protein recycling from endosomes to the plasma membrane (Ullrich O. et al., *J. Cell Biol.* **135.4**: 913-924, 1996). Furthermore, it has been implicated in regulating several other membrane transport pathways, including phagocytosis (Cox D. et al., *PNAS* **97**: 680-685, 2000), apical targeting in epithelial cells (Wang X. et al., *J. Biol. Chem.* **275**: 29138-29146, 2000), insulin-dependent glucose transporter 4 (GLUT4) transport to plasma membrane (Kessler A. et al., *Diabetologia* **43.12**: 1518-1527, 2000) and protein transport from endosomes to the Golgi vesicles (Wilcke M. et al., *J. Cell Biol.* **151.6**: 1207-1220, 2000). Therefore, cycling between GTP- and GDP-bound forms of Rab11 regulate the recruitment of various effector proteins to cellular membranes, thereby affecting the targeting and fusion of transport vesicles (Peden AA. et al., *Mol. Biol. Cell.* **15.8**: 3530-3541, 2004). Accordingly, Gaf1 (gamma-SNAP associated protein, Figure 10), also called Rab11FIP5 (Rab11 family interaction partner 5) or Rip11, was the first of six recently identified Rab11 effector proteins (Prekeris R. et al., *Mol. Cell.* **6.6**: 1437-1448, 2000), that all share a highly homologous Rab11-binding domain (RBD) at their C-termini (Figure 10). Upon binding to Rab11, Gaf1 gets recruited to endosomal membranes, while the interaction of its C2 domain with neutral phospholipids regulates its association with the plasma membrane by a phosphorylation and dephosphorylation cycle (Prekeris R. et al., *Mol. Cell.* **6.6**: 1437-1448, 2000). Among the six Rab11FIPs, regarding their N-terminal end, Rab11FIP3 and Rab11FIP4 contain EF-hand domains (class II RabFips), whereas Rab11FIP1, Rab11FIP2 and Rab11FIP5 (Gaf1) enclose a C2-domain (Figure 10) (class I Rab11FIPs). Both domains, C2-domains and EF-hands are well known to react in Ca^{2+}-dependent way unless to bind Ca^{2+}-depentent phospholipids or Ca^{2+} itself. C2-domains are found in many proteins that are involved in cell signaling or membrane targeting and serve as protein-protein or protein-phospholipid modules. As previously described this domain is also essential for the translocation of PKC to specific regions

(1.7). For Rab11FIP5 it was shown in HeLa and A431 cells to traffic between endocytic recycling compartments (ERC) and the PM in a C2-depentent manner. Hence, mutants lacking their C2-domain were unable in endosomal recycling and were not able to translocate to the PM, while a 65 aa C-terminal mutant including the Rab binding domain (RBD) was sufficient for binding to intracellular membranes. (Lindsay AJ. et al., *J. Biol. Chem.* **277**: 12190-12199, 2002; *J. Cell Sci.* **117**: 4365-4375, 2004). According to its Rab11 interaction it has been reported in several studies that Gaf1 contains a highly conserved α-helical structure of 20 amino acids at its C-terminal end, the Rab11 binding domain (RBD), forming a hydrophobic Rab11 patch (Prekeris R. et al., *J. Biol. Chem.* **276.42**: 38966-38970, 2001; Hales CM. et al., *J. Biol. Chem.* **276.42**: 39067-39075, 2001). In addition, it has been demonstrated that all Rab11FIPs possess a similar RBD like Gaf1. These compete with each other for the binding to Rab11 and therefore regulate Rab11 localization by recruiting it to distinct membranous organelles. Thus, it has been proposed by the authors of these studies that each of this Rab11FIPs forms part of a Rab11-regulated scaffold that mediates its function (Wallace DM. et al., *Biochem. Biophys Res. Commun.* **292**: 909-915, 2002; Meyers JM. et al., *J. Biol. Chem.* **277.50**: 49003-49010, 2002).

Interestingly exclusively Gaf1 was also shown to interact with γ-SNAP, a member of the soluble NSF (*N*-ethylamine-sensitive factor) attachment protein with unknown function (Chen D. et al., *J. Biol. Chem.* **276.16**: 13127-13135, 2001; Kawase K. et al., *Biochem. Biophys. Res. Commun.* **303.4**: 1042-1046, 2003). Chen and co-workers showed that overexpression of GFP-γ-SNAP results in the appearance of a reticular network of γ-SNAP that partially colocalize with Gaf-1 and mitochondria. Notably, Gaf1 and γ-SNAP were demonstrated to colocalize with mitochondria in HEK-293, CHO and HepG2 cells. Furthermore, Gaf1 was also shown in this study to bind γ-tubulin and therefore gets associated with both, cytoskeletal and mitochondrial elements. Therefore the binding of γ-SNAP to Gaf1 is accomplished by the same motif responsible for the Rab11 binding (RBD). Using these abilities, Gaf1 may constitute as a scaffold or a hydrophobic patch that can accommodate Rab11 as well as γ-SNAP (Tani K. et al., *J. Biol. Chem.* **278.15**: 13531-13538, 2003). In addition to that, a splicing variant of Gaf1 has been identified, Gaf1b, which has also been shown to interact with both proteins, Rab11 and γ-SNAP (Kawase K. et al., *Biochem. Biophys. Res. Commun.* **303.4**: 1042-1046, 2003).

Thus, regarding these studies Gaf1 is obviously able to interact with different proteins from different cellular pathways.

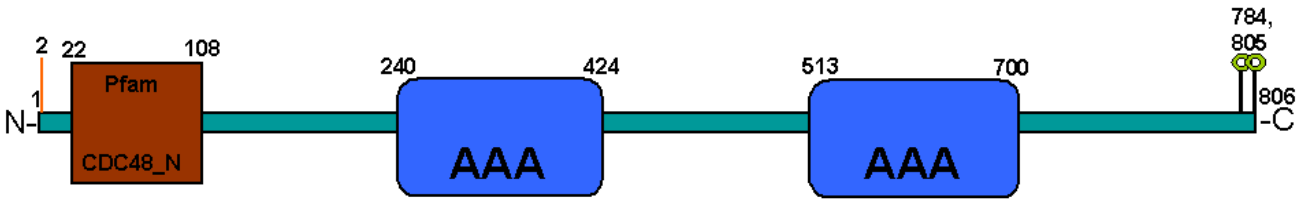

Figure 8: Schematic illustration of the VCP
The mammalian VCP also termed p97 weighs about 89 kDa consisting of 806 aa and is a hexameric ATPase of the AAA family. The two conserved AAA-domains are highlighted (240-424 aa and 513-700 aa). Additionally it has an acetylated alanine at position 2 and contains two phosphorylation sites near its C-terminal end (784: phosphoserine and 805: phosphothyrosine).

Figure 9: Schematic illustration of the Prdx1
Peroxiredoxin 1 is a ~ 22 kDa protein of 199 aa: Oxidatve thioredoxin domain (6-165 aa); Disulfid interchain spanning from aa pos. 52 to aa pos. 173.

Figure 10: Schematic illustration of Gaf1
Domain mapping of the Gaf1 protein (~ 70 kDa) consisting of 653 aa: C2-domain (20-128 aa) and Rab binding domain (RBD, 601-648 aa) are indicated.

Maps of functional domains of the three proteins (Figure 8-10) were created according to the databases of http://www.hprd.org/, http://www.expasy.org/, http://pfam.sanger.ac.uk/ and http://smart.embl.de/smart/.

2 Aim of this study

The aim of this study was to identify new Ca^{2+}-activated proteins. As calcium serves as an important second messenger, it is able to initiate various signaling pathways upon different stimuli (diverse agonists, oxidative stress, shear stress, cyclic stretch or cell to cell interaction).

To accomplish the goal of identifying new Ca^{2+}-dependent scaffold proteins or their clients, two independently different studies were aimed, a proteomic and a bioinformatic approach:

The proteomic approach is based on the isolation of distinct cellular organelles after stimulation with 100 µM histamine for 5 minutes. The purified protein extracts of stimulated and non-stimulated Ea.hy926 cells deriving from the different cell compartments are analyzed by 2D-electrophoresis for changes in the abundance of the various proteins. Significant increase or decrease of a proteins' abundance on the 2D-gel refers to protein translocation upon histamine stimulation. These proteins are further analyzed by mass spectrometry for their identification.

The bioinformatic approach is based on a combined sequence and structure annotation of proteins with regard to their motifs and already known interactions that may indicate a Ca^{2+}-dependency. Accordingly, various selection criteria are exerted to elect such putative candidate protein(s).

3 Materials and Methods

3.1 Cell Culture and Transfection

Two different types of cells were used in the experimental approach:

1. The Ea.hy926 cell line is a hybrid of human umbilical vein endothelial cells (HUVEC) and A549 human lung carcinoma epithelial cells (Edgell CJ. et al., *PNAS* **80**: 3734-3737, 1983).
2. The HeLa is an immortal cell line that is widely-used in medical research. Originally this cell line was derived from cervical cancer cells taken from Henrietta Lacks, who died from her cancer in 1951.

Cells were cultured on plasticware (100 mm tissue culture dish) at 37 °C in a humid atmosphere containing 5 % (v/v) CO_2 in air. Cells were grown in Dulbecco's modified Eagles medium (DMEM) supplemented with 10 % fetal calf serum (FCS), penicillin (100 $U \cdot mL^{-1}$), streptomycin (100 $\mu g \cdot mL^{-1}$), amphothericin B (1.25 $\mu g \cdot mL^{-1}$) and 1 % HAT (100 µM hypoxanthine, 0.4 µM aminopterin, 16 µM thymidine).

3.1.1 Transfection protocol for adherent cells

Cells of passage 40 or higher were grown on glass cover slips (Ø = 30 mm), placed in a 6-wel,l in DMEM containing 10 % FCS, 5 mM D-glucose and 1 % HAT. After they reached approximately 80 % of confluence, the cells were transiently transfected with 1-4 µg of purified plasmid DNA using TransFast™ Transfection Reagent (Promega, Mannheim, Germany).

The day before transfection the cells were seed to reach about 80 % confluence on the day of transfection.

The total volume of medium, DNA and TransFast ™ reagent to add per 30 mm plate was 1 ml.

To a steril tube, 1-4 µg of plasmid DNA were diluted in 1 ml cell growth medium containing no serum, protein and antibiotics (to avoid interference with complex formation).

4 µl TransFast ™ transfection reagent was added to the DNA solution and vortex immediately.

The mixture was incubated for 15 min at room temperature to allow transfection-complex formation.

While the complex formation took place, growth medium was gently aspirated from the culture dish, and cells were washed with PBS.

Briefly, the TransFast™ reagent/DNA complex was vortex and 1 ml was added to each glass cover slip (plate) and then the cells were immediately returned into the incubator for 1 hour.

1 ml complete medium (containing medium and antibiotics) was overlaid. Cells were placed in the incubator for 3 or 4 hours.

At the end of the incubation time, fresh medium was replaced.

Cells were used for experiments 24 or 48 hours after transfection.

3.1.2 Co-Transfection protocol for siRNA experiments

RNA interference (RNAi) is widely accepted as an experimental tool to analyze the function of mammalian genes. RNAi are used to bind to and promote the degradation of target RNAs, resulting in knockdown of the expression of specific genes (for mechanisms see 3.2.10). For the introduction of synthetic double-stranded small interfering RNAs (siRNAs) into Ea.hy926 or HeLa cells, Hp GenomeWide siRNAs (Qiagen) were selected from the database (3.2.10.2). These siRNAs were co-transfected with some modifications to the transfection protocol previously described (3.1.1):

Transfection reagent per well:

500 µL serum-free DMEM
+ 2 µg of plasmid DNA (e.g. mtDSRed or mtRP), to mark siRNA transfected cells
± 2.5 µL Hp GenomeWide siRNA
+ 4 µL TransFast™ transfection reagent

Briefly, the TransFast™ reagent/DNA complex was vortex and 500 µl were added to each 30 mm plate of a 6-well and then the cells were immediately returned into the incubator for 1 hour. 500 µl serum-free DMEM was overlaid and cells were placed in the incubator overnight. At the end of the incubation time, fresh medium was replaced. The cells were used for experiments 36 to 42 hours after transfection.

3.1.3 (Co-)Transfection protocol for overexpression experiments

Overexpression experiments were performed to analyze the effect of a specific protein, if expressed at higher, non-physiological levels, or to monitor a proteins´ expression pattern within a cell, when fused to a GFP.

Therefore, transfection was performed according to the protocol described in chapter 3.1.1. 1-4 µg of overexpression plasmid were added to the transfection reagent in case of GFP-fused plasmids. To mark overexpression of a non-tagged plasmid encoding the gene of interest, it was co-transfected with a marker protein (e.g. mtDSRed) in a ratio of 3:1.

3.2 Molecular Biological Procedures

3.2.1 RNeasy Mini Protocol for Isolation of Total RNA from Animal Cells

To isolate RNA from various animal cell lines the RNeasy Mini kit from Qiagen was used. RNA was isolated from HeLa, Ea.hy926, HUTAEC, HUVEC, ECV and ECA grown in a confluent monolayer according to manufacturer´s Protocol for Animal Cells I:

Cells were harvested after washing two times with PBS. For direct lysis of cells the appropriate buffer RLT containing 1 % β-Mercaptoethanol was added to the cell culture dish (700 µl for 100 mm dish and 350 µl for 30 mm well respectively) and cell lysate was collected with a rubber policeman and pipetted into a microcentrifuge tube.

The cell lysate was gently homogenized using an RNase free syringe by passing the sample at least 5 times through a 26-gouge needle.

One volume of 70 % ethanol was added to the lysate and mixed by pipetting.

The sample was applied to an RNeasy mini column placed in a 2 ml collection tube and centrifuged for 30 seconds at 8,000 x g (10,000 rpm)

700 µl buffer RW1 was added to the RNeasy column and the isolated RNA was washed by a 30 seconds centrifugation step at 8,000 x g (10,000 rpm).

The RNeasy column was transferred into a new 2 ml collection tube. 500 µl of buffer RPE containing ethanol (RPE concentrate: $EtOH_{abs}$ = 1:4) was pipetted onto the RNeasy column and centrifuged for 30 seconds at 8,000 x g.

Step 6 was repeated with 500 µl buffer RPE. After discarding the flow-through the RNeasy column containing the washed RNA was centrifuged another minute at full speed (13,000 rpm) to dry the RNeasy silica-gel membrane.

To elute the RNA, the RNeasy column was transferred to a new 1.5 ml collection tube, 30 – 50 µl of RNase free water was pipetted directly onto the RNeasy silica-gel membrane and left for 5 minutes (elution).

The RNA was isolated by a final centrifugation step, 1 min at max speed (13,000 rpm).

RNA was stored at –70 °C.

3.2.2 Measuring the concentration of nucleic acids

The concentration of RNA and DNA samples were either determined using the Beckman Coulter DU® 800 spectrophotometer or the Peqlab ND-1000 spectrophotometer.

3.2.2.1 Beckman Coulter DU® 800 spectrophotometer

The concentration of nucleic acid samples were measured in a black quartz cuvette using UV light absorption wavelengths. Nucleic acid free water was used for the reference (blank) as well as for the dilution of sample(s):

Blank: 100 µl ultrapure water

Sample: 99 µl ultrapure water + 1 µl of nucleic acid sample

Absorption at 160 nm and 280 nm of sample(s) were read. The concentration as well as the purity of the sample(s) was calculated using the acquired values:

Purity: abs260/abs280 RNA = 1.7-1.9
DNA = 1.5-1.7

Calculation of Nucleic Acid Concentration: abs260 x 4 = RNA in µg/µl
abs260 x 5 = DNA in µg/µl

3.2.2.2 Peqlab ND-1000 spectrophotometer

2 µl of a nucleic acid sample was directly applied onto the measurement spot of the Nanodrop (ND) instrument. RNA or DNA concentrations were immediately measured and calculated by the system.

3.2.3 Reverse Transcription of RNA to cDNA (RT-PCR)

Three different Reverse Transcription procedures were performed for the transcription of RNA to cDNA. Additionally a DNase treatment step was performed prior to RT-PCR:

3.2.3.1 DNase-treatment (for RT-PCR):

3 µg of RNA
3 µl 5x first strand buffer (Promega)
1 µl DNase I (Promega)
x µl DEPC-water (RNase-free)
15 µl, vortex gently, centrifuged a few seconds

- 37°C for 15 minutes
- put the probe on ice
- add 1.5 µl 20 mM EDTA (vortex gently; centrifuge a few seconds)

- 75°C for 10 minutes
- put immediately on ice (ice-cold water bath)
- centrifuge and put on ice again

3.2.3.2 First Strand cDNA Synthesis using MMuLV-RT (Promega)

To synthesize cDNA from RNA samples the M-MLV Reverse Transcriptase from Promega with modifications to manufacturer's protocol:

mastermix: 4.5 µl DEPC-water
3 µl 5x first strand buffer
3 µl 0.1 M DTT (Amersham)
0.6 µl 25 mM dNTPs (Roth)
0.4 µl RNAguard (Promega)
1 µl Random 6mer primers (Promega)
1 µl MMuLV-reverse transcriptase (Promega)
13.5 µl + 16.5 µl RNA (from DNase-treatment + EDTA)
vortex gently, centrifuge a few seconds

- 37°C for 1 hour
- 75°C for 10 minutes
- put the probe on ice
- centrifuge a few seconds
- put the probe on ice or freeze it at –20°C

3.2.3.3 First Strand cDNA Synthesis using SuperScript™ II RT Protocol

A 20 µl reaction volume can be used for 1 ng – 5 µg of total RNA:

1. Add the following components to a nuclease-free microcentrifuge tube:

250 ng random primers (Promega, Primer Hexamer)
1-3 µg total RNA
1 µl dNTP Mix (10 mM each)
Sterile, distilled water to 12 µl

2. Heat mixtures to 65°C for 5 min and quick chill on ice. Collect the contents of the tube by brief centrifugation and add:

5x First-Strand Buffer 4 µl
0.1 M DTT 2 µl
RNasin® RNase Inhibitor (Promega) 1 µl

3. Mix contents of the tube gently. Incubate at 25°C for 2 min.

4. Add 1 µl (200 units) of SuperScript™ II RT and mix by pipetting gently up and down.

5. Incubate at 42°C for 50 min.

6. Inactivate the reaction by heating at 70°C for 15 min.

The cDNA can now be used as a template for amplification in PCR.

3.2.3.4 cDNA Synthesis using High Capacity cDNA Reverse Transcription Kit

Prior to Real Time PCR experiments it is important to ensure complete reverse transcription of RNA samples into cDNA samples. An essential requirement for the relative quantitation of cDNA is that the reverse transcriptase reaction generates products in a manner directly dependent to the amount of input RNA template. This is possible using the High-Capacity cDNA Reverse Transcription Kit from Applied Biosystems. It contains random primers, which warrant that the first strand synthesis occurs efficiently with all species of RNA molecules present, including mRNA and rRNA. Furthermore it contains of a 10x RT buffer, a 25x dNTP Mix (100 mM) and the MultiScribe™ Reverse Transcriptase. To avoid RNA digestion the RNasin® RNase Inhibitor (Promega) was inserted into the reverse transcription as well. According to manufacturer´s protocol these reagents combined, form a 2x Reverse Transcription Master Mix:

Allow the kit components to thaw on ice and prepare the RT master mix on ice.

Referring to the procedure below, calculate the volume of components needed to prepare the required number of reactions:

10x RT buffer	2.0 µl
25x dNTP mix(100 mM)	0.8 µl
10x RT Random Primers	2.0 µl
MultiScribe™ Reverse Transcriptase	1.0 µl
RNase Inhibitor	1.0 µl
Nuclease-free H_2O	3.2 µl
Total per reaction	10.0 µl

Mix gently and place the 2x RT master mix on ice.

To prepare the cDNA Reverse Transcription reactions:

Pipette 10 µl of 2x RT master mix into individual tubes.

Pipette 10 µl of the RNA samples into each well, pipetting up and down two times. To prepare the appropriate amount of RNA, it has to be deluted with RNase-free water.

Seal the tubes and briefly centrifuge them to spin down the contents and to eliminate any air bubbles.

Place the tube on ice until the thermal cycler is ready to use.

To program the thermal cycling conditions:

	Step 1	**Step 2**	**Step 3**	**Step 4**
Temperature	25°C	37°C	85°C	4°C
Time	10 min	120 min	5 sec	soak

Table 1: Thermal Cycling Conditions for RT-PCR

3.2.4 Specific Polymerase Chain Reaction (PCR)

Two different Polymerases were used to perform specific PCR from cDNA templates: On the one hand a Hot Start Taq Polymerase from Solis Biodyne for the amplification of short (< 1000 bp) PCR products and on the other hand an Advantage® cDNA PCR Kit from Clontech to amplify long (1000 – 3000 bp) PCR products. For those, different PCR reaction protocols and conditions were used (3.2.4.4 and 3.2.4.5).

3.2.4.1 Primer Design

The design of a specific primer pair for a certain gene is depending on different parameters that are crucial for the success of amplifying a gene by specific PCR. For optimum design regarding primer balance, hairpins or primer-dimers, the *MS Dos Program Primer Designer – Version 2.0* was used.

The sequences of diverse genes (ORF = open reading frame) were obtained from the *National Center for Biotechnological Information (NCBI)* and copied as FASTA format into the *Primer Designer*. Start forward and stop reverse primers for every sequence were tagged with an overhang for the restriction sites to clone the gene into the multiple cloning site (MCS) of a vector. Therefore, coding sequences had to be analyzed at http://www.restrictionmapper.org or http://tools.neb.com/NEBcutter2/index.php for their restriction sites, in ordert that the restriction enzymes used for cloning must not cut inside of the insert and the unique sites must be available in the MCS of the vector too. That way designed primers were blasted in the NCBI to exclude any other target genes. All primers used, were purchased from Invitrogen and listed in Table 2 (Overhangs according to any restriction sites are marked italic):

Name	Sequence	Position	Product	Purpose
ECFP for	*AAACTCGAG*-ATGGTGAGCAAGGGCGAGGA	1		
ECFP rev	*CCGAGATCTTTA*-CACGAACTCCAGCAGGACCA	675	675 bp	expression
GAF1A for	*ATAAAGCTT*-ATGGCCCTGGTGCGGGGCG	1		
GAF1A rev	TCAGGATCCTCTATGGCGCT	662	662 bp	expression
GAF1A2 for	TTTGTCACCAGGTCCTGGGG	11		
GAF1A2 rev	CTTGTTGCGGAGGAAGAAGC	789	779 bp	expression
GAF1B for	AGCGCCATAGAGGATCCTGA	643		
GAF1B rev	GACTTAGGCCTTGGTGGTGG	1420	778 bp	expression
GAF1C for	CCACCACCAAGGCCTAAGTC	1401		
GAF1C rev	*TTTTCTAGA*-TTTGGGGGGGCCCGGGGGGAT	1959	559 bp, 1959bp	expression
GAF1xC2 for	*GACAAGCTTATG*-GCAGTGGTACAAGCTGCACT	430	1531 bp	expression

GAF1NW for	GCACACGCAGTGGTACAAGC	423		
GAF1NW rev	GTTGCTACGACTGCCTCTGG	1182	760 bp	detection
SNAP SalI for	*GGCGTCGAC*-ATGGCGGCTCAGAAGATAA	1		
SNAP BamHI rev	*GCTGGATCC*-GCATAGTCCTCCTGAGTATT	936	936 bp	expression
SNAP KpnI for	*GGCGGTACC*-ATGGCGGCTCAGAAGATAA	1		
SNAP XhoI rev	*CCGCTCGAG*-GCATAGTCCTCCTGAGTATT	936	936 bp	expression
SNAPNW for	TACCAGAGGCCGTTCAGCTA	271		
SNAPNW rev	AGCGGTGAGTTGCAGACATC	772	502 bp	detection
GPR55NW for	GCTGCCACCTCCATCTACAT	169		
GPR55NW rev	CGCTCCAGGTATCATCAGAC	535	367 bp	detection
MIRO1NW for	CAAGTCGATGGATTCCTCTC	280		
MIRO1NW rev	TCGAAGCACAGTCCAAGTAG	815	536 bp	detection
MIRO2NW for	GGTGTGTGTGGTGTATGACG	230		
MIRO2NW rev	AGATAGTCCGCAGTCAGCTC	859	630 bp	detection
GST for	*GCGAAGCTT*-ATGCCGCCCTACACCGTGG	1		
GST rev	*AGTGGATCC*-CTGTTTCCCGTTGCCATTGA	630	630 bp	expression
POXI for	*GGGAAGCTT*-ATGTCTTCAGGAAATGCTA	1		
POXI rev	*TACGGATCC*-CTTCTGCTTGGAGAAATA	600	600 bp	expression
VCPA for	*CCGAAGCTT*-ATGGCTTCTGGAGCCGATT	1		
VCPA rev	GCATCAGGAATTCCAATATC	1121	1121 bp	expression
VCPB for	TTGGAATTCCTGATGCTACAG	1106		
VCPB rev	*GGGGGATCC*-GCCATACAGGTCATCATCA	2418	1313 bp	expression
VCPV for	GACAGGGAGGTAGATATTGG	1090		
VCPV rev	GAACTCCAAGTCCACATCCT	2022	933 bp	detection
VCPH for	AGTTGCCAAGGATGTGGACT	1995		
VCPH rev	*GTTGGATCC*-GCCATACAGGTCATCATCA	2418	424 bp	expression
ORAI1NW for	TGTCCTGGCGCAAGCTCTAC	220		
ORAI1NW rev	ATGCCGCTGGTGCTGACGTT	685	466 bp	detection
ORAI1 MCSI for	*AAAGTCGAC*-ATGCATCCGGAGCCCGCC	1		
ORAI1 MCSI rev	*AAATCTAGA*-GGCATAGTGGCTGCCGGG	903	903 bp	expression
STIM1NW for	GAAGGCATGGAAGTCATCAG	362		
STIM1NW rev	TCCAACTCCTCCTCAGCATA	964	603 bp	detection
STIM1 MCSI for	*CCGGGTACC*-ATGGATGTATGCGTCCGTCT	1		
STIM1 MCSI rev	*CGCCTCGAG*-CTTCTTAAGAGGCTTCTTA	2054	2054 bp	expression
Venus for	*GAGCTC*-ATGGTGAGCAAGGGC GAGGA	Venus 10		
Venus rev	*TCTAGA*-TTACAGCTCGTCCTT GTACAGCTCGTCCATGC	Venus 726	717 bp	expression
citrine/eCFP BamHI for	*GGAGGATCC*-ATGGTGAGCAAGGGCGAGCA	1		
citrine/eCFP EcoRI rev	*AGAATTC*-TTAGCCGAGAGTGATCCCGGC	717	717bp	expression
pBud MCSI for	CACTGCTTACTGGCTTATCG	614		detection
pBud MCSI rev	TGCATTCTAGTTGTGGTTTGTCC	854		detection

Table 2: Primer list

3.2.4.2 Dilution of Primers

The primers were dissolved with sterile double deionized water (ddH_2O) according to the provided data sheet to a concentration of 100 µM (stock, stored at –20°C). Stock solutions were diluted 1:10 with ddH_2O to 10 µM (working solution).

3.2.4.3 Dilution of dNTPs

Separated dNTPs (dATP, dCTP, dGTP, dTTP) were obtained from Roth in 100 mM stock solutions. Equal amounts of these were mixed and diluted 1:10 with sterile ddH_20 to an end concentration of 2.5 mM (working solution) or 2:5 to an end concentration of 10 mM respectively.

3.2.4.4 Standard PCR reaction and condition (Hot Start Taq Polymerase)

Standard PCR Reaction:
2.5 µl of cDNA or 5-50 ng of plasmid DNA
25-100 pmol of a gene specific forward primer
25-100 pmol of a gene specific reverse primer
5 µl of the supplied 10 x polymerase reaction buffer
4 µl of the supplied 25 mM $MgCl_2$
4 µl of 2.5 mM dNTPs
0.15 µl of Hot Start Taq Polymerase (Solis Biodyne)
ddH_2O to a final reaction volume of 50 µl

The temperature settings of the thermocycler for the amplification cycles depend on the total length of the target gene and the annealing temperature of the primers used in the individual PCR reactions:

Standard PCR Conditions:			
	95°C	15 min (Initial denaturating step)	
	94-95°C	1 min (denaturating)	} 30 - 40 cycles
	50-65°C	1 min (primer annealing)	
	72°C	1 min (extension)	
	72°C	10 min (final extension step)	
	4°C	soak	

3.2.4.5 Standard PCR reaction and condition (Advantage® cDNA PCR Kit)

Standard PCR Reaction:
5 µl of cDNA or 5-50 ng of plasmid DNA
10 pmol of a gene specific forward primer
10 pmol of a gene specific reverse primer
5 µl of the supplied 10 x polymerase reaction buffer
4 µl of 10 mM dNTPs
1 µl of Advantage cDNA Polymerase Mix (Clontech)
ddH_2O to a final reaction volume of 50 µl

Standard PCR Conditions:	94°C	1 min (Initial denaturating step)	
	94°C	30 sec (denaturating)	} 25 - 35 cycles
	68°C	3 min (annealing/extension)	
	68°C	3 min (final extension step)	
	4°C	soak	

3.2.5 Purification of DNA fragments obtained by PCR

Prior proceeding to further applications like sequencing, reamplifications, restriction enzyme digestion or cloning, the DNA fragments obtained from PCR were separated by agarose gel electrophoresis and extracted from agarose gels.

3.2.5.1 Agarose Gel Electrophoresis

Solid agarose applied to 1x TAE buffer (40 mM Tris, 20 mM Na^+-acetat, 1 mM EDTA, pH=7.2) and melted in the microwave oven. Ethidium bromide was added to a final concentration of 0.5 µg/ml, and then the liquid gel was poured into a horizontal gel-forming chamber. DNA fragments as well as an appropriate amount of the GeneRuler™ DNA Ladder Mix, ready-to-use purchased from Fermentas (Figure 11) were applied into the gel slots of the solidified agarose gel. Gels were run using 1x TAE buffer for about one hour at 80 V and documented under UV-light (360 nm). For further procedures the desired DNA band was cut under UV-light and extracted from the gel slice (3.2.5.2).

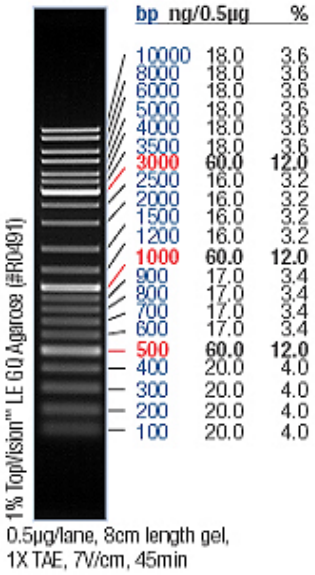

Figure 11: GeneRuler™ DNA Ladder Mix

3.2.5.2 Isolation of DNA fragments

DNA fragments were extracted and purified from agarose gel slices using the Wizard® SV Gel and Clean-Up System (Promega Corp.) according to manufacturer's protocol.

3.2.6 Cloning

3.2.6.1 Preparative Restriction

Restriction enzymes for preparative restriction or control restriction were either obtained from Promega or New England Biolabs for usage in following protocols:

1-5 µg plasmid-DNA / 5-10 µl miniprep-DNA
10 µl 10x buffer (according to the enzymes)
1 µl 100x BSA (if necessary according to the enzyme)
2 µl enzyme
x µl ultrapure water
100 µl, 37°C (or according to the enzyme) for 3 – 6 hours

For enzymes, that cut in the same buffer system double digestion was performed by adding two enzymes in the restriction protocol. Otherwise the second restriction was done after a precipitation step (3.2.9).

The restricted vector and insert(s) (inserts in case of three point ligation) were run in an agarose gel electrophoresis to separate them from the cut overhangs. DNA containing gel slices were cut out from the gel and again extracted using the Wizard® SV Gel and PCR Clean-Up System from Promega (3.2.5.2). DNA from the aqueous phase was precipitated overnight and the DNA pellet was rinsed, dried, and suspended in deionized water.

3.2.6.2 Ligation

The linearized vector and the purified insert DNA fragment(s) were together subjected to ligation at a molar ratio of 3:1:

1 µl vector
1-11 µl insert(s) or DNA fragment(s)
2 µl 10x ligase buffer (ATP containing → always keep / thaw on ice)
1 µl T4-ligase (Promega)
x µl water to a final volume of 20 µl
16°C, 16-20 hours

Once the insert(s) was ligated with the vector, the constructed plasmid was transformed into competent E. coli cells (3.2.6.4).

3.2.6.3 Preparation of competent *E.coli* strain XL1

5 ml LB medium were inoculated with the *E.coli* strain XL1 and pre-cultured overnight (3.2.6.7). Thereafter the pre-culture was transferred into 250 ml LB medium and grown in the shaker at 37°C to an OD_{600} of 0.5-0.7 that was obtained after ~ 3 hours.

Bacterial cultures of a cell density of OD_{600} = 0.6 are standing in an exponential growth stage. E.coli strains harvested at this point of time are ideal to get electrocompetent for the uptake of plasmids.

The cells were then collected by centrifugation in a cold rotor at 4,000 x g for 15 min. The supernatant was wasted and the sediment was resuspended in 250 ml ice-cold sterile 10 % glycerol and again centrifuged at 4,000 x g for 15 min. Thereafter, the cells

were resuspended in 10 ml ice-cold sterile 10 % glycerol, followed by another centrifugation step at 4,000 x g for 15 min. At last, the cells were resuspended in a final volume of 1.5 ml ice-cold sterile glycerol and shock-frozen in aliquots (80 µl) by use of liquid nitrogen. These were stored at – 70°C and electrocompetent stable for at least 6 month.

3.2.6.4 Transformation of competent *E.coli* strains

Competent cells were thawed on ice and mixed with 1-9 µl ligation mixture in a chilled reaction tube. Thereafter the mixture was transferred in a UV-light sterilized (stratagene crosslinker → autocrosslink, maximal power, 3x) 2 mm BioRad electroporation cuvette and pulsed with 2.5 kV at a constant time of 4-5 ms to open the membranes of *E.coli* for a short moment. In order to that they were able to take up the plasmids from the mixture. Then the transformed *E.coli* strains were transferred into another sterile reaction tube containing 600 µl LS or LB medium (see recipes below), depending on the antibiotic resistance of the vector. The cells were then gently shaken for either 1 hour at 37° C (in case of Zeocin or Kanamycin resistant plasmids) or 15-20 min (in case of Ampicillin resistant plasmids) to let them regenerate for plate pouring (3.2.6.5).

LB medium:	per liter H_2O	LS medium:	per liter H_2O
	10 g Tryptone		10 g Tryptone
	10 g NaCl		5 g NaCl
	5 g Yeast Extract		5 g Yeast Extract

The media were autoclaved after adjusting the pH to 7.4 with NaOH.

3.2.6.5 Plate pouring

Regenerated cells were spread on LS or LB plates containing 2 % Agar-Agar and the appropriate antibiotics. The transformed *E.coli* were then grown overnight at 37°C until antibiotic resistant colonies have been formed, that may contain the ligated plasmid.

3.2.6.6 Picking Colonies

Some *E.coli* colonies were picked from the plate using a pipette tip and each tip was put into a sterile tube filled with 5 ml bacterial medium containing the selective antibiotic (3.3.6.8).

3.2.6.7 Vector selective antibiotics

Antibiotic	1000x Stock conc.	Final conc.	Medium	Vectors
Ampicillin	100 mg/ml in ddH_2O	100 µg/ml	LB	pcDNA3.1/V5-His-TOPO, pcDNA3
Kanamycin	50 mg/ml in ddH_2O	50 µg/ml	LB	pENTR^{TM}221, pDS_SP
Zeocin	100 mg/ml in ddH_2O	25 µg/ml	LS	pBudCE4.1

Table 3: Antibiotic media and plates

3.2.6.8 Pre-Culture

The pre-culture consisted of 5 ml LS or LB medium with antibiotic and was either inoculated with a picked colony (3.2.6.6) or 100 – 200 µl of an E. coli glycerine stock (3.2.6.9) containing the desired plasmid. It was shaken in the incubator at 37°C overnight (small ONC) in case of picked colony or during the daytime in case of glycerine stock.

3.2.6.9 Overnight culture

Pre-cultures from the daytime were inoculated in 250 ml of the same culture medium and grown over night on the shaker at 37°C.

3.2.6.10 Freezing of *E.coli*-clones in glycerine stocks

500 µl of ONC were mixed with 350 µl sterilized glycerine (50 %) and store at –70° C.

3.2.7 Isolation of plasmids

Depending on the desired purity of plasmids three different methods were performed to isolate plasmids from E. coli strains.

3.2.7.1 STET-minipreparation

The STET-minipreparation was exclusively performed for the isolation of constructed plasmids derived from small ONC pre-cultures of picked colonies. These were centrifuged at 3,000 rpm for 10 min to pellet bacteria and the supernatants were removed to waste.

- 200 µl of Buffer P1 was added; the tube was vortex to resuspend the pellet and incubated at RT for 5 min.
- 200 µl of Buffer P2 was added; the tube was gently inverted to mix and incubated at RT for 5 min.

- 200 µl of Buffer P3 was added; the tube was gently inverted to mix and then incubated at RT for a few minutes before being spun at 13,000 rpm for 15 min.

During the centrifugation step fresh Eppendorf tubes filled with 650 µl of isopropanol was prepared to be mixed with the supernatant.

The mixture was centrifuged at 13,000 rpm for 20 min., the supernatant was removed and the pellet air-dried for about 10-20 min. Then the pellet was solved in 40 µl of sterile H_2O. Since not every picked colony may contain the right constructed plasmid, they were to check by four different procedures (3.2.8) as follows.

Buffer P1:	Buffer P2:	Buffer P3:
50 mM Tris/HCl (pH=8.0)	200 mM NaOH	3 M Sodium acetate
10 mM EDTA	1 % (w/v) SDS	pH=5.5 with glacial acetic
100 µg/ ml RNaseA	*store at RT*	acid
store at 4°C		store at RT

3.2.7.2 Plasmid maxi-preparation

Isolation of high-quality plasmid DNA from transformed *E.coli* for the use in eukaryotic cell transfection was performed using the PureYield™ Plasmid Maxiprep System (Promega, Madison, USA) according to the manufacturer's protocol: All steps were done at RT. Briefly, *E.coli* containing the desired plasmid derived from an over night culture (3.2.6.9) were harvested by a centrifugation step at 5,000 x g for 10 min. The cell pellet was resuspended in 12 ml of Cell Resuspension Solution, 12 ml of Cell Lysis Solution were added and the mixture was gently inverted for 3-5 times. After 3 min at room temperature, 12 ml of Neutralization Solution were added for precipitation and gently inverted to mix for 10-15 min. Then the lysate was centrifuged at 14,000 x g for 20 min. To purify the plasmid DNA the blue Clearing Column was assembled on top of the white Binding Column and the column stack was placed onto the vacuum manifold. One-half of the lysate was poured into the Clearing Column and maximum vacuum was applied until the lysate had passed through both columns. Then the remaining lysate was added and vacuum maintained until the liquid has cleared both columns. The Clearing Column was removed and the plasmid DNA bound to the Binding Column was washed once with 5 ml of Endotoxin Removal Wash and once with 20 ml of Column Wash until the solution was pulled through the column by the vacuum. Hence, the membrane was dried by applying vacuum for 5 min. The column was then removed and placed into a sterile 50 ml centrifugation tube. To elute the plasmid DNA from the

Binding Column, 1.5 ml of Nuclease-Free water were added and the tubes were centrifuged for 5 min at 2,000 x g. Finally the concentration of the obtained plasmid DNA was measured (3.2.2) transferred to a sterile 1.5 ml tube and stored at 4°C to keep it stable for transfections.

3.2.8 Control of Clones

3.2.8.1 Colony PCR

The Colony PCR is the fastest but imprecise option to verify which clone contain the right insert. 2 µl of each pre-culture were directly added to specific PCR experiments by using the appropriate primers to detect the sequence that should have been ligated into the vector.

3.2.8.2 Restriction Control

The Restriction Control is the common way to check clones. In the following procedure two restriction enzymes were added in the best restriction buffer for both to cut out a defined sequence of the ligated insert from the vector:

2-5 µl miniprep-DNA
2.5 µl 10x buffer (according to the enzymes)
0.25 µl 100x BSA (if necessary according to the enzyme)
0.5 µl enzyme 1 + 0.5 µl enzyme 2
x µl ultrapure water

25 µl, 37°C (or according to the enzyme) for 3 – 6 hours

Restricted plasmid DNA deriving from the different clones was run in an agarose gel electrophoresis after the inactivation of restriction enzymes by precipitation (3.2.9).

3.2.8.3 Sequencing

3.2.8.4 Transfection of minipreparation

In case of clones that consisted of a tagged FP, 5-10 µg of the respective plasmid DNA minipreparation were directly transfected in HeLa cells, which were likely to take up plasmid DNA easier than other cell lines. The various clones were then checked upon their protein expression using the Nipkow imaging system (3.4.10).

3.2.9 Precipitation

In some cases, it is necessary to do a precipitation step. In this work it was either used to inactivate restriction enzymes or to purify DNA. To precipitate DNA samples, the appropriate volumes of solutions listed below were added prior to the precipitation procedure:

1/10 volume 3M NaAcetate
2 volumes ethanol absolute
-20°C overnight (at least 5 hours or 30 min –70°C; depends on DNA concentration; the lower DNA concentration is, the longer the sample has to be precipitated)

- centrifuge 15 min 14,000 rpm 4°C
- wash once with 500 µl of 70 % ethanol
- dry DNA at 37°C (just a few minutes; otherwise DNA cannot be resolved)
- solve DNA with x µl H_2O

3.2.10 siRNA

3.2.10.1 Mechanism of siRNA

Double-stranded RNAs (ds-RNA; typically > 200 nt) can be processed into 20-25 nucleotide with 3'-overhangs small interfering RNAs (siRNAs) by an RNase III-like enzyme called DICER. In vitro studies with *Drosophila* indicate that the siRNA/protein complexes are then transferred to a second enzyme complex, the RNA-induced silencing complex (RISC), which contains an endoribonuclease that is distinct from DICER. RISC uses the sequence encoded by the antisense siRNA strand to find and destroy mRNAs of complementary sequence. The siRNA acts as a guide, restricting the ribonuclease to cleave only mRNAs complementary to one of two siRNA strands. It is not clearly understood how the RNA-degrading capacity of the ribonuclease is constrained by the siRNA guide. (Hammond SM., Boettcher S. et al., *Science*; **293**: 1146-50, 2001; Figure 12).

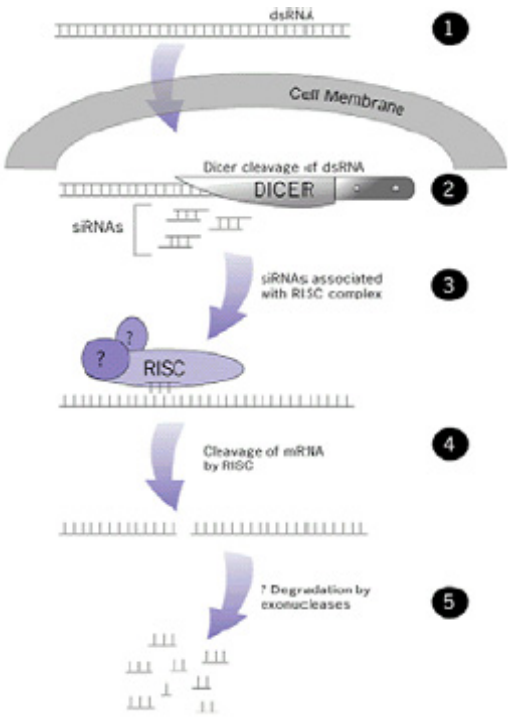

Figure 12: Model for RNAi in *Drosophila*

1. dsRNA is introduced in the cell. 2. DICER digests dsRNA in ~ 21 bp dsRNA. 3. The siRNAs are integrated into RISC complex. 4. The siRNAs undergo strand separation the antisense strand then binds to its complementary/target RNA.
5. Nucleases within the RISC degraded the targeted mRNA

Intracellular transcription of small RNA molecule can be achieved by cloning the siRNA templates into RNA polymerize III transcription units, which normally encode the smaller nuclear RNA (snRNA) U6 or the human RNAse P RNA H1. Two approaches have been developed for expressing siRNA (Figure 13): in the first, sense and antisense strands constituting the siRNA duplex are transcribed by individual promoters (Lee, N.S. et al. *Nat. Biotechnol.* **20**: 500-505, 2002; Miyagishi M. & Taira K., *Nat. Biotechnol.* **20**: 497-500, 2002); in the second, siRNAs are expressed as fold back stem-loop structures that are processed into the siRNAs. (Brummelkamp TR et al., *Science* **296(5567)**: 550-553, 2002; Paul CP et al., *Nat. Biotechnol.* **20**: 505-508, 2002; Paddison PJ. et al. Genes & Dev. **16 (8)**: 948-958, 2002). U6 and H1 promoters are members of the type III class of polymerize III promoters. U6 and H1 are different in size but contain the same conserved sequence elements or protein binding sites (Myslinski, E. et al. *Nucleic Acid Res.* **29**: 2502-2509)

The +1 nucleotide of the U6-like promoters is always guanosine, whereas the +1 for H1 promoters is adenosine. The termination signal for these promoters is defined by 5 thymidines, and the transcript is typically cleaved after the second uridine. Cleavage at this position generates a 3' UU overhang in the expressed siRNA, which is similar to the 3' overhangs of synthetic siRNAs. Any insert sequence shorter than 400 nucleotides can be transcribed by this promoter; therefore they are ideally suited to the expression of ~21-nucleotide siRNAs of ~50-nucleotide RNA stem-loops.

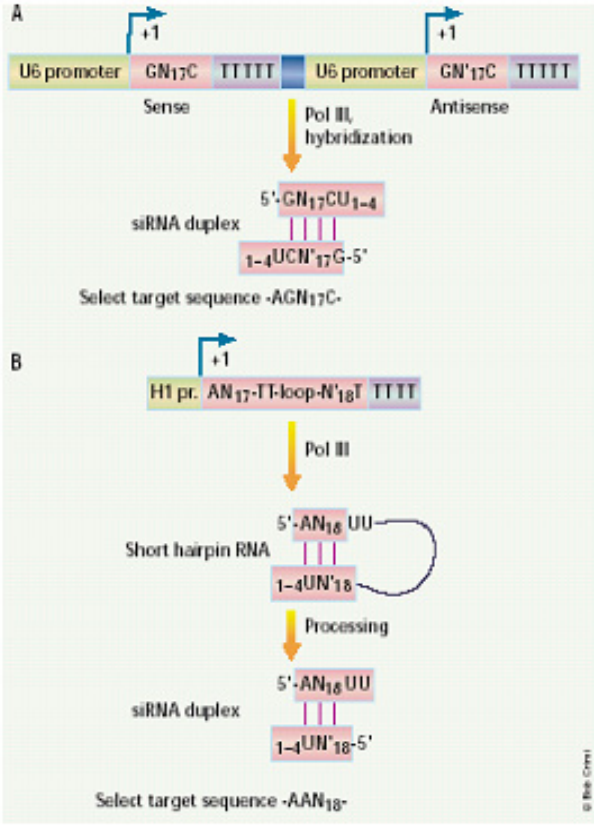

Figure 13: Endogenous expression of small hairpin forming siRNA:

A. Expression cassette for sense and antisense using the U6 snRNA promoter. The 250 bp U6 snRNA promoter is illustrated as a yellow box, the Pol III terminator signal composed for a run of thymidines is shown as a light purple box, and the spacer between sense and antisense (indicate with a prime symbol) expression element is shown as a blue box. The siRNA is highlighted in pink.
B. H1-based Pol III cassette for expressing hairpin RNAs that are subsequently processed to siRNAs. The H1 RNA Pol III promoter is only 100 bp in size, but contains all the essential sequence motifs present in the U6 snRNA promoter (Tuschl T., *Nat. Biotech.*, **20(5)**:446-, 2002).

3.2.10.2 HP GenomeWide siRNAs

HP GenomeWide siRNAs were purchaised from Qiagen and contain sense and antisense small RNA sequences to form a short hairpin RNA for the downregulation of any desired gene. Therefore it goes the pathway described in Figure 13A.

Prior to transfection they were prepared in order to the manufacturer's protocol: siRNA Suspension Buffer was added to the lyophilized siRNA to obtain a 20 µM solution (5 nmol/tube in 250 µl or 20 nmol/tube in 1 ml). The tube was heated to 90°C for 1 minute and incubated at 37°C for 60 minutes afterwards. siRNA was divided in 30 µl volume portions and stored at –20°C to keep it stable till use of transfection.

HP GenomeWide siRNAs are predesigned siRNAs which are available for every gene of the human, mouse, and rat genomes. These siRNAs were designed using cutting-edge HP OnGuard siRNA Design ensuring high potency and specificity (http://www1.qiagen.com/Products/GeneSilencing/HPOnGuardsiRNADesign.aspx.).

siRNA design is then checked for homology to all other sequences of the genome using an up-to-date, nonredundant sequence database and a proprietary homology analysis tool which incorporates exciting features. However, most available siRNAs have not been validated. Therefore all siRNAs, used in this work (Table 4), were verified in real-time RT-PCR experiments.

Accession Number	Definition	Product Name	Catalog Number	Target Sequence	Sense	Antisense
NM_005683 (GPR_55)	Homo sapiens G protein-coupled receptor 55	Hs_GPR55_5_HP siRNA	SI02635717	CCG GTT CTT GGC CAT CCG TTA	r(GGU UGU UGG CCA UCC GUU A)dTdT	r(UAA CGG AUG GCC AAG AAC C)dGdG
NM_015470 (Gaf1) (RAB11FIP5)	Homo sapiens RAB11 family interacting protein 5	Hs_RAB11FIP5_2_HP siRNA	SI00697214	CAG GGA CAA GAT GAA GGG CAA	r(GGG ACA AGA UGA AGG GCA A)dTdT	R(UUG CCC UUC AUC UUG UCC C)dTdG
NM_001033566 (RHOT1) (MIRO1)	Homo sapiens ras homolog gene family, member T1	HS_RHOT1_1_HP siRNA	SI00702975	CTG CAT GAA GTT AAA CAA GAA	r(GCA UGA AGU UAA ACA AGA A)dTdT	r(UUC UUG UUU AAC UUC AUG C)dAdG
NM_003355 (UCP2)	Homo sapiens uncoupling protein 2 (mitochondrial proton carrier)	Hs_UCP2_5_HP siRNA	SI03082898	AAG CAC CGT CAA TGC CTA CAA	r(GCA CCG UGA AUG CCU ACA A)dTdT	r(UUG UAG GCA UUG ACG GUG C)dTdT
		Hs_UCP2_6_HP siRNA	SI03032729	CCT GTT ACA GAT CCA AGG AGA	r(GGU UAC AGA UCC AAG GAG A)dTdT	r(UCU CCU UGG AUC UGU AAC C)dGdG
-	-	AllStars Neg. Control siRNA	1027281	-	Proprietary	Proprietary

Table 4: HP GenomeWide siRNA list

3.2.10.3 Vector containing siRNAs

SYK was downregulated with the GeneSuppressor™ System of IMGENEX and BMX was knocked down with the siRNA vector constructed by Zoratti C. using siRNA primers chosen at position 1482 bp of cDNA. Additionally scrambled siRNA containing vectors for SYK or BMX respectively were used as their negative controls.
Thus, these siRNA were expressed as fold back stem loop structures and they go the pathway described in Figure 13B. Since these siRNA derived from a vector, the conventional transfection protocol for plasmids (3.1.1) was performed.

Accession Number	Definition	Vector	Target Sequence	Primer for	Primer rev
NM_203281 (BMX)	Homo sapiens BMX non-receptor tyrosine kinase (BMX)	BMX1482 + mtDSRed in pBudCE4.1	Self-made (Zoratti)	-5' TCG ATG GCT GCT TGC TGA ATT ACC TGA GTC GTC GAG GTA ATT CAG CAA GCA GCC ATT TTT 3'	-5' CTA GAA AAA TGG CTG CTT GCT GAA TTA CCT CGA CGA CTC AGG TAA TTC AGC AAG CAG CCA 3'
		(BMX751 + mtDSRed in pBudCE4.1)	Self-made (Zoratti)	-	-
NM_003177 (SYK)	Homo sapiens spleen tyrosine kinase (SYK)	SYK siRNA plasmid (IMG-808-1)	GeneSuppressor™ System of IMGENEX	-	-
		negative control plasmid (IMG-800-6)		-	-

Table 5: Vector containing siRNA list

3.2.11 Real-time RT-PCR

The real-time RT-PCR technology was used to define the RNA-degrading capacity of a distinct gene by its siRNA.

3.2.11.1 LightCycler 480 Instrument (Roche)

The LightCycler instrument basically consists of two different components: a cycler component and a fluorimeter component. The thermal chamber is directly connected to the optical system of the fluorimeter. The homogeneous, 470 nm light beam (excitation) is subsequently focused onto the individual wells of a 96 well plate and hence onto the samples to be measured. The detection channel within the LightCycler fluorimeter is equipped with a filter. This permit analyzes at certain emission wavelengths, which allow exact measurements of emission from a distinct fluorophore.

3.2.11.2 QuantiFast™ SYBR Green PCR Master Mix

SYBR Green I is a dye that binds specifically to double-stranded DNA. Its inherent fluorescence is enhanced when it binds to the minor groove of double-stranded DNA. During PCR, SYBR Green I binds to DNA products as soon as they are synthesized. Thus, the increase in SYBR Green I fluorescence, when measured at the end of each elongation cycle, indicates the amount of PCR product formed during that cycle. Dye staining can detect from approximately 1 to 10^9 copies of a target sequence. The maximum excitation of SYBR Green I dye occurs at 497 nm. Maximal emission of DNA stained with SYBR Green I occurs at 521 nm.

The components of QuantiFast™ SYBR Green PCR Master Mix include HotStartTaq *Plus* DNA Polymerase, QuantiFast SYBR Green PCR Buffer, SYBR Green I, and ROX passive reference dye.

3.2.11.3 Primers for real-time RT-PCR

For the amplification of the specific genes QuantiTect® Primer Assays for (Qiagen Corp.) were inserted in the RT-PCR reaction.

QuantiTect® Primer Assays are validated genomewide primer sets that provide highly specific and sensitive results in SYBR Green based real-time RT-PCR. The assays are ideal for gene expression analysis applications, such as validation of RNAi or microarray results.

To reconstitute 10x QuantiTect Primer Assay, it was dissolved in 1.1 ml H_2O and portionized in aliquots to avoid repeated freezing and thawing. The Primer Assay for GAPDH was used for the amplification of human Glyceraldehyde-3-phosphate dehydrogenase in all RT-PCR experiments acting as a housekeeping gene.

Assay Name	Gene Symbol	Catalog Nr	Length of detected transcript	Amplicon lenght
Hs_GAPDH_2_SG	GAPDH	QT01192646	1310 bp	119 bp
Hs_GPR55_1_SG	GPR55	QT00019124	2629 bp	94 bp
Hs_RAB11FIP5_1_SG	RAB11FIP5 = Gaf1	QT00006755	4362 bp	134 bp
Hs_UCP2_1_SG	UCP2	QT00014140	1646 bp	114 bp
Hs_BMX_1_SG	BMX	QT00071015	2514 bp	95 bp
Hs_SYK_1_SG	SYK	QT00050043	2672 bp	83 bp

Table 6: QuantiTect® Primer Assays

3.2.11.4 Preparation of samples

Cells were grown on 6 cm dishes (~10^6 cells) and transfected according to 3.1.2, one dish transfected with 10 µl negative control siRNA and the other dish(es) with 10 µM of the respective siRNA(s), whichhas to be tested for its potency to downregulate a specific gene. 42 hours after transfection cells were harvested and the RNA was isolated from the various dishes (3.2.1). Usually 3 µg of each RNA sample was subsequently reverse transcribed to cDNA (3.2.3.4). To quantify specific genes in cDNA samples with the LightCycler instrument it was necessary to make a pool containing an appropriate amount of cDNA from the various samples. Thereafter different dilutions of each cDNA sample were made, dilutions 1:10, 1:100 and 1:1000 from the pool and dilutions 1:50 from the negative control and siRNA samples. The pools were used to generate standard curves to calculate the PCR efficiency. The generated amplificons were measured in the siRNA (1:50) as well as in their negative control samples (1:50) in threefold measurements during one RT-PCR experiment. This experiment was repeated for three times. The out coming data from the LightCycler instrument represented the crossing point of each amplicon. Thus, the efficiency of the active siRNAs was identified by higher crossing points in comparison to their negative controls. That means the amplification in siRNA samples start at a later point of time.

3.2.11.5 Reaction Setup

- Each well of the 96 well plate was filled with 2 µl of cDNA sample
- 5 µl QuantiFast™ SYBR Green PCR Master Mix, 1 µl QuantiTect® Primer Assay and 2 µl RNase free water were added from a master mix.
- After a brief centrifugation step at 1,000 rpm for 10 sec the LightCycler instrument was loaded with a 96 well plate.

3.2.11.6 Real-Time Cycler Conditions: Two-step RT-PCR

Step	Time	Temperature
PCR initial activation step	15 min	95°C
Two-step cycling		
Denaturation	10 s	95°C
Combined annealing/extension	30 s	60°C
Number of cycles	40	

Table 7: Real-Time PCR Cycling Conditions

3.2.11.7 Analysis of quantitative RT-PCR

The out coming crossing points of the particular PCR-reactions were analyzed by the REST software version 384® (Relative Expression Software Tool), which was downloaded from http://rest.gene-quantification.info/.
Accordingly, the downregulation of the gene in its siRNA samples was calculated and plotted in percentage to their negative controls.

3.3 Proteomic Procedures

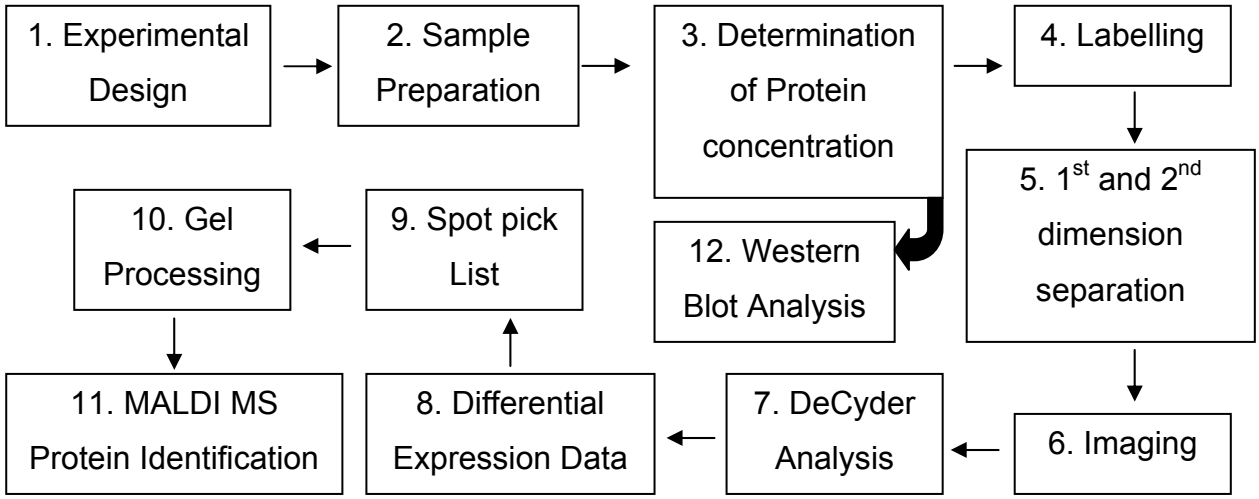

Figure 14: Overview of the Proteomic Workflow

3.3.1 Experimental Design

Two different procedures have been performed to determine interorganelle protein compositions upon histamine treatment in comparison to untreated cells. First to detect any proteins, that might have been attached to the plasma membrane or that have been changed in their abundance upon histamine stimulation (sucrose gradient centrifugation, 3.3.1.3); second to detect protein migrations within nucleus and membranes after histamine stimulation (speed sedimentation, 3.3.1.4).

3.3.1.1 Cell treatment

Ea.hy926 cells were grown on 10 cm dishes and washed twice with 5 ml Hanks buffered salt solution (HBSS) without phenol red (Sigma) prior to treatment. 10 dishes (~10^8 cells) were treated with 5 ml of CB (Table 14) containing 100 µM Histamine for 5 min to stimulate cells, while another 10 dishes remained untreated in CB representing control cells. Cells from both conditions were then scraped from the dishes with a rubber policeman using ice cold 200 µl of HBSS for each and separately combined.
Ea.hy926 cells of both conditions were then isolated in ice cold 200 µl HBSS using a rubber policeman. From the first step of isolating cells until the fractionation, all procedures have been performed at maximum 4°C.

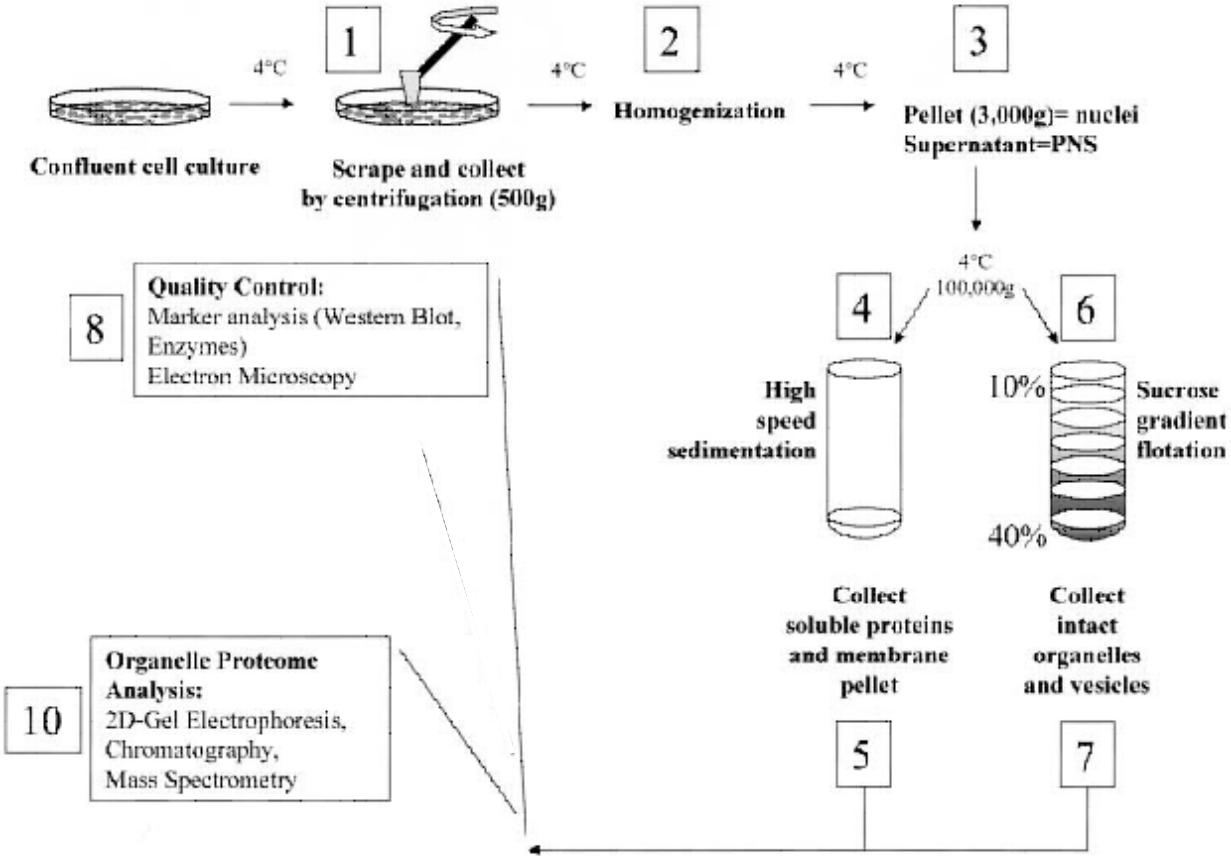

Figure 15: Schematic outline of the stepwise preparation and analysis of subcellular fractions as discussed in the text (Huber A. et al., *Circ Res*. **92**, 962-968,2003.)

3.3.1.2 Cell disruption (Homogenization)

Prior to homogenization the harvested cell suspensions were centrifuged at 200 x g for 5 minutes at 4°C. The supernatants were discarded and the cell pellets were suspended in ten volumes of cold 5 mM Tris HCl pH 8.0, 75 mM sucrose and incubated at 4°C for 15 minutes. The hypotonic buffer causes the Ea.hy926 cells to swell but not to lyse. Immediately after homogenization, 0.25 volume of compensating buffer (0.95 M sucrose, 20 mM Tris HCl, pH 7.4, 26 mM $MgCl_2$, 1.5 mM EDTA, 5 mM DTT, 0.15 M NaCl, 0.15 M KCl) was added.Treated and untreated cells were homogenized by sonication. The two cell suspensions were subjected to 3 treatments of 15 seconds with a sonication rod chilling the suspensions on ice after each of the three sonication steps for one minute.

3.3.1.3 Isolation of Plasma Membrane Proteins

The plasma membrane enriched fractions were separated by Sucrose gradient centrifugation (Figure 15, Step 6) according to a modified procedure described by

Remold-O´Donell, *Preparative Biochemistry*, **7(6)**: 441-455, 1977. In brief, the lysed cell suspension was transferred to a graduated cylinder. By adding 1.28 volume of concentrated sucrose solution (2.30M sucrose, 10 mM Tris HCl pH 7.6, 5.3 mM $MgCl_2$, 0.3 mM EDTA, 1 mM DTT, 30 mM NaCl, 30 mM KCl) the sucrose concentration of the homogenate was brought to 40.5 % (a solution less dense than nuclei, lysosomes and mitochondria, but more dense than membranes). Using a syringe with a long needle, this homogenate was introduced under preformed sucrose gradients in 11 ml cellulose nitrate swinging bucket centrifuge tube. The gradients were performed from 3.1 ml each of 40.0 and 34.0 w/w % sucrose solutions which had been made by addition to solid sucrose of 10 mM Tris HCl, pH 7.6, 5.3 mM $MgCl_2$, 0.3 mM EDTA, 1 mM DTT, 30 mM NaCl, 30 mM KCl. The tube was filled by layering 20 % sucrose in the same buffer on the top of the gradients. Then it was centrifuged in a Beckman ultracentrifuge at 40,000 rpm for 6 hours at 4°C using a SW 40 Ti rotor (Beckman Instruments). In these experiments the plasma membrane was found as a single band in the gradient at a sucrose concentration of 33.5 % (density = 1.14). Fractions of 500 µl (usually 18-21) were collected from the top of the tube using an arcuated needle to obtain each fraction from the surface area. For later use the fractions were stored at -70°C. Plasma membrane enriched fractions were detected by Western Blot analysis (3.3.12) using antibodies against Caveolin 1 or Scavenger Receptor Class B1 (SRB1) as PM marker proteins.

3.3.1.4 Separation to Membrane, Nucleic and Cytosolic Fractions

This protocol allowed fractionation of cells into three major constituents, membranes, cytosol, and nuclei. Nuclei pellets were collected from the first low-speed centrifugation step (Figure 15, Step 3). The postnuclear supernatant (PNS) obtained was additionally fractionated by high-speed sedimentation/centrifugation (100,000 x *g*), which separated the total membrane fraction from all soluble proteins (Figure 15, Step 4). Membrane and Nucleic fractions were further prepared for 2D-electrophoresis.

3.3.2 Sample Preparation

Pre-treatment of samples for 2D PAGE involved precipitation, solubilization, denaturation and reduction to completely break up the interactions between the proteins.

3.3.2.1 Protein Precipitation

Precipitation of protein samples was done to deionize and concentrate the protein samples according to the method of Wessel D. and Fluegge UI. using methanol and chloroform (Wessel D. et al., *Anal. Biochem.* **138**, 141-143, 1984). Briefly, an appropriate number of Eppendorf tubes (usually 10) were filled with 150 µl of sample in aquous solution at room temperature. 4 volumes of MeOH (600 µl) and 1 volume of $CHCl_3$ (150 µl) were added, vortexed, and checked that there is only one phase. Thereafter 3 volumes of H_2O (450 µl) were added and thoroughly vortexed. Then the tubes were centrifuged in an Eppendorf table centrifuge at full speed (16,000 x g) for 1 min and the upper organic phase was removed with a drawn out pasteur pipet without disturbing the interphase (contains the proteins). Another 3 volumes of MeOH (450 µl) were added, vortexed and spun down for 2 min at full speed. The supernatant was again removed with the Pasteur pipet and the pellet was air dried, but not completely to allow a better dissolving (3.3.2.2).

3.3.2.2 Solubilization of Proteins

The most widely used solubilization procedure is that based on O'Farrell PH., *J. Biol. Chem.* **250**, 4007-4021, 1975 using a mixture of 2 % NP-40, 9 M urea, 1 % DTT and 0.8 % carrier ampholytes (Pharmalyte pH 3-10). Instead of NP-40, the zwitterionic detergent CHAPS was used (Lysis buffer).

The two different protein samples deriving from treated and untreated cells were solubilized after the protein precipitation step. Each protein precipitate was dissolved in 10 µl of Lysis Buffer and combined to a total volume of 100 µl (in case of 10 precipitates). According to that 100 µl protein extract of the untreated and 100 µl of treated condition were generated.

3.3.3 Determination of Protein Concentration

Protein concentrations derived from the various fractions were determined using the Protein Assay Dye Reagent Concentrate from Bio-Rad, which is based on the Bradford assay (Bradford M., *Anal. Biochem.*, **72**: 248,1976), according to the Microassay Procedure. The Bio-Rad Protein Assay is a dye-binding assay, in which a differential color change of a dye occurs in response to various concentrations of protein resulting in an anionic (bound) form with an absorbance maximum at 595 nm (blue) and a cationic (unbound) form with an absorbance maximum at 470 nm (red). According to

that, the increase of absorbance 595 nm is proportional to the amount of protein, which had been bound on the dye. Different concentrations of Bovine Serum Albumin (BSA; 0.1, 0.2, 0.5, 1 mg/ml) were used to generate a standard curve for calibration to calculate the protein amounts in the various samples. The protein extract was then equilibrated by diluting the higher amount sample to the concentration of the lower.

3.3.4 Labeling

From the beginning of Labeling (Figure 14, Step 4) until the end of Gel processing (Figure 14, Step 10) all procedures have been performed according to the Ettan™ DIGE (Difference Gel Electrophoresis) technology, that was developed by GE Healthcare, formerly Amersham. The Ettan™ DIGE comprises a system of DIGE dyes, Typhoon™ 9400 scanner and DeCyder™ image analysis software and is based on a prelabeling method of protein samples prior to 2D-Electrophoresis for differential analysis.

3.3.4.1 Principle of Labeling using CyDye DIGE

The CyDye DIGE fluors are 3 spectrally resolvable CyDye fluors (Cy2™, Cy3™ and Cy5™) matched for mass and charge. That means that the same protein labeled with any of the CyDye DIGE fluors, will migrate to the same position on the 2–D gel. This eliminates intra-gel variation. The dyes have great sensitivity with detection of 125 pg from a single protein and a linear response in protein concentration over at least five orders of magnitude (10^5). CyDye DIGE fluors contain a NHS ester reactive group, and are designed to covalently bond to the epsilon amino group of lysine of proteins via an amide linkage. The fluors are added to the proteins so that the fluors are limiting within the reaction. This ensures that the fluors label approximately 1–2 % of lysine residues. Therefore the CyDye DIGE fluors are just labeling a small proportion of the total protein in a sample. For that reason, this type of labeling has been called minimal labeling. The lysine amino acid in proteins carries an intrinsic +1 charge at neutral or acidic pHs. CyDye DIGE fluors also carry a +1 charge which, when coupled to the lysine, replaces the lysine's +1 charge with its own, ensuring that the pI of the protein does not significantly alter. CyDye DIGE fluors when coupled to the protein add approximately 500 Da to the protein's mass. This mass shift is not routinely visible.

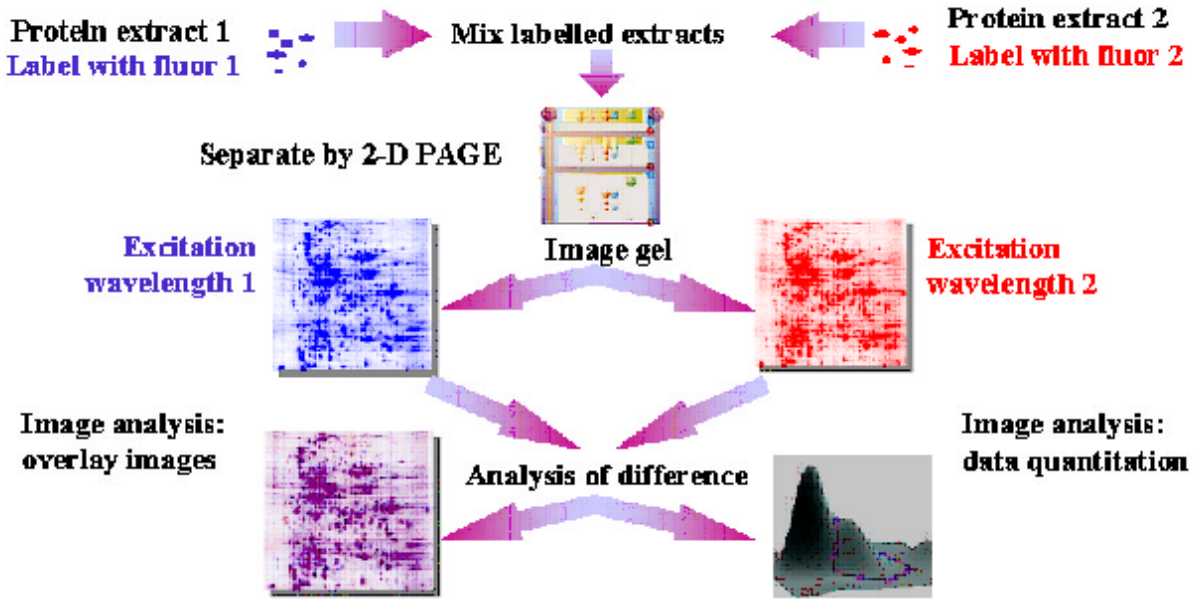

Figure 16: Outline of the basic Ettan DIGE Technology
(Images for Figures 6-13 taken from: Ettan DIGE User Manual 18-1164-40 Edition AA, Amersham Bioscience)

3.3.4.2 Protocol for labeling a sample with a Cy DIGE flour

- Add 0.4 µl (400pmol) of a Cy DIGE flour to the protein extract – 75 µl for each
  (Cy3 was used for the untreated, Cy5 for the treated protein extract)
- Centrifuge at 13,000 rpm for 1 minute and incubate 30 minutes on ice
- Add 1 µl of 10 mM Lysine and incubate another 10 minutes on ice
- After addition of 1.0 volume (75 µl) 2x Lysis buffer, labeling is completed.

Lysis buffer: 9 M urea, 2 % (w/v) CHAPS, 0.8 % (w/v) Pharmalyte pH 3-10, 1 % (w/v) dithiothreitol (DTT) and 5 mM Pefabloc

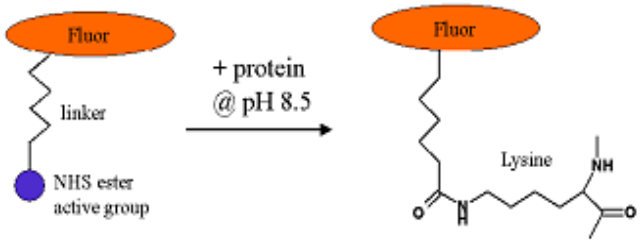

Figure 17: Schematic of labeling reaction
CyDye DIGE fluor containing NHS ester active group covalently binds to lysine residue of protein via an amide linkage.

Thereafter the two labeled protein extracts were mixed to a total volume of 300 µl.

3.3.5 2D-Electrophoresis: 1st and 2nd dimension separation

Two-dimensional electrophoresis (2D-electrophoresis) is a powerful and widely used method for the analysis of complex protein mixtures extracted from cells, tissues or other biological samples. This technique sorts proteins according to two independent properties in two discrete steps: The first-dimension step, isoelectric focusing (IEF), separates proteins according to their isoelectric points (pI); the second-dimension step,

SDS-polyacrylamide gel electrophoresis (SDS-PAGE), separates proteins according to their molecular weights (MW). Each spot on the resulting two-dimensional array correspond to a single protein species in the sample. Thousands of different proteins can thus be separated, and information such as the protein pI, the apparent molecular weight and the amount of each protein can be obtained.

3.3.5.1 Isoelectric Focusing: 1st dimension

3.3.5.1.1 Principle of IEF

Inter-laboratory comparisons of 2 D-electrophoresis had been achieved for the first time by the development of immobilized pH gradients (IPG) in 1982, based on the use of bifunctional Immobiline® reagents, a series of ten chemically well defined acrylamide derivatives with general structure CH_2=CH-CO-NH-R, where R contains either a carboxyl or a (tertiary) amino group. These form a series of buffers with different pK values between pK 1 and 13. Since the reactive end is c-polymerized with the acrylamide matrix, extremely stable pH gradients are generated, allowing true steady-state IEF with increased reproducibility. IPGs can be cast in different pH ranges between pH 2.5 and pH 12, as well as in different lengths, usually from 7-24 cm. Accordingly, GE Healthcare offers a large number of IPG strips differing in their pH.

For fast and efficient screening to gain a broad overview of total protein distribution Immobiline DryStrips pH 3-10 NL, 24 cm were purchased. IPG-IEF for 2D electrophoresis can be simplified by the use of an integrated instrument, the Ettan IPG*phor* (Figure 18). The IPG*phor* (Islam R. et al., *Science Tools* **3**: 14-15, 1998) includes a Peltier element for temperature control (between 18°C and 25°C) and a programmable power supply (8000V, 1.5 mA). The central part of this instrument are so-called strip holders made from an aluminium oxide ceramic (Figure 19), in which IPG strip rehydration with sample solution and IEF are performed.

Figure 18: Ettan IPG*phor* Instrument

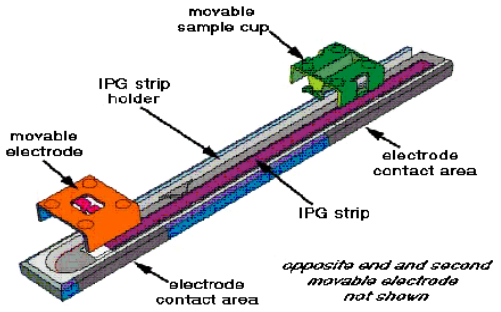

Figure 19: Cup Loading strip holder

3.3.5.1.2 Rehydration of IPG DryStrips

Prior to Isoelectric Focusing (IEF), IPG DryStrips were placed in strip holders to get rehydrated at least for 10 hours (usually overnight, 16-18 hours) to their original thickness of 0.5 mm using a rehydration solution containing 7 M urea, 2 M thiourea, 1 % CHAPS, 0.4 % DTT, 0.5 % v/v Pharmalyte 3-10 and 0.002 % BPB. Therefore, the mixture of the two labeled protein samples was mixed with the rehydration solution (dilution: 1:1 for micropreparative runs) and applied by in-gel rehydration (Rabilloud T. et al., *Electrophoresis* **15**: 1552-1558, 1994; Sanchez JC. et al., *Electrophoresis* **18**: 324-327, 1997) to a final volume of 600 µl. These were pipetted evenly along each 240 mm long IPG strip and covered with 3 ml IPG DryStrip Cover Fluid® (Amersham) to prevent them of running dry. The strip holders were then placed in the IPG*phor* and the electrodes were positioned and pressed down gently on top and bottom of the strip holders (Figure 19). Low voltage (30 V) was applied during the rehydration step for improved sample entry of high Mr proteins into the polyacrylamide gel which otherwise can be a problem with sample in-gel rehydration.

3.3.5.1.3 Procedure of IEF

Running conditions for the IEF depend on the pH gradient and the length of the IPG strips. In case of using Immobiline DryStrips pH 3-10 NL, 24 cm, Table 8 gives an appropriate time schedule to program the IPG*phor* for running an IEF (Görg A. et al., *Electrophoresis* **21**: 1037-1053, 2000). Furthermore, the IPG*phor* was set up to a max. current of 0.05 mA and a max. power of 0.2 W per strip. Optimum focusing temperature was set to 20°C (Görg A. et al., *Electrophoresis* **12**: 653-658, 1991.

Protocol	**Voltage (V)**	**Time (h)**	**Voltage hours (Vh)**	**Total Vh (tVh)**
Step-n-hold	150	3	450	450
Step-n-hold	300	3	900	1350
Step-n-hold	600	3	1800	3150
Gradient	600 → 8000	3	12900	16050
Step-n-hold	8000	~ 4	~ 32000	~ 48000

Table 8: IPGphor-Program for running the IEF

3.3.5.2 IPG strip equilibration

To diminish endoosmotic effects and to guarantee a better transfer of proteins from the IPG-strip into the SDS-gel, the strips have to be equilibrated between the 1st and 2nd dimension.

3.3.5.2.1 Principle and Materials for IPG strip equilibration

The IPG gel strips were equilibrated twice, each time for 15 min in 2x10 ml equilibration buffer 6 M urea, 30 % (w/v) glycerol and 2 % (w/v) SDS in 0.05 M Tris-HCl buffer, pH 8.8 (Laemmli UK. et al., *Nature* **227**: 680-685, 1970). The equilibration buffer contains 6 M urea and 30 % glycerol in order to diminish electroendosmotic effects (Görg A. et al., *Electrophoresis* **9**: 531-546, 1988) which are held responsible for reduced protein transfer from the first to the second dimension. During the 2nd equilibration step, 260 mM iodoacetamide (Amersham) is added to the equilibration buffer in order to remove excess DTT (responsible for the 'point streaking' in silver stained patterns) (Görg A. et al., *Electrophoresis* **8**: 122-124, 1987).

3.3.5.2.2 Procedure for IPG strip equilibration

1. 100 mg of DTT were dissolved in 10 ml of equilibration buffer (= equilibration buffer I). The focused IPG strips were shaken for 15 min in this buffer.
2. For the second equilibration step 400 mg of iodoacetamine were dissolved in 10 ml (=equilibration buffer II) and equilibrated as above for another 15 min.

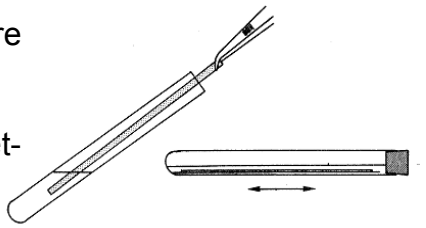

Figure 20: IPG-strip equilibration

3.3.5.3 Second Dimension

3.3.5.3.1 Principle and equipment for the SDS-PAGE

In the second dimension, the SDS-PAGE, the focused proteins were separated by their mass. Accordingly low mass proteins were able to go easier through the gel, while proteins of higher masses stay rather on top of the gel.

The SDS-PAGE gels were cast in the DALT*six* Gel Caster using low fluorescence glass plates for Ettan™ DIGE gels. The second dimension was run on a vertical system (Görg A. et al., *Electrophoresis* **16**: 1079-1086, 1995), the Ettan™ Dalt*six* electrophoresis unit consisting of a power supply, a Multitemp II thermostatic circulator for cooling and the Ettan™ DALT*six* electrophoresis chamber.

3.3.5.3.2 Casting gels

DALT*six* Gel Caster accommodates six 1.0 mm gel cassettes with separator sheets. Fewer gels can be cast by inserting blank cassettes to minimize the volume of casting solution.

The casting cassettes (gel size 200 x 250 x 1 mm³) consist of two glass plates connected by a hinge strip, and two 1.0 mm thick spacers in between them. The gel solution was mixed according to Table 9 (Laemmli UK. et al., *Nature* **227**: 680-685, 1970) and poured into the funnel of the caster, taking care to avoid introducing any air bubbles into the feed tube, until it was about 1 to 2 cm below the final desired gel height. Immediately, 2 ml of water saturated n-butanol (Roth) was pipetted onto each gel and the homogenous gels were allowed to polymerize for at least 1 hour. Then the caster was disassembled and butanol was accurately removed.

Reagents for vertical SDS gels	**Source**	**12 % T, 2,6 % C**
Acrylamide/Bisacrylamide (30.8 %T, 2.6 %C)	Sigma	89 ml
1.5M Tris (pH 8.8)	Serva	56 ml
Deionized water		75 ml
SDS solution (10 %)	Serva	2.2 ml
TEMED (added just before casting)	Sigma	111.5 µl
APS (10 %) (added just before casting)	Sigma	1.33 ml
Total volume		~ 223.5 ml

Table 9: Recipe for 12 % homogenous vertical SDS gels: (volumes for preparing 2 gels)

3.3.5.3.3 IPG strip transfer

Prior to SDS-PAGE, the equilibrated IPG strips were placed on top of the vertical SDS gels and embedded in low melting agarose (Nueve) containing 0.002 % BPB to ensure a better contact between the strip and the gel. The agarose was then allowed to solidify for at least 5 min.

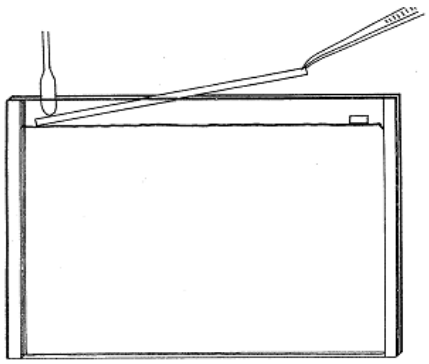

Figure 21: Loading an IPG striponto a SDS gel

3.3.5.3.4 Running the SDS-PAGE

The Ettan™ Dalt*six* tank was filled with 4 l of 1x electrophoresis buffer (Table 10) and blank cassettes were inserted into any unoccupied slots (depending on the number of gels). Then the MultiTemp II temperature controller was switched on and the gel cassettes were placed in the tank when the temperature was adjusted to the running setting of 18°C. Thereafter the upper buffer chamber was seat over the gels and filled with 2x electrophoresis buffer (Table 10). Finally the safety lid was placed on the electrophoresis unit and SDS-PAGE was started at 30 mA for about 18 h. The run was terminated when the BPB tracking dye has migrated off the lower end of the gel.

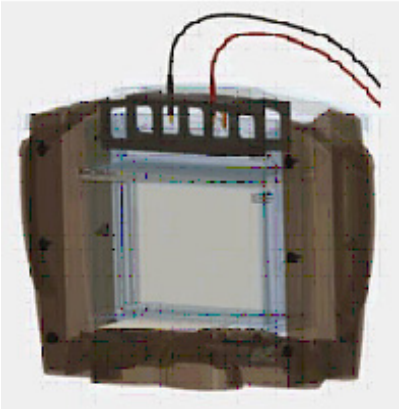

Figure 22: Ettan™ Dalt*six* instrument

10x SDS electrophoresis buffer (Storage solution)		**Dilution in Ettan DALT*six* (to use): Lower anode chamber (1x buffer):**	**Dilution in Ettan DALT*six* (to use): Upper cathode chamber (2x buffer)**
Tris (Serva)	60.5 g	Dilute 450 ml 10x SDS electrophoresis buffer with MilliQ-water to a final volume of **4.5 l**	Dilute 200 ml 10x SDS electrophoresis buffer with MilliQ-water to a final volume of **1 l**
Glycine (Merck)	288.0 g		
SDS (Serva)	20.0 g		
MilliQ-water	to **2 l**		

Table 10: Recipes for electrophoresis buffers
Laemmli buffer system (Laemmli, UK. Et al., *Nature* **227**: 680-685, 1970)

3.3.6 Imaging

The gels in the glass cassettes were directly scanned after second dimension using a Typhoon 9400 scanner (Amersham Biosciences) to ensure that all gels have the same dimensions; doing so simplifies spot matching of different gels. The exterior of the glass plates must be carefully cleaned with deionized water and dried with a lint free laboratory wipe before gel cassette is positioned on the scanner in the right direction (23 Figure).

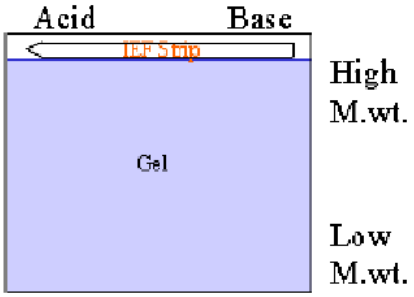

Figure 23: Orientation of a 2D-gel

Each flourescent dye was consecutively excited to avoid fluorescence crosstalk and scanned at resolution of at least 200 µm with the proper filter (Table 11). The two out coming images of protein distribution deriving from the different fluorescent labeling of treated and untreated sample were subsequently analyzed with the DeCyder Software.

Dye	Sample	Abs. Max.	Fluoresc. Max.	λ(Lasers)	Emission Filter
Cy3	untreated	553 nm	569 nm	532 nm	580 nm, band pass 40
Cy5	treated	645 nm	664 nm	633 nm	670 nm, band pass 40

Table 11: Emission filters and laser combinations for detecting Cy flours

3.3.7 DeCyder Analysis

DeCyder Differential Analysis Software DIA processes images from a single gel, performing spot detection and quantification. The DIA module algorithms detect spots on a cumulative image derived from merging up to three individual images from an in-gel linked image set. This co-detection ensures that all spots are represented in all images processed. The DIA module algorithms then quantify spot protein abundance for each image and express these values as a ratio there by indicating changes in expression levels by direct comparison of corresponding spots.

DeCyder Differential Analysis Software DIA graphical user interface is divided into four equally sized inter-linked views. All four views are linked, therefore selecting a spot in, for example the Image View, will display the spot in the Histogram View (in magenta), the 3-D View and the Table View (Figure 24).

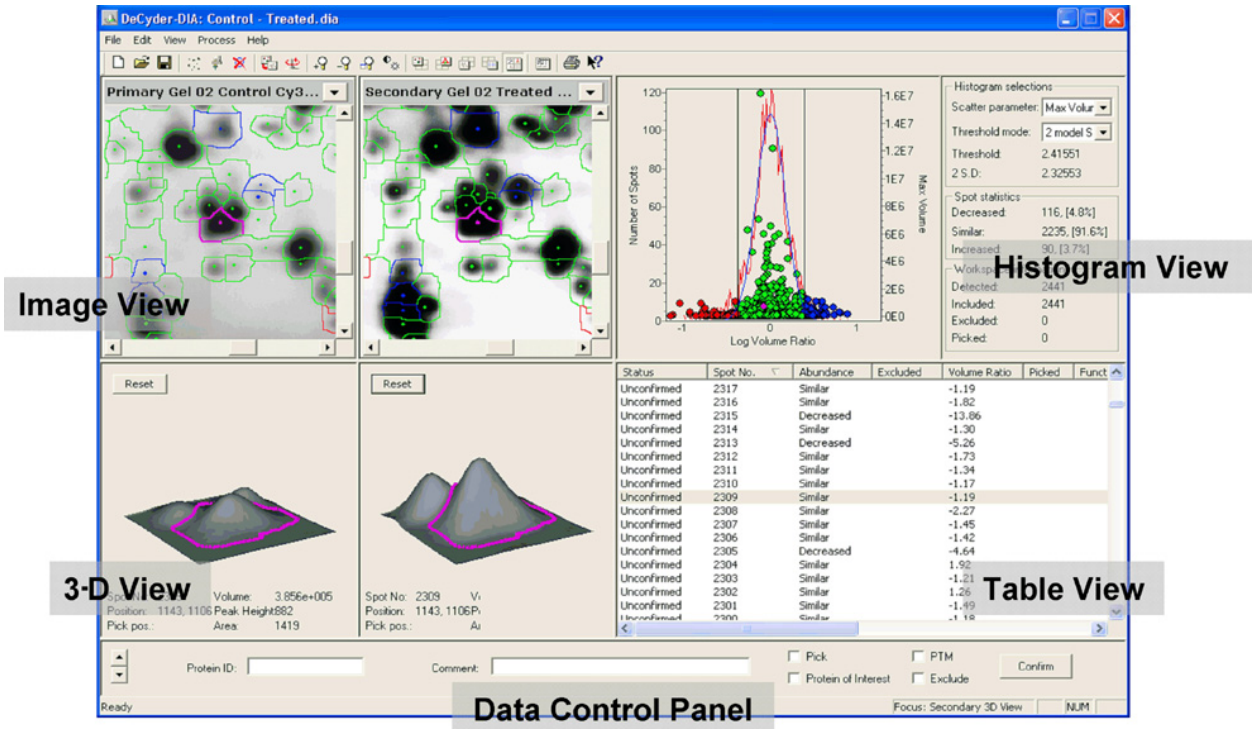

Figure 24: DIA Graphical User Interface

- **Image View:** primary and secondary gel images
- **3-D View:** a three dimensional representation of the gel localized on the spot
- **Histogram View:** graphical representation of data associated with the spots displayed in the image view
- **Table View:** tabulated data associated with selected spots displayed in the image view

Below the four views the **Data Control Panel** is found. This panel contains tools and user definable functions associated with the specific data displayed in each mode.

(DeCyder Differential Analysis Software, Version 5.0, User Manual, 18-1173-16 AA, Amersham Bioscience)

3.3.8 Differential Expression Data

Proteins of the treated Cy5 image, that differed in their abundance a range higher than 1.2 fold or lower than 0.8 fold in comparison to the control Cy3 image were selected and set on a list for proteins of interest.

3.3.9 Spot Picking

After the scan, the gel was released out of the glass plates and fixed in 30 % isopropyl alcohol / 10 % acetic acid for one hour at least preparing the gel for later spot picking procedure. The fixed gel was placed in a Hoefer Easy Breeze Drying Frame (Amersham) and cast with two reference markers in the middle left and right side of the gel. Thereafter it was scanned for a second time and proteins of interest were set on the picking list by the DeCyder software. Using the reference markers the spot picker was then able to pick all these proteins automatically from the gel. Each picked gel slice containing the individual protein was put into a Protein LoBind tube (Eppendorf), in which Gel Processing (3.3.10) took place.

3.3.10 Gel Processing

Proteins separated by SDS-PAGE for identification by mass spectrometry needs to be digested before analysis (usually with trypsin). However, as it is difficult to extract intact proteins from the polyacrylamide gel, the digestion of the protein was done within the gel (*in situ*). The generated peptides are usually < 3000 Da and these readily diffuse out of the gel (Shevchenko A. et al., *Anal. Chem.* **68**: 850-858, 1996). Accordingly the tryptic in-gel digestion took place in the Protein LoBind tubes (Sigma) and was performed using the solutions listed in Table 12 as follows:

3.3.10.1 Tryptic in-gel digestion

1. Add approximately 50 µl ACN (Sigma) / H_2O (1:1). Incubate for 15 min at RT. Remove and discard the fluid. Repeat this step.
2. Add 50 µl of 100 % ACN and leave to incubate for 15 min at RT. Remove and discard the ACN. The gel pieces will appear white and are dehydrated now.
3. Add 50 µl 0.1 M NH_4HCO_3 and incubate for 15 min at RT. Do not remove fluid.
4. Add 50 µl ACN, mix, and incubate for 15 min at RT.
5. All fluid is removed and the gel pieces get vacuum-dried using a speed-vac centrifuge for ~15 min.

6. Add 10 µl of trypsin solution and incubate for 10 min until fluid has been absorbed.
7. Add 25 µl of 50 mM NH_4HCO_3 (the gel pieces should be covered completely).
8. Incubate overnight at 37°C (water bath).

3.3.10.2 Extraction of Peptides

Peptides generated by tryptic in-gel digestion were extracted from the gel slice:

9. Freeze the probes at – 20°C for 60 min to stop the enzymatic activity of trypsine
10. Evaporate the trypsin solution in an Eppendorf Vacuum Concentrator 5301
11. Add 50 µl of extraction solution onto each dried gel slice and incubate for 60 min at RT on the shaker (alternatively 20 min at 37°C) to extract the peptides from the gel.
12. Transfer the supernatant into a fresh Protein LoBind tube and repeat steps 10 and 11 for a second extraction. Combine 2nd extraction with the 1st.
13. Dry the extracts in the Eppendorf Vacuum Concentrator 5301. The dried extracts are stable at – 20°C for at least one week.

Ammonium bicarbonate NH_4HCO_3 buffer 25 mM	**Trypsin solution (keep ice cold)**	**Extraction solution**
NH_4HCO_3 (M_r=79,06) 494.13 mg	Porcine Sequencing Grade Modified Trypsin (Roche) 10-15 µg	ACN 500 µl
MilliQ-water to **250 ml**	NH_4HCO_3 buffer to **1ml**	CF_3COOH 5 µl
Adjust pH to 8.0	(freeze in aliquots at –70°C)	MilliQ-water to **1 ml**

Table 12: Solutions and buffers for Gel Processing

3.3.11 MALDI MS Protein Identification

3.3.11.1 Principle of Mass spectrometry and MALDI–TOF

The peptides generated by proteolysis of a protein represent the fingerprint of this protein (Peptide mass fingerprint). When a complex mixture of proteins is digested by e.g. trypsin, and analyzed by mass spectrometry a large number of masses will be detected. These masses represent unique peptides from the proteins present in the mixture. The masses detected are submitted to a database containing all known proteins of the relevant organism. Using specialized software, a hypothetical digest of the proteins in the database is generating the peptides of the used protease (in this case trypsin). The masses of the peptides detected by mass spectrometry are then compared to the *in silico* generated peptides. The higher the number of identified peptides representing one protein (sequence coverage) the higher is the possibility that this protein was present in the mixture analyzed.

The MALDI technique is based on an ionization approach using a nitrogen UV laser (337 nm) to generate ions from high mass, non-volatile samples such as peptides and proteins (Figure 25). The key to this technique is that in the presence of an aromatic matrix large molecules like peptides ionize instead of decomposing. A number of matrices are available to assist the analysis of both peptides and intact proteins. Although the mechanism remains uncertain, it may involve absorption of UV light by the matrix followed by transfer of this energy to the peptide, which then ionizes into the gas phase as a result of the relatively large amount of energy absorbed. To accelerate the resulting ions into a flight-tube of the mass spectrometer, the ionized peptides are subjected to a high electrical field. The peptide ions generated by MALDI are predominantly single charged and carry just one proton.

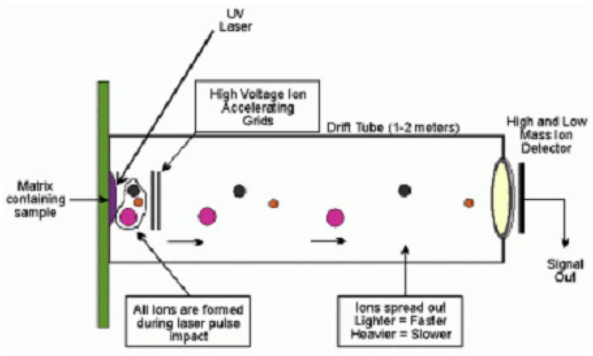

Figure 25: Schematic of MALDI

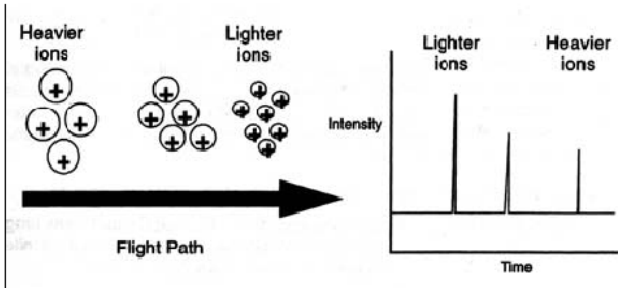

Figure 26: Time-of-Flight analysis

The mass-to-charge ratio of an ion can be measured by determining its velocity after acceleration in the electrical field. In practice this is done by accelerating an ion electrostatically to a defined kinetic energy and measuring its time-of-flight (TOF) through a field free region (no acceleration). The pulsed laser used for MALDI is an ideal technique for coupling with TOF mass spectrometry since there is a precisely defined time of ion generation. A detector positioned at the end of the field-free region determines the flight-time for each m/z. At a fixed kinetic energy, small ions travel at higher speed than large ions (Figure 26). In practice, the mass spectrometer is calibrated using peptides of known mass (Calibration Standards; 3.3.11.2.1). In this way the time-of-flight is correlated with mass.

3.3.11.2 Materials for MALDI–TOF Analysis

All regents for MALDI–TOF Analysis were taken from the ProteoMass™ Peptide & Protein MALDI-MS Calibration Kit (Sigma: MS-CAL1). For tryptic digested samples it is recommended to use α-cyano-4-hydroxycinnamic acid (CHCA) as the matrix and a

mixture of Bradykinin fragment 1-7, Angiotenesin II (human), $P_{14}R$ (synthetic peptide) and ACTH fragment 18-39 (human) as standard for calibration.

3.3.11.2.1 Preparation of Calibration Standard stock solutions

- The 0.1 % TFA solution is provided ready for use in the preparation of standard solutions, except bradykinin.
- Mix 5 ml of the 0.1 % TFA and 5 ml of ACN to give a solution of 50 % ACN in 0.05 % TFA. This solvent is used in the preparation of bradykinin.

Standard	$(M+H)^+$ Monoisotope	nmol	Solvent	Conc. of Stock
Bradykinin fragment 1-7	757.3997	10	250 µl	40 pmol/µl
Angiotensin II (human)	1,046.5423	10	250 µl	40 pmol/µl
$P_{14}R$ (synthetic peptide)	1,5433.8582	10	250 µl	40 pmol/µl
ACTH fragment 18-39	2,465.1989	10	250 µl	40 pmol/µl

Table 13: Calibration Standard Stocks for MALDI-MS

Stock solutions were stored in 5 µl aliquots at –70°C and mixed up to 10 pmol/µl on the day of MS Analysis. The resulting 20 µl mixture was then mixed with 20 µl of the CHCA-Matrix just prior the application on the MALDI-TOF target plate (Standard Mix).

3.3.11.2.2 Preparation of MALDI Matrix solution (CHCA)

10 mg of CHCA were dissolved in 1 ml of the 50 % ACN in 0.05 % TFA solution and stored in the dark. Once dissolved, it can be used for maximum one week.

3.3.11.3 Procedure

The dried peptide extracts obtained from Trypsine in-gel digestion (3.3.10) were dissolved in 3 µl 0.1 % TFA and 1 µl of each sample was applied on the spots of the target plate.

1 µl of the Matrix solution was added to each spot.

1 µl of the Standard Mix was applied directly next to the sample spot on the target plate (Calibration Spot).

Spots were dried in the dark → dried droplet.

Plate was adjusted into the MALDI-TOF system.

Calibration Spots and Sample Spots were alternately pound by the nitrogen UV laser.

Resulting Mass spectra were saved for following analysis.

3.3.11.4 Analysis of Mass spectra

Each sample mass spectrum was calibrated using its appropriate Calibration mass spectrum. Accordingly the sample mass spectrum peaks were fit applying a virtual baseline. The calibrated mass spectra of each individual sample spot were then analyzed using the MASCOT database (http://www.matrixscience.com/). In order to that, the corresponding protein for each sample mass spectrum was identified.

3.3.12 Western Blot Analysis

Western blot analysis was performed to identify plasma membrane enriched fractions (3.4.1.3). Briefly, 20 µl of each odd-numbered fraction was mixed with 40 µl of a sample buffer (10 % Glycerol, 130 mM SDS, 110 mM Tris, 6 % ME, 0.002 % BPB). The probes were applied into the slots of a stacking gel onto a 12 % SDS gel (12 % Acrylamid, 0.35 % Bis-acrylamid, 0.25 M Tris, 0.1 % SDS, 0.09 % APS, 0.05 % TEMED, pH=8.8). The first lane was loaded with a LMW (Amersham Corp.) to mark molecular weights of proteins. SDS-PAGE was run in an electrophoresis chamber (Biorad) containing 1 x SDS electrophoresis buffer (Table 10) at $U_{const.}$=130 mV until the BPB tracking dye has reached the lower end of the gel (~ 90 min). The gel was then blotted on a PVDF membrane (7 x 9 cm) in a blotting chamber (Biorad) filled with blotting buffer (10 mM Tris, 40 mM Glycine, 20 % MeOH) at $I_{const.}$=150 A for 1h. Then the blot was stained with Coomassie-blue R250 by loading the blot for 5 sec with Coomassie blue solution (0.1 % Coomassie, 40 % MeOH, 10 % acetic acid). The blot was washed with washing buffer (0.05 % Tween, 154 mM NaCl, 10 mM Tris, pH=7.4). The bands of the protein marker were signed with a pencil and the blot was destained in a Coomassie destaining solution (10 % MeOH, 20 % acetic acid) thereafter. Two different specific antibodies, for Caceolin 1 and SRB1, were used to detect plasma membrane enriched fractions. Accordingly, the blot was divided into two parts just below the 45 kDa mark. The lower blot containing the low molecular weight proteins (0-45 kDa) were analyzed with a primary antibody (Rabbit Polyclonal anti-CaveolinI; Abcam, Cambridge, U.K.) for Caveolin 1, a 22 kDa plasma membrane protein, while the upper blot containing the high molecular weight proteins (45-200 kDa) was exposed to a primary antibody (Rabbit Polyclonal anti-SR BI; Abcam, Cambridge, U.K.) for Scavanger receptor B1 (SR B1), another 82 kDa plasma membrane protein. In order to that, the blots were loaded 1:2000 with 6 µl of the anti-Caveolin 1 in 12 ml blocking buffer (washing buffer containing 5 % NFDM) and 1:1500 with anti-SR B1 antibody, respectively and shaken

overnight at 4°C. The next day the blots were washed several times with aqua dest., then transferred into another blocking solution containing 1:4000 of the secondary antibody, an anti-goat HRP, and shaken for 2 h. The PVDF membranes were again washed several times with aqua dest. and shaken in washing buffer for another 1.5 h. The blots were detected with ECL reagent for 1 min and developed in the dark on a x-ray photograph after 1 or 10 min exposure incubation.

3.4 Imaging Procedures

3.4.1 Buffers and Solutions

Frequently used buffers (Table 14) were made at room temperature and solutions were generated by adding the correct amount of any compound(s) of need (Table 15 and 16) from their stock solution(s) to obtain the right molar concentration of a working solution according to the laboratory´s recipes:

Storage-buffer (mM) (EH-Loading, SB):	2 $CaCl_2$, 138 NaCl, 1 $MgCl_2$, 5 KCl, 10 Hepes, 10 D-glucose, 2.6 $NaHCO_3$, 0.44 KH_2PO_4, 0.1 % vitamins, 0.2 % essential amino acids, 1 % penicillin/streptomycin, 1 % fungizone; pH adjusted to 7.4
Ca^{2+}-free-buffer (mM) (EGTA, EB):	1 EGTA, 138 NaCl, 1 $MgCl_2$, 5 KCl, 10 Hepes, 10 D-glucose; pH adjusted to 7.4
Ca^{2+}-buffer (mM) (2CaNa, CB):	2 $CaCl_2$, 138 NaCl, 1 $MgCl_2$, 5 KCl, 10 Hepes, 10 D-glucose; pH adjusted to 7.4

Table 14: Frequently used buffers

Substance	Source	Molecular Weight	Solvent	Conc. of Stock solution	Conc. of Working solution(s)
Histamine	Sigma	184.07	H_2O	100 mM	100, 10, 1 µM
CGP37157	Tocris	324.22	DMSO	100 mM	20 µM
BHQ	Sigma	222.33	DMSO	100 mM	15 µM
ATP	Sigma	507.20	H_2O	100 mM	10 µM
Rotenone	Sigma	394	DMSO	100 mM	50 µM
Oligomycine	Sigma	786.78	DMSO	10 mM	2 µM
Antimycine	Sigma	534.645	$EtOH_{abs}$	100 mM	10 µM
Ionomycine	Sigma	709.01	DMSO	3 mM	5 µM
Digitonin	Sigma	1229.34	H_2O	10 mM	5 µM
FCCP	Sigma	255.97	DMSO	10 mM	4 µM
Anandamide	Cayman	347.54	$EtOH_{abs}$	143.87 mM	10 µM
(= AEA)	Tocris	347.54	$EtOH_{abs}$	10 mM	10 µM
ACPA	Cayman	343.6	$EtOH_{abs}$	145.52 mM	10 µM
O-1602	Cayman	258.4	CH_3COOCH_3	38.7 mM	10 µM
LPI	Sigma	605.1	H_2O	10 mM	3 µM
SB366791	Sigma	287.74	DMSO	10 mM	10 µM
AM251	Cayman	555.20	DMSO	10 mM	10 µM
LFM-A13	Sigma	360.00	DMSO	50 mM	10 µM
U73122	Tocris	464.65	DMSO	5 mM	1, 2 µM
PP2	Tocris	301.78	DMSO	10 mM	10 µM
Wortmannin	Sigma	428.44	DMSO	2.5 mM	0.1 µM

Table 15: Compounds

Compound	Description
Histamine	Endogenous H_1 and H_2 histamine receptor agonist; H_1 activation mobilizes Ca^{2+}; activates nitric oxide synthetase; potent vasodilator. Fu LW. et al., *Am. J. Physiol.* **273(6 Pt 2)**: 2726, 1997.
CGP37157	Selective antagonist of the mitochondrial Na^+-Ca^{2+} exchanger (IC_{50} = 0.4 µM). Enhances the export of calcium from isolated mitochondria. Also reported to directely inhibit voltage-gated calcium channels. Cox et al., *J. Cardiovasc. Pharmacol.* **21**: 595, 1993.
BHQ	A selective inhibitor of endoplasmic reticulum Ca^{2+}-ATPase. Hassessian et al., *Br. J. Pharmacol.* **112**: 1118, 1994.
ATP	P_2 purinergic agonist; increases activity of Ca^{2+}-activated K^+ channels; Berger L. et al., *Biochim. Biophys. Acta* 20: 23, 1956.
Rotenone	Inhibitor of mitochondrial electron transport by inhibiting the transfer of electrons from Fe-S centers in Complex I to ubiquinone. This prevents NADH from being converted into usable cellular energy (ATP). The compound breaks down when exposed to sunlight. Fukami JI. et al., *Science* **155**: 713, 1967.
Oligomycin	Macrolide antibiotic; Inhibits respiration in mitochondria by inhibiting mitochondrial ATPase and phosphoryl group transfer. Nagamune H. et al., *Biochim. Biophys. Acta* **1141**: 231-237, 1993
Antimycin	Inhibitor of electron transfer at complex III. Induces apoptosis. Izzo G., *FEBS Lett.* **93**: 320, 1978.
Ionomycin	Ca^{2+} ionophore = mobile ion carrier for Ca^{2+}; non-fluorescent; used to study Ca^{2+} transport across biological membranes. Toeplitz BK. et al., *J. Am. Chem. Soc.* **101**: 3344, 1979.
Digitonin	Mild nonionic detergent used to solubilize receptors and permeabilize cellular and nuclear membranes. Liu J. et al., *Methods* **19**: 403, 1999.
FCCP	Very potent uncoupler of oxidative phosphorylation in mitochondria; is used to “uncouple” ATP synthesis and reduction of oxygen in oxidative phosphorylation. Heytler and Pritchard, *Biochem. Biophys. Res. Comm.* **7**: 272, 1962
Anandamide (= AEA)	Endogenous cannabinoid neurotransmitter that binds to both CB_1 and CB_2 receptors. Felder CC. et al., *Proc Natl Acad Sci USA* **90**:7656-7660, 1993.
O-1602	Synthetic regioisomer of cannabidiol that fails to elicit either CB_1 or CB_2 responsiveness and is without psychotropic activity; it induces endothelium-dependent vasodilation via a CB_1/CB_2/nitric oxide-independent mechanism. Járai Z. et al., *Proc Natl Acad Sci USA* **96(24)**: 14136-14141, 1999.
LPI	Predicted selective GPR55 agonist. Oka S. et al., *Biochem. And Biophys. Res. Comm.* **362**: 928–934, 2007.
SB366791	Potent, selective and competitive vanilloid TRPV1 (VR1) receptor antagonist (pA_2 = 7.71 at hVR1); antagonises hTRPV1 receptors activated by agonists, noxious heat, but not protons. Fowler et al., *Biochem. Pharmacol.* **66**: 757, 2003.
AM251	Selective CB_1-antagonist with a Ki value of 7.5 nM. Rinaldi-Carmona M. et al., *FEBS Lett* **350**: 240-244, 1994.
ACPA	Potent and selective CB_1 agonist (K_i = 2.2 nM). Displays 325-fold selectivity over CB_2 receptors. Hillard et al., *J. Pharmacol. Exp. Ther.* **289**: 1427, 1999.

LFM-A13	Potent and selective inhibitor of Bruton's tyrosine kinase (BTK). Mahajan S. et al., *Vit. E: A Comprehensive Treatise* **274**: 9587, 1999.
U73122	Phospholipase C inhibitor. Bleasdale et al., *J. Pharmacol. Exp. Ther.* **255**: 756, 1990.
PP2	Selective inhibitor of Src-family tyrosine kinases. Hanke et al., *J. Biol. Chem.* **271**: 695, 1996.
Wortmannin	Potent, selective, cell-permeable and irreversible inhibitor of phosphatidylinositol 3-kinase (PI 3-kinase). Arcaro and Wymann, *Biochem. J.* **296**: 297, 1993.

Table 16: Description of Compounds

3.4.2 Fura-2(AM); $[Ca^{2+}]_{cyto}$

Cytosolic Ca^{2+}, $[Ca^{2+}]_{cyto}$ was monitored in single cells using the conventional fura-2 technique as described previously (Graier WF. et al., *J. Physiol*. **506.1**: 109-125.,1998; Paltauf-Doburzynska J. et al., *J. Physiol.* **513.2**: 369-379, 1998; *J. Physiol.* **524.3**: 701-713, 2000). Briefly, cells were loaded for 45 min at room temperature in the dark in SB containing 2 µM Fura2/AM, washed twice and equilibrated further 30 min in SB. The cover slip (Ø 30 mm) was mounted in an experimental chamber and perfused (~ 1.5 ml min^{-1}) with Ca^{2+}-buffer. To measure $[Ca^{2+}]_{cyto}$, cells were excited alternately at 340 and 380 nm (340HT15 and 380HT15; Omega Optical, Brattleboro, VT, USA). Emission was monitored at 510 nm (510WB40; Omega Optical). Fura-2 is a widely used UV-excitable fluorescent calcium indicator, developed by Tsien RY. et al., *J Biol Chem* **260**: 3440, 1985. Upon calcium binding, the fluorescent excitation maximum of the indicator undergoes a blue shift from 363 nm (Ca^{2+}-free) to 335 nm (Ca^{2+}-saturated), while the fluorescence emission maximum is relatively unchanged at ~510 nm. For ratiometric measurements, excitation at 340 and 380 nm has usually been preferred because the absorption peak of Ca^{2+}-free fura 2 is quite close to its isobestic point and Ca^{2+}-free fura 2 emits greater than Ca^{2+}-bound fura 2 when excited by wavelengths longer than 370 nm (for review see Takahashi A. et al., *Physiol. Rev.* **79.4**: 1089-1125, 1999). The ratio (F_{340}/F_{380}) of the fluorescent emission intensities corresponding to the two excitations is used in calculating the intracellular Ca^{2+} concentration.

3.4.3 History and functionality of fluorescent proteins

The Green Fluorescent Protein (GFP) was discovered by Shimomura et al., *J. Cell. Comp. Physiol.* **59**: 223–39, 1962 as a companion protein to aequorin, the famous chemiluminescent protein from jellyfish *Aequorea victoria*, which is able to produce both aequorin and GFP. Fluorescence means, that a compound takes up electromagnetic waves (for example light) and emits light thereafter. In order that this process spends

energy, the emitted light is of lower energy than the light, that is absorbed. That means that the emitted light has a lower wavelength. In the jellyfish the emitted light is green (Figure 27), whereas the absorbed light of higher energy is blue. This blue light comes from the photoprotein aequorin. The aequorin contains the chromophoric compound, coelenterazin that changes its conformation to coelenteramid after binding of calcium from the sea. This initiates a chemical reaction that results in the production of CO_2 and blue light. Hence, it subsequently excites the GFP, which then emits green light (Tsien RY., *Annu. Rev. Biochem.* **67**: 509-544, 1998).

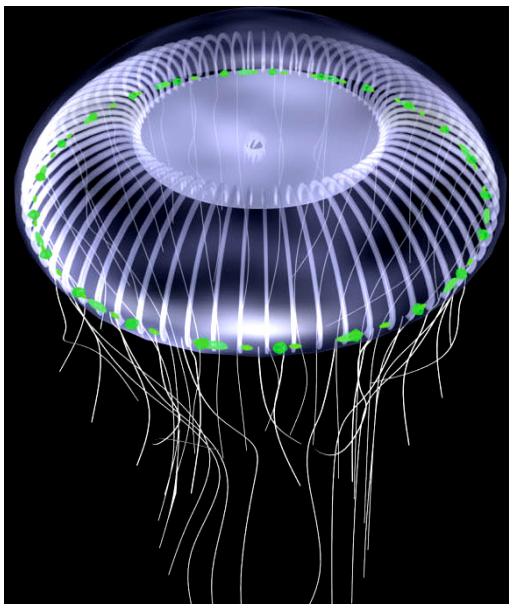

Figure 27: Bioluminescence of A. victoria
Green dotted ring = GFP

In 1992 the cDNA of GFP was first cloned and two years later it lighted in E. coli and C. elegans (Chalfie M. et al., *Science* **263**: 802–805, 1994). In the laboratory the GFP is excited by the exposure to blue light. Furthermore it was found, that the chromophore of the GFP consists of 3 amino acids, serine^{65}-thyrosine^{66}-glycine^{67}. In order that the wtGFP has a very broad excitation spectrum from λ_{uv}=395 nm to λ_{blue}=475 nm, the chromophore was genetically modified by the exchange of serine to threonine at position 65 (Ser^{65}Thr) → enhanced GFP (eGFP, Figure 28). The eGFP (Heim R. et al., *Nature* **373**: 663-664, 1995) has its excitation maximum at 488 nm and emits light at about 530 nm outshining sixfold of the wtGFP.

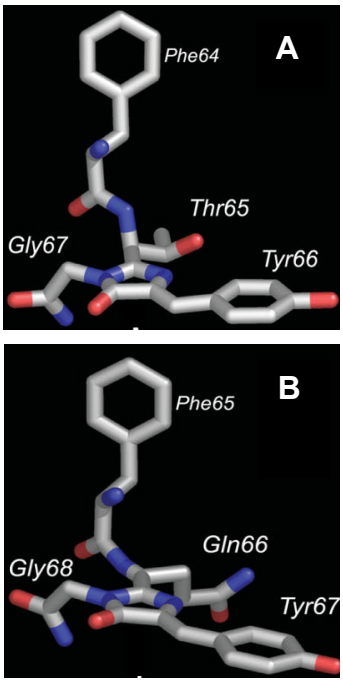

Figure 28: Chromophores of different FPs
A: eGFP, **B:** DSRed

Due to the fact that green is not the only color of fluorescent proteins in nature, in 1999 another protein was isolated from the coral Discosoma shining red (DSRed) (Matz et al., *Nature Biotechnology* **17**: 969-973, 1999). In case of the DSRed protein an additional oxygen reaction takes place, which includes the neighbored Phe^{65} resulting in a larger electron system. Accordingly its excitation λ_{max}= 550 nm and its emission λ_{max}= 580 nm. In comparison to the eGFP chromophore the DSRed chromophore is moved by one amino acid. Additionally the DSRed protein just occurs as a tetramer and therefore

needs several hours for the correct protein folding whereas the eGFP exists as a monomer.

In the meantime more and more GFP similar proteins were isolated from other marine organisms (e.g.: Anthozoa, Hydrozoa, Siphonophora, Copepoda,…), cloned and genetically enhanced. Accordingly, today a lot of fluorescent proteins are available in a variety of different colors becoming an indispensable tool in live cell imaging.

3.4.4 Fusion of Yellow Fluorescent Proteins (YFP)

Yellow fluorescent mutants of GFP (YFP) contain the modification $Ser^{65}Gly$. Due to the fact that especially eucaryotic cells contain diverse organic (e.g. metabolites), that are fluorescent, it is not that easy to distinguish this 'autofluorescence' from the background. Accordingly the YFP variants are very attractive, hence they possess the best illuminating power (citrine, 174 % of eGFP photon efficiency; Griesbeck O. et al., *J. Biol. Chem.* **276**: 29188–29194, 2001) and are folding fast (Venus, 156 % of eGFP photon efficiency; Nagai T. et al., *Nat. Biotechnol.* **20**: 87–90, 2002).
To monitor specific proteins, their coding gene sequences were fused with the YFP citrine or Venus sequence (3.3.6) on the C-terminal side in order to conserve the function of any domains that were mostly located on the N-terminal side of proteins. Such constructed plasmids were transfected in cells and observed using a confocal imaging system (3.4.10).

3.4.5 mitochondrial targeted DSRed (mtDSRed)

The Cox VIII sequence that is fused with the DSRed sequence in the mtDSRed vector (Figure 29), is mitochondria specific and targets the DSRed protein (176 % of eGFP brilliancy) exclusively into the mitochondria of cells transfected with this plasmid (3.1.1). On the one hand it was used as a marker protein for non-tagged overexpression proteins or siRNA and monitored on a Nikon inverted microscope (Eclipse 300TE, Nikon, Vienna) and excited at 558 nm (575DF25 Omega Optic). Emission was detected at 583 nm (528-633DBEM Omega Optical).

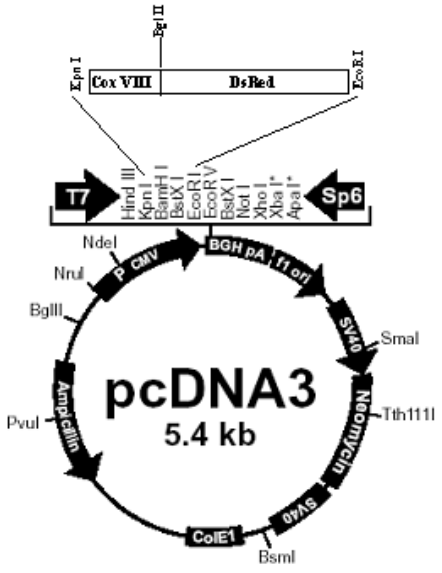

Figure 29: Vector map of mtDSRed

On the other hand it was used to record mitochondrial motility using a confocal imaging system (3.4.10 and 3.4.11).

3.4.6 mitochondrial targeted ratiometric pericam (mtRP); ($[Ca^{2+}]_{mito}$)

Curiously fluorescent proteins would also shine, if they were divided into two parts and each the halfs were fused to a protein 'X' and 'Y'. If the proteins 'X' and 'Y' then interact in a cell, the two FP parts are close-by and a fluorescence signal can appear.
This method is called multicolor fluorescence complementation analysis and is used to monitor the interaction between two proteins (Hu CD. et al., *Nat. Biotechnol.* **21**: 539–545, 2003).

The functionality of so called a circularly permuted GFP (cpGFP) is similar to that. Accordingly the GFP is divided between the amino acid position 144/145 and the two parts were subsequently interchanged. Pericam Ca^{2+} sensors are designed on the basis of a circularly permuted yellow fluorescent protein (cpYFP) that is sandwiched between a Calmodulin (CaM) and a M13 sequence. The protein CaM is an ubiquitous intracellular calcium sensor that responds to changes in calcium concentration. Each CaM molecule has four binding sites for Ca^{2+}. The molecule undergoes a conformational change after calcium-binding.

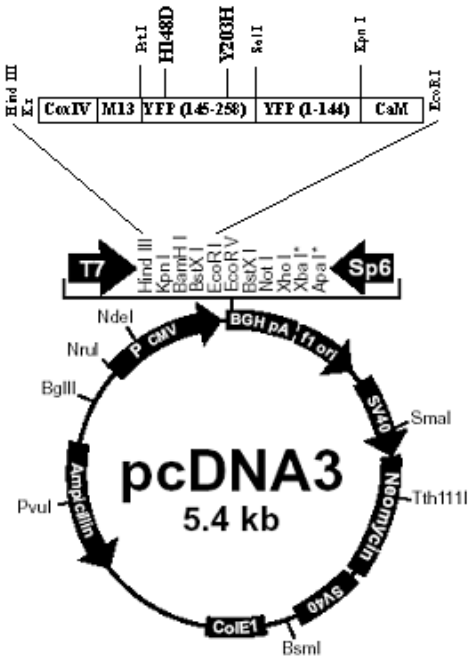

Figure 30: Vector map of mtRP

This conformational change of CaM after binding calcium causes an interaction with the M13 peptide (Calmodulin binding domain of myosin light chain kinase M13). Random or rational mutations introduced into the sequence generated three variants of pericams, one of these was named ratiometric pericam, because it was first described to allow ratiometric measurements. The conformational change that leads to alterations in the fluorescent properties upon Ca^{2+} binding can be monitored at excitation wavelength of ~ 430 nm (430DF15; Omega Optical). Excitation of ~ 480 nm reveal the sensitivity of this probes to changes in pH and more less to Ca^{2+} concentrations. Emission is monitored at 535 nm. For the measurements of mitochondrial free Ca^{2+} concentration ($[Ca^{2+}]_{mito}$) in single cells we used mitochondrial targeted ratiometric pericam (mtRP), that is fused with a COX IV mitochondrial targeting sequence (Figure 30; Nagai et al., *PNAS* **98(6)**:

3197-3202, 2001). Due to the recognized pH-sensitivity of mtRP at 485/488 nm excitation (Malli R. et al., *J. Biol. Chem.* **278(45)**: 44769-79, 2003), $[Ca^{2+}]_{mito}$ was monitored by the fluorescence of the pH-insensitive but Ca^{2+}-sensitive 430 nm excitation and $[Ca^{2+}]_{mito}$ was expressed as $1-(F_{433}/F_0)$.

3.4.7 Förster Resonance Energy Transfer (FRET)

Over the past few years, the rapid development of fluorescent proteins and their application as fusion products and biosensors have significantly expanded the molecular toolkit available for probing the mysteries of cellular physiology and pathology. In this regard, Förster resonance energy transfer (FRET) is emerging as a powerful optical microscopy technique for examining physiological processes with high temporal and spatial resolution.

FRET is transfer of the excited state energy from the initially excited donor (D) to an acceptor (A). The donor molecules typically emit at shorter wavelengths that overlap with the absorption of acceptor. The process is a distance-dependent interaction between the electronic excited states of two molecules without emission of a photon. FRET is the result of long-range dipole-dipole interactions between the donor and acceptor (Figure 31; Wu P. et al., *Anal Biochem.* **218**: 1-13, 1994). FRET occurs when the donor and acceptor molecules are within a specified range, usually < 10 nm or 10 - 100 Å. In the process of FRET, the excited-state energy of a donor is transferred to an acceptor molecule. Once excited, the acceptor can return to the ground state and emit light at its characteristic wavelength, which is always longer than the emission wavelength of the donor. The cyan-colored CFP as donor and the yellow YFP as acceptor, named cameleon, are well suited for FRET experiments in living cells, since the emission spectrum of CFP partially overlaps the spectrum of YFP (Figure 32).

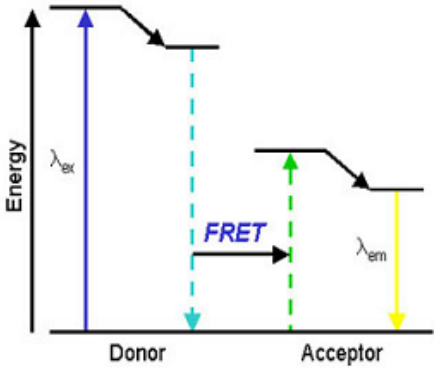

Figure 31: Diagram of FRET process
From donor to acceptor molecule

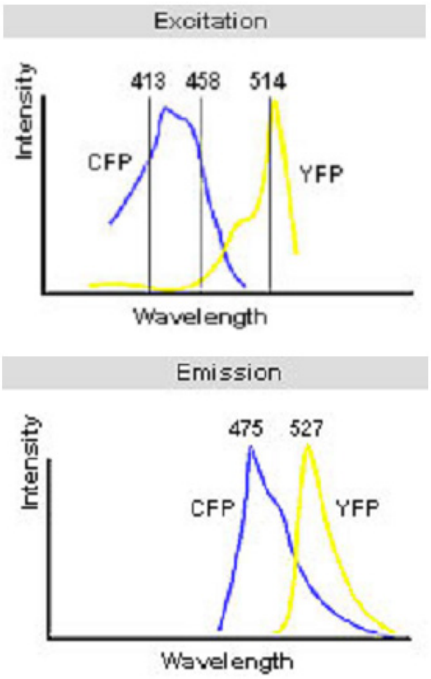

Figure 32: Excitation and Emission spectra
For CFP/YFP in FRET system

The cyan fluorescent protein (CFP) is another variant of GFP with the modification $Tyr^{66}Trp$ of the chromophore. Blue light, λ_{em}= 480 nm, is emitted upon λ_{exc}=430 nm of the CFP, if the YFP is to far away from the CFP to form a FRET signal. In contrast yellow light, λ_{em}= 535 nm, is just emitted upon λ_{exc}=430 nm, if CFP and YFP are so close to each other, that the energy gets transferred from the CFP to the YFP (3.4.8).

3.4.8 D1ER; ($[Ca^{2+}]_{ER}$)

Measuring of ER calcium ($[Ca^{2+}]_{ER}$) using the D1ER plasmid (Figure 33) is based on the FRET technology (Figure 34).

D1ER consists of a mutant CaM / peptide pair, designated as Design 1 (D1), that was cloned between CFP and citrine to yield a reengineered cameleon. Additionally of the calreticulin signal sequence and a KDEL ER-retention tag led to effective and specific localization of the cameleon to the ER in mammalian cells (Palmer et al., *PNAS* **101(50)**: 17404–17409, 2004).

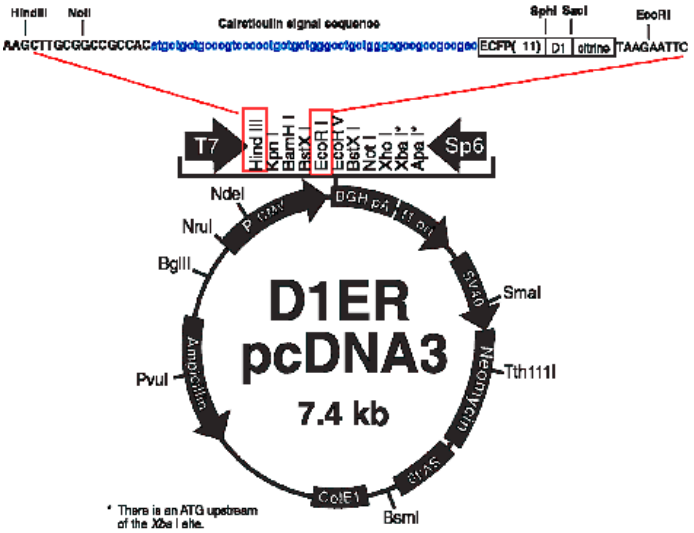

Figure 33: Vector map of D1ER

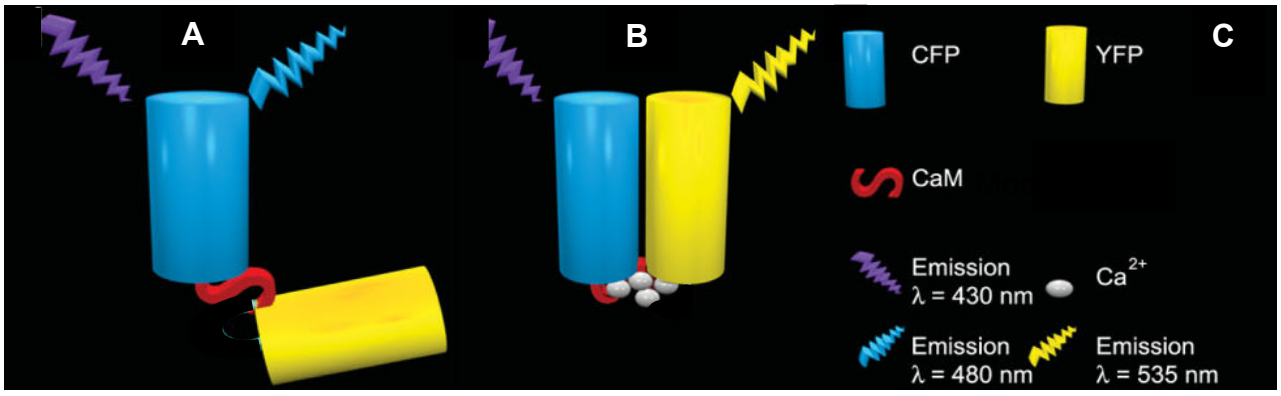

Figure 34: Schematic of FRET Technology using D1ER
A-C: A cyan (CFP, blue barrel) and a yellow (YFP, yellow barrel) shining FP are connected via a reactive Ca^{2+}-sensitive peptide bridge (D1); **A:** Without Ca^{2+} CFP and YFP are separated from each other and upon λ_{exc}=430 nm just the CFP gets excited and emits blue light (λ_{em}=480 nm). **B:** After binding of Ca^{2+} the YFP gets close to the CFP upon a conformational change resulting in a FRET signal by emitting yellow light (λ_{em}=535 nm), although λ_{exc}=430 nm was used for excitation. **C:** Legend
Images for Figures 27, 28 and 34 taken from Veith D. and Veith M.: Biologie fluoreszierender Proteine, *Biologie unserer Zeit* **6**: 304-404, Wiley-VCH Verlag GmbH & Co. KGaA, Weinheim, 2005.

For measuring the free Ca^{2+} concentration within the lumen of the ER Ca^{2+} dependent FRET of the ER targeted cameleon construct D1ER was monitored as described previously (Osibow K. et al., *J. Biol. Chem.* **281**: 5017-5025, 2006). Transfected cells were excited at 440 ± 15 nm (440AF21, Omega Optical) and emission was monitored simultaneously at 535 and 480 nm with one given camera using an optical beam splitter (535 and 480, Dual-View MicroImager^{TM}, Optical insights, Visitron Systems, Puchheim, Germany). To account for photobleaching or photochromism of D1ER the bleaching function F_0 was calculated for each individual cell using a one phase exponential decay equation for curve fitting according to the individual decay of Ratio F_{535}/F_{480} that were collected at the beginning and the end of each experiment.

3.4.9 Data acquisition for Calcium measurements

All experiments for measuring $[Ca^{2+}]_{cyto}$, $[Ca^{2+}]_{mito}$ or $[Ca^{2+}]_{ER}$ were performed on a deconvolution microscope that consists of a Nikon inverted microscope (Eclipse 300TE, Nikon, Vienna) equipped with CFI Plan Flu or 40x oil immersion objective (NA 1.3; 0.171 µm pixel^{-1}, Nikon, Austria), an epifluorescence system (150W XBO; Optiquip, Highland Mills, NY, USA), a computer controlled z-stage (Ludl Electronic Products, Haawthrone, NY, USA) and a liquid-cooled CCD camera (-30°C; Quatix KAF 1400G2, Roper Scientific, Acton, MA, USA). Excitation wavelengths were selected using a computer controlled filter wheel (Ludl Electronic Products, Haawthrone, NY, USA). All devices were controlled: by either Metafluor 4.0 (Visitron Systems, Puchheim, Germany) for Ca^{2+} measurements.

3.4.10 Confocal Imaging

Cells transfected with YFP-tagged proteins and/or mtDSRed were monitored in performing z-scans or time-lapse experiments using a Nipkow-disk-based array confocal laser scanning microscope (ACLSM; Malli R. et al., *J. Biol. Chem.* **278**: 10807-10815, 2003). The ACLSM was built on a Zeiss Axiovert 200M (Zeiss Microsystem, Jena, Germany) equipped with VoxCell Scan® (VisiTech, Sunderland, UK), a 150 mW Ar- laser (laser Physic; West Jordan, UT, USA) and controlled by Metamorph 6.2r6 (Universal imaging, Visitron System, Puchheim, Germany). Fluorescent proteins were imaged with a 100 x objective (α Plan-Fluar 100 x / 1.45 oil objective, Zeiss Micro-system, Jena, Germany). The YFP (citrine or venus) probe targeted to the protein of interest was excited using the 488 nm Ar-laser line for illumination. The emitted light

was filtered at 535 nm using an emission filter 535/30 (Chroma Technology Corp., Rockingham, VT, USA), which was mounted in a computer-controlled fastfilter wheel (Ludl, Electronic Products, Hawthrone, NY, USA). The mtDSRed probe was imaged with the 100 x objective as previously described and excited using the 514 nm Ar-laser line. The emitted light was filtered at 570 nm with the emission filter E570LPv2 (Chroma Technology Corp., Rockingham, VT, USA), that was mounted as aforementioned. Z-scans were performed in z-intervals of 0.1 µm between the planes. Mitochondrial motility was recorded in time-lapse experiments between 600 and 780 seconds by taking an image each second after 1000 ms exposure time.

3.4.11 Analysis of mitochondrial motility

Mitochondrial motility was measured as according to a recently established protocol by Malli R. using a programmed journal on the MetaMorph 6.2r6 software were used to analyze the time dependent changes of moving mitochondria. In brief, a background area was selected and subtracted from each image plane of the movie. In order to prevent any influences from photobleaching of the mtDSRed, that may have occurred during the experiment, a threshold was set and every plane was subsequently binarized. The binarized stack was then divided into sets of ten consecutive images. By subtraction of sequential images (1-s interval), the fluorescence change for each pixel was calculated, and pixels that exhibited a change (positive or negative) greater than the threshold were counted for each time point and added for each set of images. The resulting pixel image for each set of images were calculated according to the motility of mitochondria during each 10-s interval. Changes in the pixel number were normalized to the initial value calculated for cells before stimulation.

4 Results

Two different approaches were performed for the identification of putative Ca^{2+}-dependent scaffold proteins:
A Proteomic Approach (1.8; 4.1) and a Bioinformatic Approach (1.9; 4.2).

4.1 Proteomic Approach

The major problems concerning the visualization of total cell or tissue extract proteins lie in the high dynamic range of expression, and the diversity of proteins with respect to molecular weight, isoelectric point and solubility. Although a one-step procedure for protein extraction would be highly desirable with regard to simplicity and reproducibility, there is no single method of sample preparation that can be universally applied to all kinds of samples analyzed by 2-D PAGE (Görg A., **A laboratory Manual**, 1-77, 2003).
Proteases present within samples have to be inactivated to prevent protein degradation which can result in artificial spots (4.1.1).
The fundamental steps in sample preparation are (a) cell disruption, (b) inactivation or removal of interfering substances and (c) subsequent solubilization of the proteins. Although a large number of 'standard' protocols has been published, these protocols have to be adapted and further optimized for the type of sample (*e.g.* microbial cells or mammalian tissue) to be analyzed.
(a) Cell disruption was experimentally optimized for Ea.hy926 cells (4.1.1.2).
(b) Interfering substances like sucrose (4.1.2.3), salts, polysaccharides, lipids (4.1.3) or nucleic acids (4.1.4) have to be inactivated or removed. The drawback of these procedures is a possible loss of proteins.
(c) Detergents for the solubilization of proteins have to be adapted to the proteins of interest (*e.g.* 'soluble' or highly 'insoluble' membrane proteins, respectively; 4.1.2.4).
Protein extracts should not be too diluted to avoid loss of protein due to adsorption to the wall of the vessel (glass or plastic). The minimum protein concentration should not be less than 0.1 mg/ml, and optimum concentration is 1-5 mg/ml.

4.1.1 Ideal Protease Inhibitor

Crude cell extracts contain a number of endogenous enzymes, such as proteases and phosphatases, which are capable of degrading the proteins present in the extract. The best way to improve the yield of intact proteins is to add inhibitors of these enzymes known to be present in the source material.

The Protease Inhibitor Cocktail for mammalian tissue (P 8340, Sigma-Inc., St. Louis, Missouri) was found to be ideal for the inhibition of proteases from an endothelial cell line like the Ea.hy926. Accordingly, it was found out that 20 µl of this mixture supplied to 2 ml of homogenization buffer (HB) was the optimum concentration to inhibit proteases without any interference in the following procedures.

4.1.2 Optimization of Sample Preparation for Plasma Membrane Proteins

4.1.2.1 Optimization of Homogenization

One major limitation in the successful fractionation of tissue culture cells is the production of an ‘‘ideal’’ homogenate, that is, the release of organelles and other cellular constituents as a free suspension of intact, individual components. Very often cytoplasmic aggregates are observed which contain cytoskeletal elements as well as various organelles. However, aggregates can reflect some pre-existing cellular organization, particularly due to the cytoskeleton, which may cause the cytoplasm to maintain some degree of organization after homogenization. Consequently organelles remain associated with the cytoskeletal elements surrounding the nucleus and/or become entrapped in large aggregates which readily sediment. A potential source for those are nuclei which break under harsh homogenization conditions and subsequently release DNA. This in turn will result in significant loss of components of the homogenate during the initial centrifugation step for removal of nuclei. Since the cytoplasmic and cytoskeletal organization of different tissue culture cells varies enormously, homogenization conditions must be optimized for each cell line (Pasquali C. et al., *J. of Chromatography B* **722**: 89–102, 1999).

The quality of the homogenization should be assessed by morphological means; e.g., by phase contrast microscopy, it is possible to assess the extent of cellular disruption, i.e., the appearance of unbroken nuclei and the absence of large aggregates.

To optimize cell disruption homogenization was performed by three different procedures, (1) Homogenization using a 22G needle and a 1-ml syringe (Pasquali C. et

al., *J. of Chromatography B* **722**: 89–102, 1999), (2) Homogenization using a Dounce homogenizer with a tight fitting pestle (Desjardins M. et al., *J. of Biol. Chemistry* **269(51)**: 32194-32200, 1994; Remold-O´Donell, *Preparative Biochemistry*, **7(6)**: 441-455,1977), (3) Homogenization by Sonication (Podolsky DK. et al., *PNAS* **71(3)**: 904–908, 1974; Boone CW. et al., *The J. of Cell Biology* **41**: 378-392, 1969). (1) Cells were disrupted by 3-4 strokes passing the 22G needle. This kind of homogenization was not useful for this endothelial cell line as it breaks open the nuclei. (2) The cell suspension was homogenized with 10 strokes using a glass/Teflon homogenizer after Potter.

(3) The suspension was sonicated in nine 15-second bursts and 30-second intervals using a Labsonic 2000 sonifier (Braun, Melsungen, Germany).

The quality of the two different homogenization methods (2) and (3) was verified by phase contrast microscopy. Accordingly it was not clearly seen, which of these two homogenization methods was more powerful as unbroken nuclei, unbroken cells and other cell compartments were found in both samples. Therefore protein concentrations were measured in the plasma membrane enriched fractions 2-4 (according to 4.1.2.2, Figure 36) after sucrose gradient centrifugation.

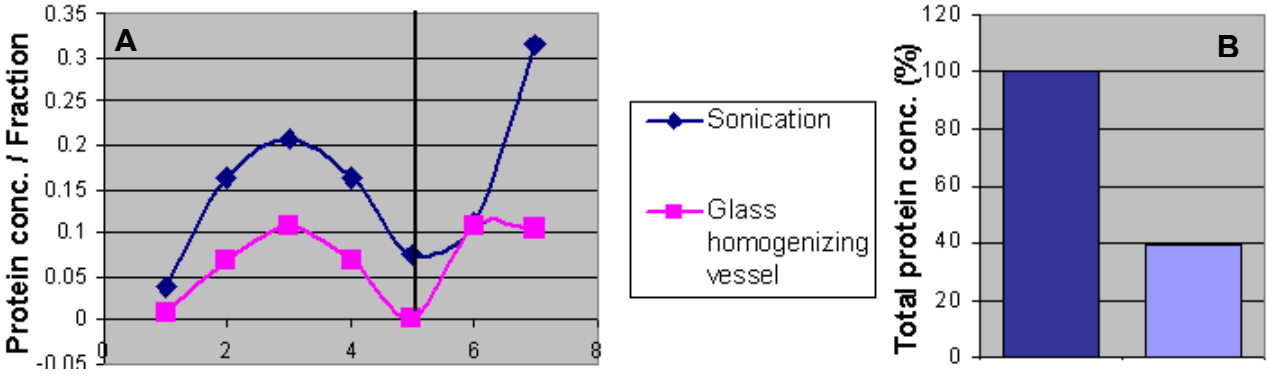

Figure 35: Overlay of Plasma Membrane enriched fractions
A: Protein determination of Plasma Membrane enriched fractions (µg/ml) **B:** Comparison of Plasma Membrane Protein Recovery in % after Homogenization by Sonication versus Mechanical Force (39.6 %)

As a result in optimizing homognization of Ea.hy926 cells, Figure 35 clearly shows that cells get better disrupted by sonication and therefore higher amounts of protein concentrations were revealed within plasma membrane enriched fractions. In comparison, protein concentration was about 60 % decreased, if homogenized by mechanical force. Accordingly this data indicate that more cells remained unbroken under these conditions.

4.1.2.2 Verification of Plasma Membrane enriched fractions

Isolation of Plasma membrane from Ea.hy926 cells was performed as previously discussed (3.3.1.3) after homogenization by sonication (4.1.1.1). The various fractions (~20 x 500 µl) were subsequently taken after sucrose gradient centrifugation and analyzed in Western blot experiments using either a Caveolin 1 antibody or a SR B1 antibody (3.3.12) to identify plasma membrane enriched fractions.

Therefore, the protein concentrations were determined from the fractions (Figure 36). Accordingly the amount of protein was calculated for each fraction and plotted in order to their cell compartments as predicted (Remold-O´Donell E., *Preparative Biochemistry*, **7(6)**: 441-455, 1977; Aronson NN. et al., *Methods Enzymol.* **31(Pt.A)**: 90-102, 1974). The average yield of plasma membrane protein was 250 µg per 5 mg (~ 5 % of the cell protein), that is in line with Emmelot P. et al. *Methods Enzymol*. **31(Pt.A)**: 75-90, 1974.

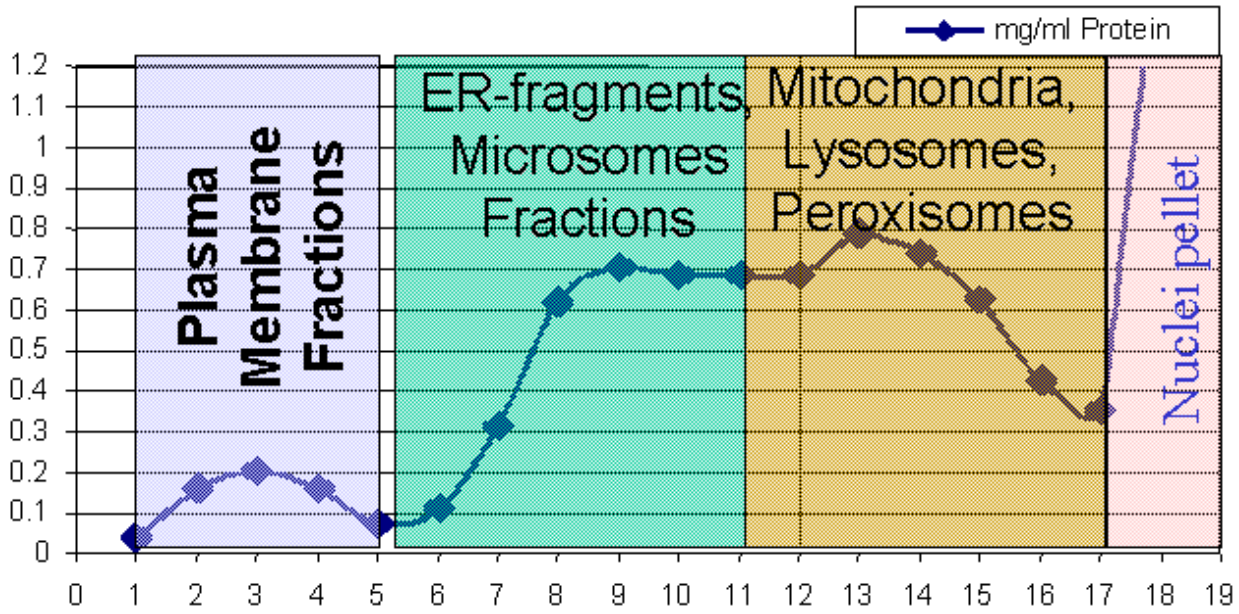

Figure 36: Protein concentrations of the various fractions
Colored bars indicate fractions containing the proteins of the various cell compartments as predicted. Total Protein Weight from 20 x 10 mm dishes of confluent Ea.hy926 cells: 4.715 mg

For Western Blot Analysis 450 ng of each odd-numbered fraction was transferred into each slot of the stacking gel. Caveolin 1 was detected in Western Blot Analysis indicating plasma membrane enriched fractions (Figure 37). Unfortunately SR B1 was not detected within any fraction.

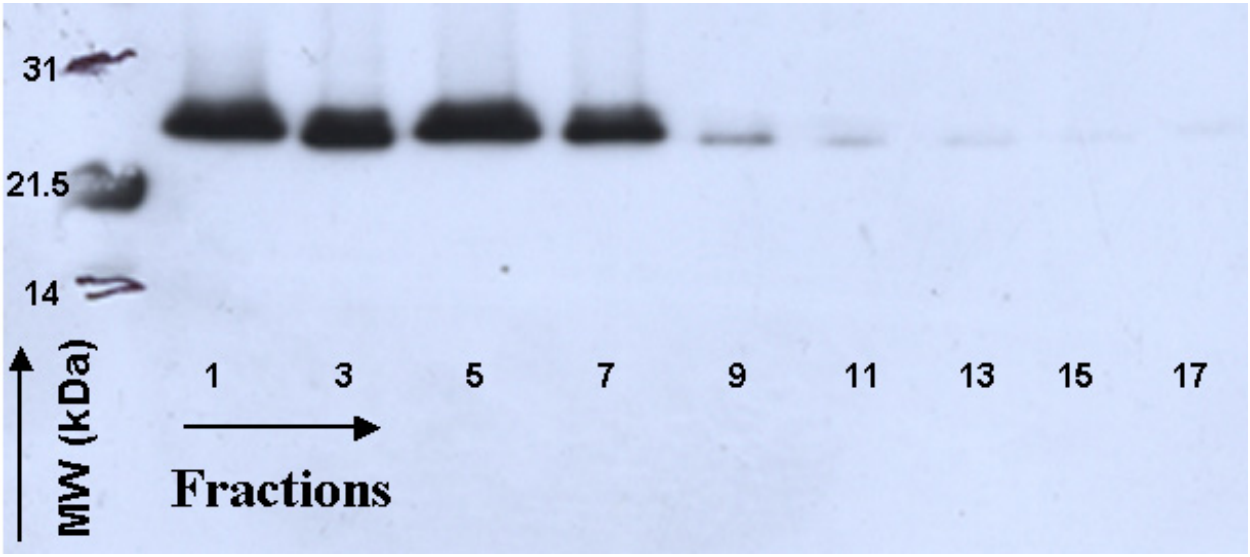

Figure 37: Distribution of Caveolin 1 containing fractions

Comparing the plasma membrane enriched fractions with their protein concentrations, the quality of plasma membrane enriched fractions was improved by just pooling the fractions 2-4 to avoid any contamination derived from other cell compartments.

4.1.2.3 Purification and Extraction of plasma membrane proteins

Plasma membrane protein enriched fractions obtained after sucrose gradient centrifugation contain a lot of interfering compounds like sucrose, proteolytic enzymes, salts, lipids or polysaccharides. These have to be removed prior to 2D-gel electrophoresis. Therefore the pooled fractions 2-4 were dialyzed in an Argon-gas inerted dialysis tube for 15 hours in 2 l of double destilled water at 4°C (Owens GP. et al. *Journal of Virological Methods* **68**: 119-125, 1997). Thus, interfering compounds got removed, but the volume of the protein sample was still to high for the labelling procedure. Accordingly, the sample was concentrated from 2500 µl to 500 µl using the Centriprep® Centrifugal Filters (Millipore Corp., County Cork, Ireland).

4.1.2.4 Solubilizaton of Plasma Membrane Proteins

The ideal sample solubilization procedure for 2-D PAGE would result in the disruption of all non-covalently bound protein complexes and aggregates into a solution of individual polypeptides which remain soluble during the 2-D electrophoretic separation.
Whereas satisfying results with modified O'Farrell's lysis buffer are obtained with the more hydrophilic proteins, this standard IEF sample buffer is not ideal for the solubilization of all protein classes, in particular not for membrane or other hydrophobic proteins. Improvement in the analysis of hydrophobic proteins was achieved by thiourea

(Rabilloud T., *Electrophoresis* **19**: 758-760, 1998) and zwitterionic detergents like CHAPS. Merits and limits of these new detergents, chaotropes, and reducing agents have been thoroughly discussed by Rabilloud T. et al., *Electrophoresis* **18**: 307-316, 1997 and *Proteome Research:* **Springer**: 9-29, 2000.

4.1.3 Optimization of Sample Preparation for Membrane Proteins

The membrane enriched protein fraction obtained as described in 4.1.2.1 contained lipids, polysaccharides or salts that may interfere in two-dimensional electrophoresis:
Lipids may interact with membrane proteins and consume detergents (Görg A. et al., *Proteomics* **4**, 3665–3685, 2004). Polysaccharides (especially the charged ones) can interact with carrier ampholytes and proteins, and give rise to streaky 2-D patterns. Moreover, these macromolecules may also increase the viscosity of the solutions and clog the pores of the polyacrylamide gels (Görg A. et al., *Proteomics* **4**, 3665–3685, 2004). High concentrations of salts may effect electrophoresis separation as they can give rise to excessive local differences of heating due to high current (Cañas B. et al., *Journal of Chromatography A* **1153**: 235–258, 2007).
To remove these interfering compounds, the protein sample was precipitated as described (3.3.2.1). Thereafter the precipitated sample was dissolved in the sample buffer mentioned before (4.1.2.4).

4.1.4 Optimization of Sample Preparation for Nuclear Proteins

Nuclei obtained after low speed sedimentation (3.3.1.4) were homogenized for a second time using a 22G needle and a 1-ml syringe (4.1.2.1) to disrupt them.
The presence of nucleic acids, especially DNA, interferes with isoelectric focusing of proteins. DNA is negatively charged and binds to proteins resulting in artifacts in protein migration during IEF. Under denaturing conditions DNA complexes are dissociated and markedly increase the viscosity of the solution. This inhibits entry of the protein to the gel matrix and slows their movement during focusing. Nucleic acids can be removed by enzymatic digestion (GE Healthcare, *2-D Electrophoresis: Principles and Methods*, Handbook **80-6429-60AC**: 19, 2004).
Therefore, the samples were treated with a protease-free DNase/RNase mixture to reduce the nucleic acids to mono- and oligonucleotides. This was done after cooling first at room temperature for 5 min and then on ice. The cell extracts were then treated with nucleases by adding 0.5 ml of nuclease buffer (1 mg of DNase I/ml (Sigma Inc.), 0.25

mg of RNase A/ml (Sigma Inc.), 24 mM Tris base, 476 mM Tris HCl, and 50 mM $MgCl_2$) and incubated on ice for 15 min (Marouga R. et al., *J. of Bacteriology* **178(3)**: 817-822, 1996).

The nucleic protein sample was then subsequently precipitated and solubilized as previously discussed (4.1.3). The DNase and RNase proteins may appear on the 2-D map resulting in a smear (Figure 42).

4.1.5 2D Gel Analysis

4.1.5.1 Plasma Membrane Proteins

The average concentration of total purified plasma membrane proteins yielded about 80-100 µg/500 µl. However equal amounts of protein (30 µg) from the untreated and treated sample were labeled with 400 pmol of their corresponding CyDyes (3.3.4.2) and combined. 2D gel electrophoresis was run as described (3.3.5). Several proteins were picked from the resulting gel outlined in Figure 38, tryptic in-gel digested and applied to MALDI-TOF for protein identification.

According to the low amount of protein concentration supplied to 2D-electrophoresis it seemed unclear, if any protein could be identified by mass spectrometry. Thus, just one protein was identified (marked with yellow number 1) from this 2D gel (Table 17), which was 1.29 fold increased in the treated sample.

4.1.5.2 Membrane Proteins

The average concentration of total purified membrane proteins yielded about 800-1000 µg/100 µl. Accordingly, 672.5 µg of each protein extract, untreated or treated, were labeled for 2D gel electrophoresis in the presented 2D gel map (Figure 39, Table 18).

Additionally, the mass spectrum (40 Figure) and the Mascot Search Result (Figure 41) of Peroxiredoxin 1 (Prdx1) is outlined as one example for protein identification after MALDI-TOF analysis.

4.1.5.3 Nuclear Proteins

The average concentration of total purified nuclear proteins after subtracting the amount of inserted nucleases yielded about 1000-1200 µg/200 µl.

The presented 2D gel map (Figure 42, Table 19) contained 900 µg of total nuclear protein, 450 µg of each, treated and untreated protein extract.

4.1.6 2D Gel Maps

General Guidelines for Reading the presented 2D Gel Maps and Tables:

1. pI value: pI (left end): ~3 pI (right end): ~10
2. Molecular weight: Mass (upper end): ~200 kDa Mass (lower end): ~9 kDa
3. Picked Spots: encircled black
4. Identified Proteins: numbered yellow and listed in the particular tables
5. Abundance: Increased: positive values Decreased: negative values
6. Selected Client Proteins: Bold marked

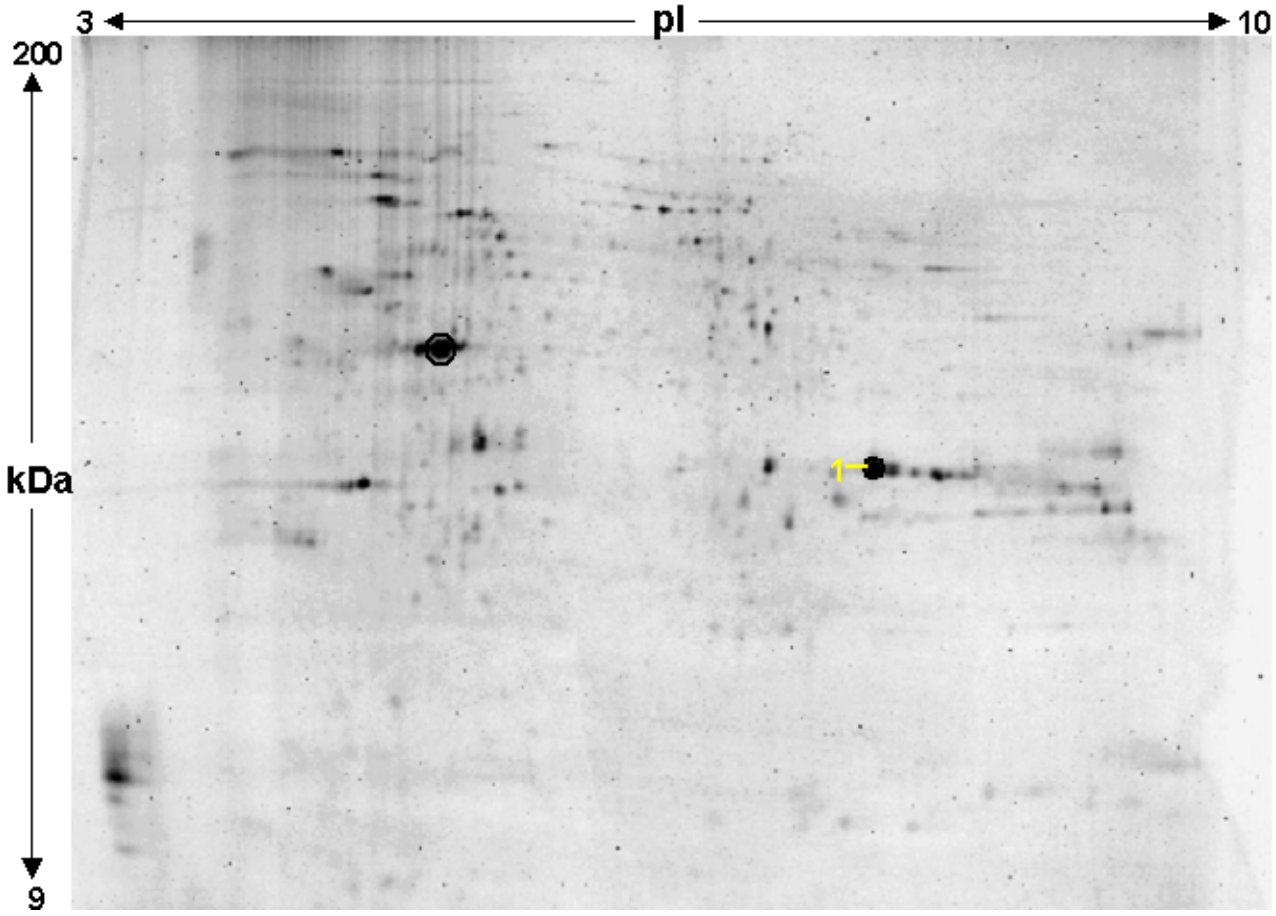

Figure 38: 2D Gel containing Plasma Membrane Proteins from Ea.hy926 cells

Number	Identified Protein	Mass (Da)	pI value	Abundance
1	Annexin A2 isoform 2	38594	7.57	1.29

Table 17: Identified Plasma Membrane Protein (corresponding to Figure 38)

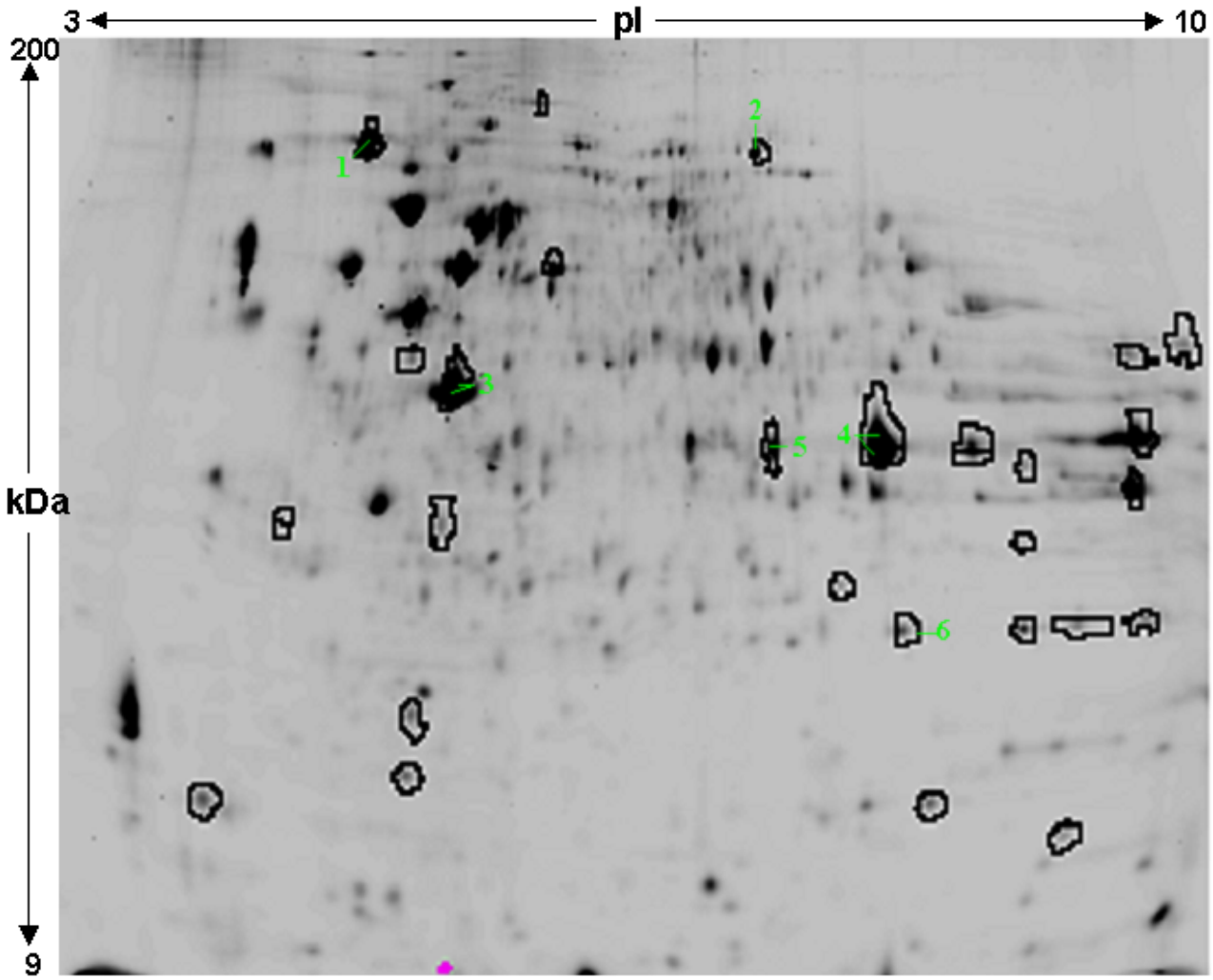

Figure 39: 2D-gel containing Membrane proteins from Ea.hy926 cells

Number	Identified Protein	Mass (Da)	pI value	Abundance
1	Heat shock protein gp96	90138	4.73	1.15
2	Eucaryotic translation elongation factor 2	95277	6.41	1.43
3	ACTB protein	40194	5.55	-1.22
4	Annexin A2 isoform 2 variant	40505	8.41	1.25
5	ANXA2 protein	38564	7.57	1.22
6	Peroxiredoxin 1	22096	8.27	1.31

Table 18: Identified Membrane Proteins (corresponding to Figure 39)

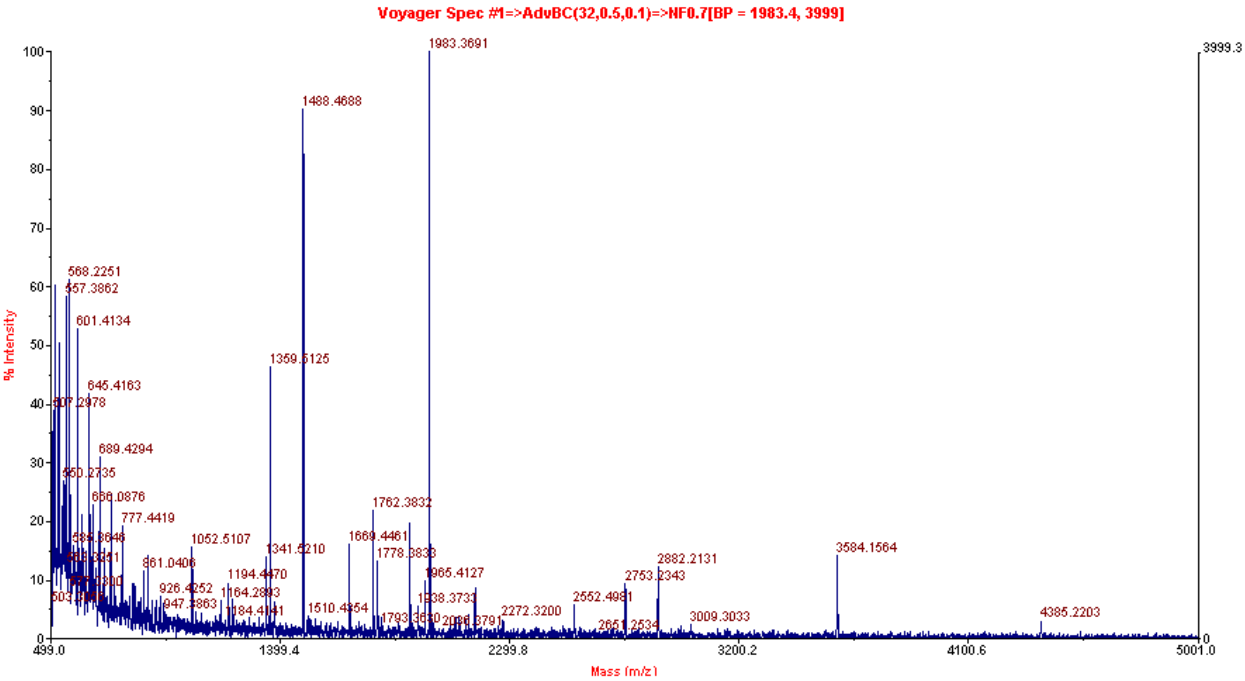

Figure 40: Mass spectrum of Peroxiredoxin 1
Protein Mass Fingerprint of Peroxiredoxin 1 after tryptic in-gel digestion

Mascot Search Results

User : helga reicher
Email : helga.reicher@meduni-graz.at
Search title : Peroxiredoxin 1
MS data file : D:\Markus\2005-10-10\spot 972-2_0001.txt
Database : NCBInr 20051110 (3023944 sequences;)
Taxonomy : Homo sapiens (human) (138675 sequences)

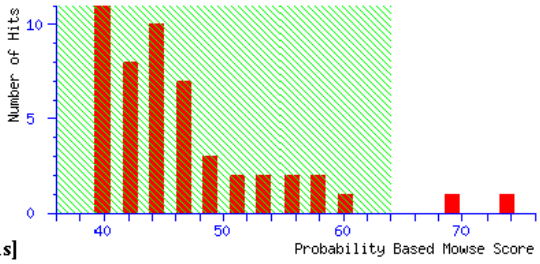

Protein Summary Report

Top Score : 74 for gi|55959887, peroxiredoxin 1 [Homo sapiens]

Probability Based Mowse Score

Ions score is -10*Log(P), where P is the probability that the observed match is a random event. Protein scores greater than 64 are significant (p<0.05).

Index

	Accession	Mass	Score	Description
1.	gi|55959887	18964	74	peroxiredoxin 1 [Homo sapiens]
2.	gi|32455264	22096	70	peroxiredoxin 1 [Homo sapiens]
3.	gi|55770895	145996	61	ERBB2 interacting protein isoform 7 [Homo sapiens]
4.	gi|8923909	153831	59	ERBB2 interacting protein isoform 2 [Homo sapiens]
5.	gi|14582259	158140	58	densin-180-like protein [Homo sapiens]
6.	gi|3327094	70977	56	KIAA0540 protein [Homo sapiens]
7.	gi|440306	22113	56	enhancer protein
8.	gi|55635297	68954	53	PREDICTED: similar to SWAP-70 protein [Pan troglodytes]
9.	gi|30911101	68955	53	SWAP-70 protein [Homo sapiens]
10.	gi|21752372	41034	52	unnamed protein product [Homo sapiens]
11.	gi|21739458	134708	52	hypothetical protein [Homo sapiens]
12.	gi|28703998	80616	49	SETDB2 protein [Homo sapiens]
13.	gi|13994282	81802	49	CLLL8 protein [Homo sapiens]
14.	gi|55662252	81842	49	SET domain, bifurcated 2 [Homo sapiens]
15.	gi|24158848	56871	47	Chain D, Human Erythrocyte Pyruvate Kinase
16.	gi|24158852	56901	47	Chain D, Human Erythrocyte Pyruvate Kinase: Thr384met Mutant
17.	gi|24158856	56901	47	Chain D, Human Erythrocyte Pyruvate Kinase: Arg486trp Mutant
18.	gi|24158860	56852	47	Chain D, Human Erythrocyte Pyruvate Kinase: Arg479his Mutant
19.	gi|16741315	111579	47	MIB2 protein [Homo sapiens]
20.	gi|19070557	5864	46	NCX1 exchanger [Homo sapiens]

Protein View

Match to: **gi|32455264**
Score: **70** Expect: **0.015**
peroxiredoxin 1 [Homo sapiens]
Found in search of
D:\Markus\2005-10-10\
spot 972-2_0001.txt

Nominal mass (M_r): **22096;**
Calculated pI value: **8.27**
NCBI BLAST search of gi|32455264
against nr
Unformatted sequence string for
pasting into other applications

Figure 41: Mascot database analysis of mass spectrum

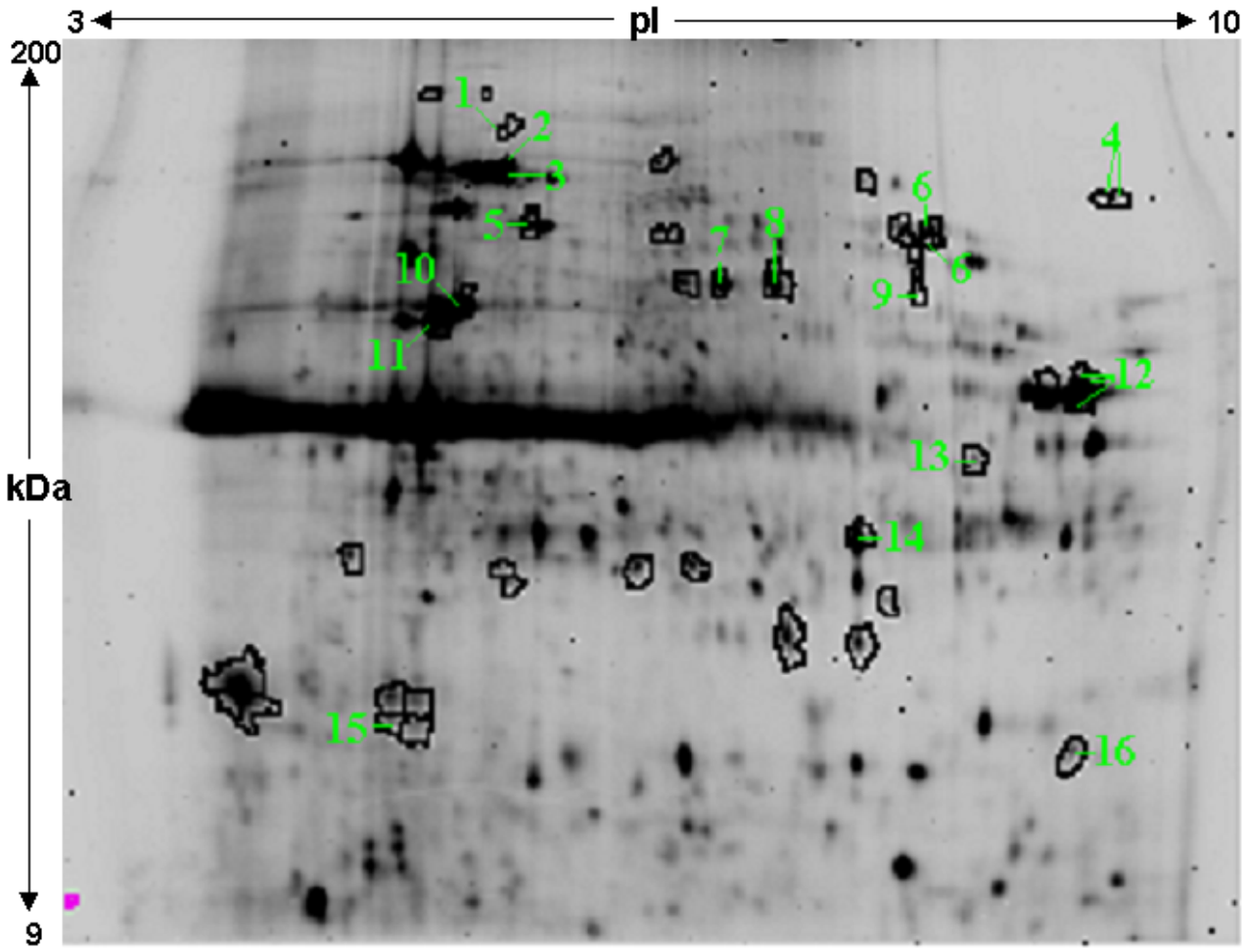

Figure 42: 2D-gel containing nuclear proteins from Ea.hy926 cells

Number	Identified Protein	Mass (Da)	pI value	Abundance
1	**Valosin-containing Protein**	89266	5.14	-2.02
2	Heat shock 70 kDa protein	73653	5.87	-1.22
3	Chaperonin	61016	5.7	-1.23
4	Enoyl CoA hydratase	82907	9.16	-2.04
5	Protein disulfide isomerase	56761	5.98	1.27
6	Pyruvate kinase 3, isoform 1	57841	7.58	1.24
7	Enolase 1 variant	47139	7.01	1.58
8	Hypothetical protein	47139	7.01	1.58
9	ATP synthase, ATP5A1 protein	48765	9.1	-1.36
10	Actin beta	40194	5.55	1.26
11	Beta Actin	41710	5.29	1.22
12	Glyceraldehyd-3-phosphate dehydrogenase	36030	8.57	-1.29
13	Annexin 1	35018	7.77	-1.28
14	Heterogenous nuclear ribonucleoprotein A2/B1	28384	7.4	1.23
15	Glutathione S-transferase	23327	5.43	-1.84
16	Non-metastatic cells 2, protein (NM23B) expr. in isoform 2	17287	8.55	1.22

Table 19: Identified Nuclear Proteins (corresponding to Figure 42)

4.1.7 Abundance of selected Client Proteins

Two Client proteins were selected from the Proteomic Approach for further investigation, Peroxiredoxin 1 (Prdx1) from the membrane protein extract and Valosin containing protein (VCP) from the nuclear protein extract.

Upon histamine stimulation the abundance of Prdx1 in the membrane fraction was found about 30 % higher compared to the untreated protein extract, whereas the abundance of VCP was about 50 % decreased in the nuclear fraction.

The 3-D view of the DeCyder Differential Analysis Software clearly showed the differences in the abundance of the two proteins derived from the various protein extracts (Figure 43). Additionally these two proteins seemed to be the most interesting in terms to be involved in Ca^{2+} homeostasis (Introduction).

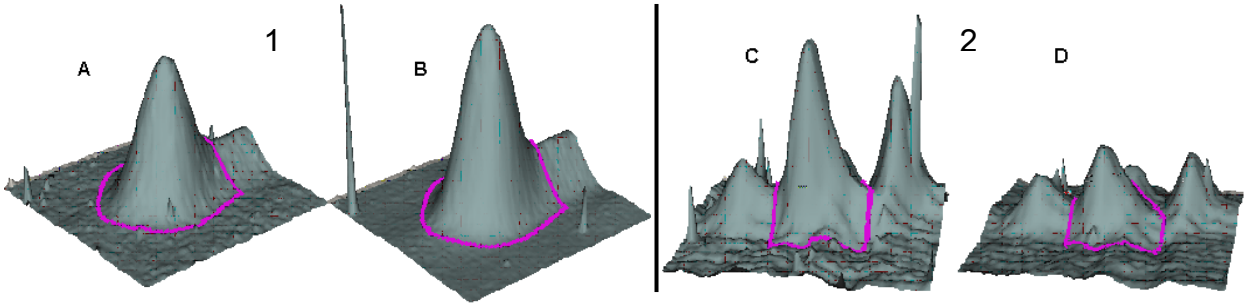

Figure 43: 3-D Views of Client Proteins (Untreated vs. Treated)
1: Peroxiredoxin 1: $\mathbf{1_A}$**:** Cy3 labelled (untreated) $\mathbf{1_B}$**:** Cy5 labelled (treated)
2: Valosin containing protein: $\mathbf{2_C}$**:** Cy3 labelled (untreated) $\mathbf{2_D}$**:** Cy5 labelled (treated)

4.1.8 Cloning Genes of Client Proteins

Both genes, Prdx1 and VCP, were amplified out of a cDNA from Ea.hy926 in a several PCR experiments. For the amplification of Prdx1 using the Primers Poxi *for* (GGG*AAGCTT*-ATGTCTTCAGGAAATGCTA) and Poxi *rev* (TAC*GGATCC*-CTTCTGCTTGGAGAAATA) in the Hot-Start Taq-Polymerase protocol (3.2.4.4) and for VCP using the Primers VCPA *for* (CCG*AAGCTT*-ATGGCTTCTGGAGCCGATT) and VCPH *rev* (GTT*GGATCC*-GCCATACAGGTCATCATCA) in the protocol for the advantage cDNA PCR kit (3.2.4.5). The citrine (YFP) was amplified from a D1ER fragment using the Primers citrine/eCFP BamHI *for* (GGA*GGATCC*-ATGGTGAGCAAGGGCGAGCA) and citrine/eCFP EcoRI *rev* (AGA*ATTC*-TTAGCCGAGAGTGATCCCGGC) in a Hot Start Taq PCR experiment.

In the face of further investigations based on finding interaction proteins the pBudCE4.1 vector (Invitrogen) was selected for the cloning procedures as it was designed to

simultaneous expression of two genes in mammalian cell lines, and therefore contains the human cytomegalovirus (CMV) immediate-early promotor and the human elongation factor 1α-subunit (EF-1α) promotor for high-level, constitutive, independent expression of two recombinant proteins.

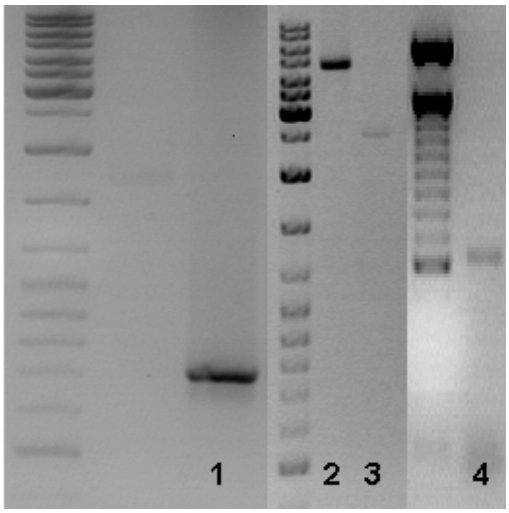

Figure 44: Restricted inserts for cloning into pBudCE4.1
1. citrine restricted BamHI / EcoRI (~ 700 bp)
2. pBud restricted BamHI / EcoRI (~ 4500 bp)
3. VCP restricted HindIII / BamHI (~ 2420 bp)
4 Peroxiredoxin 1 restricted HindIII / BamHI (~ 600 bp)

Accordingly the coding sequences of the client proteins and the citrine as well as the vector were enzymatically digested at their restriction sites and separated on an agarose gel (Figure 44). The inserts were then ligated into the CMV multiple cloning site of the pBudCE4.1 vector in one three-point or two two-point ligation resulting in citrine tagged client protein constructs (Figure 45).

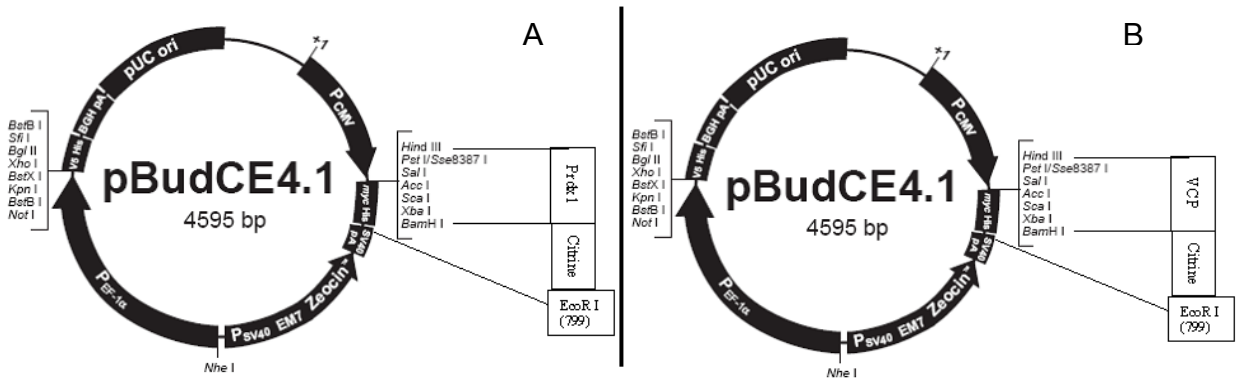

Figure 45: Gene maps of pBudCE4.1 containing citrine tagged client proteins
A: Coding sequence of Peroxiredoxin 1 fused to citrine in the CMV multiple cloning site
B: Coding sequence of Valosin containing protein fused to citrine in the CMV multiple cloning site

Both constructed plasmids were verified in a Restriction Control (HindIII/EcoRI) resulting in the expected bands (gel photographs not shown), ~ 4500 bp for the linearized vector, ~ 1300 bp for Prdx1-citrine and ~ 3000 bp for VCP-citrine. Additionally verification of clones were performed by sequencing. In order to review the correct sequences of the two genes, sequencing was performed using the gene specific primers Poxi *for* and Poxi *rev* for the Prdx1 construct and VCPA *for*, VCPA *rev*, VCPB *for*, VCPH *for* for the

VCP construct. For the purpose of the correct fusion with the citrine sequence and the correct insertion in the vector detection primers were used for both constructs (pBud MCS1 *for*, pBud MCS1 *rev*, citrine/eCFP BamHI *for* and citrine/eCFP EcoRI *rev*).

The clones that were found to be positive in containing the correct constructs for the citrine fused Prdx1 or VCP were subsequently applied to a maxi preparation.

4.1.9 Imaging of Client Proteins

The plasmids for the citrine tagged client proteins obtained from the maxi preparation were transfected into Ea.hy926 cells and visualized 24 or 48 hours after transfection.

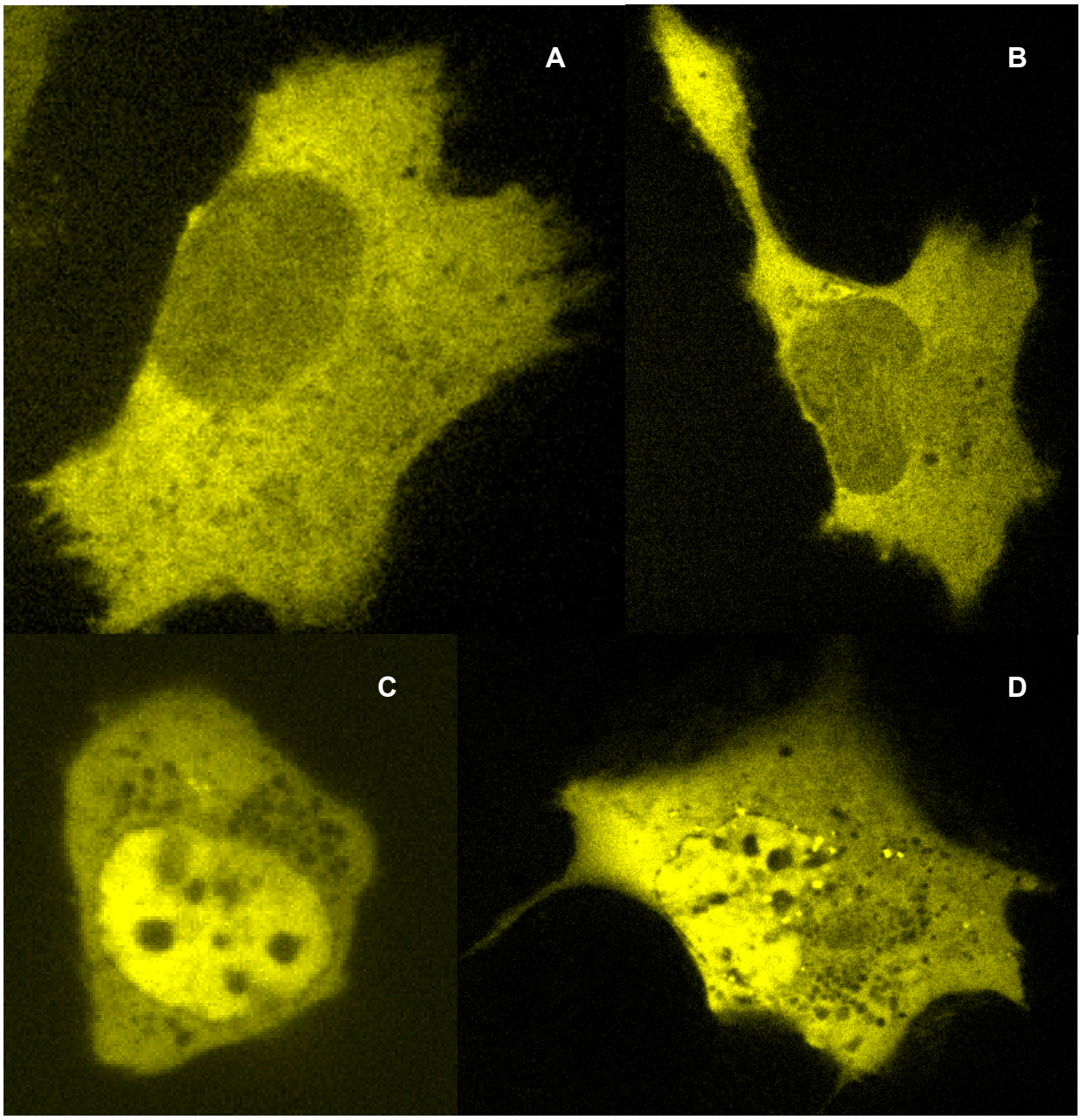

Figure 46: Distribution of client proteins overexpressed in Ea.hy926
A,B: Overexpression of citrine tagged Peroxiredoxin **A:** 24 h after transfection **B:** 48 h after transfection
C,D: Overexpression of citrine tagged VCP **C:** 24 h after transfection **D:** 48 h after transfection

Protein distribution in live cell imaging was obtainedusing the confocal imaging system. Peroxiredoxin 1 was found to be primary localized in various subcellular organelles and in the cytosol (Figure 46A,B) as recommended by Mowbray AL. et al., *J. of Biol. Chem.* **283(3)**:1622–1627, 2008.

Subcellular localization of VCP was observed to be primary in the nucleus and the cytosol of Ea.hy926 cells (Figure 46C,D), which was already found out in human cell lines by Zhang H. et al., *DNA and Cell Biology* **19(5)**: 253-263, 2000.

According to the treated situation in the proteomic approach, the two tagged client proteins were also monitored to observe their translocation during histamine stimulation. Neither Peroxiredoxin 1 nor VCP was found out to show a clear translocation upon 100 µM histamine stimulation when overexpressing Ea.hy926 cells with the citrine fused proteins for 24 or 48 hours after transfection.

4.2 Bioinformatic Approach

Based on the sequence and structure annotation (1.9) several proteins were selected that may act as putative Ca^{2+}-activated scaffolds. However, the list of such proteins presented in Table 20 is still in process, other selection criteria were established, to verify the most interesting proteins.
Due to the recent publications on mitochondrial motility (1.3) the idea was born to select a protein that may have an influence on this phenomenon. Accordingly such a protein was supposed to possess several of the following structural or functional characteristics (A-D):

A. For the induction of the Ca^{2+}-dependent mitochondrial motility, it may possess a Ca^{2+}-binding domain, which can either be a C2-domain or EF-hand domains (1.12).
B. It may be either localized within mitochondria or recommended to be mitochondria-associated.
C. As mitochondria fulfill their movements with the aid of microtubles, it may interact with tubulin.
D. It may possess a predicted kinase activity.

Among all the proteins on the list, just three proteins were found to possess two or more of these selection criteria:

1. MIRO1: EF-Hand domains, Mitochondrial Localization
2. MIRO2: EF-Hand domains, Mitochondrial Localization
3. RAB11FIP5: C2-domain, Mitochondrial Localization, Interaction with γ-tubulin

In a first series of experiments various siRNAs against RAB11FIP5 and MIRO1 (3.2.10.2) were tested to effect mitochondrial motility. Interestingly one of them does (4.2.5), RAB11FIP5, which is further named Gaf1 (gamma-SNAP interacting factor 1) in the text according to its interaction with γ-SNAP.

Scaffold	Ca^{2+} binding.	Trans-location	Location	↔ Cyto-skelet.	↔ ion channels	↔ PKC	↔ CREB	↔ Inte-grins	↔Kinases	Other interaction Partners	Ea.hy Expr.
14-3-3 α/ß			Cytoplasm Golgi		KCNK3	inhibitor	TORC2	Beta 1	ERK5, c-src, Raf1, KSR1	UCP2, UCP3, A20,TORC2	+
14-3-3 ε	CaM		Cytoplasm Nucleus		Ca-act. Cl-channel	inhibitor			MEKK1,2,3,c-src, Raf1, KSR1	A20	+
14-3-3 η			Cytoplasm Nucleus	actin	KCNH2	inhibitor			c-src, Raf1, KSR, CaMK, PDK1	CDC25, Abl1	+
14-3-3 γ			Cytoplasm, ER, Golgi	actin		inhibitor	CREBBP		c-src, Raf1, KSR1, CaMK	UCP2, UCP3, A20	+
14-3-3 σ			Cytoplasm			inhibitor			CDK2	CDC2	-
14-3-3 τ/θ			Cytoplasm Nucleus			inhibitor			PDK1, Raf1, KSR1	UCP3, UCP3, NFAT, CBL, BAX	+
14-3-3 ζ/δ			Cytoplasm Golgi		Cl-channel	inhibitor			MEKK3, AKT1	RGS3, REM1, NFAT, UCP3	+
AHNAK			Cytoplasm Nucleus, PM	actin	L-Type Ca-channel				PKA, PKB	Annexin, S100B	+
AKAP79	CaM		PM	actin	L-Type Ca-ch., K-ch.				PKA	GPCR, IQGAP, ADRB2	-
AKAP 250	CaM-like bdg.		Cytoplasm, PM	actin					PKA, GRK2	GPCR, ARRB2	+
ARRB1			Cytoplasm Nucleus, PM		Na^+/H^+ exchanger				GRK2, CSK, c-scr, MAPK(ERK), BARK	GPCR	+
ARRB2			Cytoplasm Nucleus		Na^+/H^+ exchanger				MAPK(ERK), c-scr, RAF, ASK, GRK2	GPCR	-
BANK			Cytoplasm		IP3R				Lyn, Scr	IP3R, BCL	-
Calcy-phosphin	EF hands	PH domain	Cytoplasm						PKA		-
Calsenilin	EF hands	Nucleus (Ca dependent)	Cytoplasm, ER, Golgi, Nucleus		KChIP					Caspase3, presenilin	-
CARMA1		Cytoplasma PM	Cytoplasm, PM						PDK1	Bcl10	+
CIB1	EF hands		Cytoplasm, ER, Golgi, Nucleus						FAK	Rac3, Pax3	-
CrkII			Cytoplasm Nucleus, PM						Abl, FAK, MAP4K5	Grb2, p130Cas	+
Filamin A	↔ CaR		Cytoplasm Nucleus		K^+-channel				MAPK, FAK, PKA	RhoA, caveolin1, ROCK	+

Scaffold	Ca^{2+} binding	Trans-location	Location	↔ Cyto-skelet.	↔ ion channels	↔ PKC	↔ CREB	↔ Inte-grins	↔ Kinases	Other interaction Partners	Ea.hy Expr.
GIPC			Cytoplasm, PM						TrkA	GAIP, TGFR	+
Homer1			Cytoplasm, ER, Nucleus		RyR				PI3K	TRPC, PIKE	+
IQGAP1	CaM		Cytoplasm, PM, Golgi		Cl^--channel				PKA, ERK2	S100, AKAP, E-cadherin, catenin	+
MAGI-1			PM	actin	Cl^--channel					Actinin, Catenin, JEAP, ESAM	+
MAGI-3			Nucleus, PM							RTPT, TGFβ	-
MIRO 1	EF hands		Mitochondria								+
MIRO 2	EF hands		Mitochondria								+
MORG1			Cytoplasm						MAPK	unknown	-
MP1			Cytoplasm, Endosomes	actin					MEK1, ERK1/2	KSR2	+
NHERF-2			Cytoplasm		TRPC, Na^+/H^+ ex.				ERK, c-scr	AKAP, Gq_α, NOS β-catenin	+
POSH			Cytoplasm						JNK, MAPK, PKB	RACGAP1, Akt2	+
RAB11FIP2			PM, Cytoplasm, Endosomes							RAB11, 14-3-3γ, RAB11FIP4,	+
RAB11FIP5			PM, Mitochondr. Endosomes,	γ-tubulin						RAB11, γ-SNAP, 14-3-3γ	+
RACK1			Cytoplasm Nucleus, PM		IP3R				c-scr, Raf1, TYK2, JAK1	RACGAP, GRID, TNFR, NHERF	+
RGS2	CaM		Cytoplasm Nucleus, PM						PKG1	Gq_α, Gs_α	+
RGS5			Cytoplasm Nucleus, PM						MAPK	Gi_α, Go_α, CB1R	+
SKRP1			Cytoplasm						ASK1, MKK7	unknown	+
Sorcin	EF hands	Ca, pH dep.	Cytoplasm, PM		L-Type Ca-ch., RyR					Grancalcin, Annexin	+
Striatin	CaM									Caveolin, PP2A	+
Tamalin			Cytoplasm, PM		HCN				c-scr, Fyn, CASK	Cytohesin, SHP2	-
Vinexin ß			PM						ERK1/2, FAK, JNK, PKA, PAK	Vinclulin, Sos, Cbl	+

Table 20: List of putative Ca^{2+}-activated Scaffolds from Bioinformatic Research

4.2.1 Identification of Gaf1 gene expression in various human cell lines

Reverse Transcription-PCR was performed to investigate gene expression of Gaf1 in Ea.hy926, human umbilical vascular endothelial cells (HUVEC), human uterine artery endothelial cells (HUtAEC), ECA, ECV and HeLa cells.

Using the Advantage® cDNA PCR Kit, the gene expression of Gaf1 was detected with two different primer pairs in a 40 cycle PCR experiment. The primer pairs used were found to yield amplification products of the expected sizes in all human cell lines tested (Figure 47).

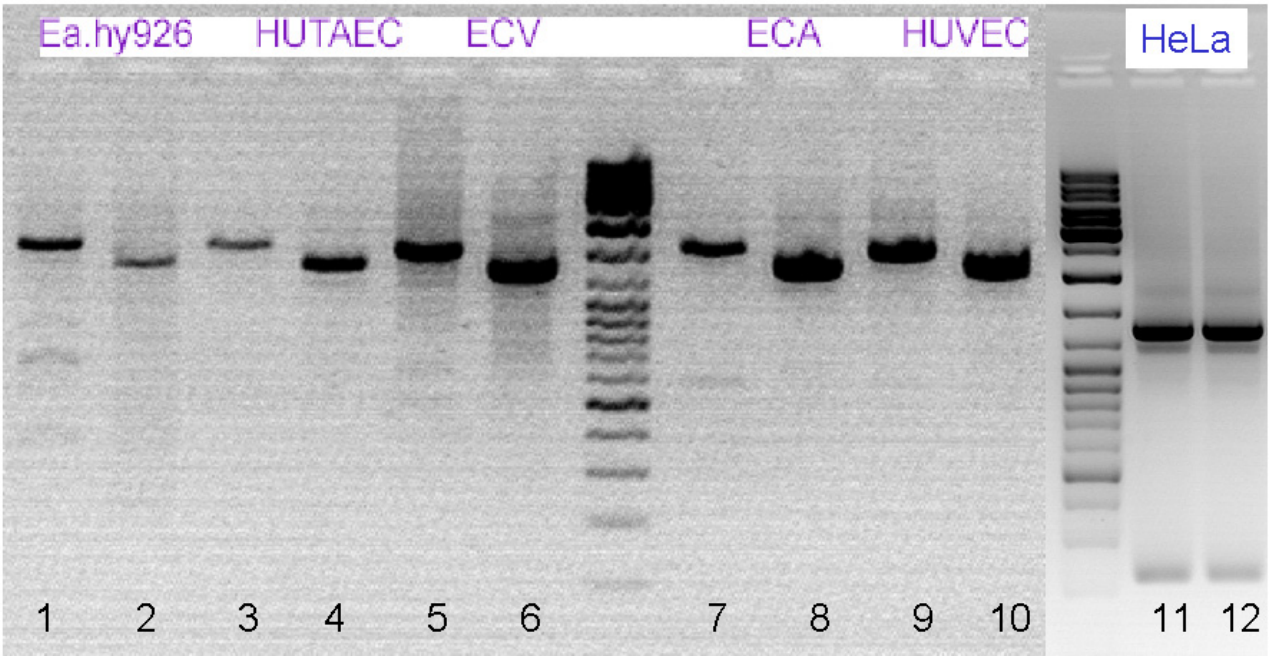

Figure 47: Gaf1 mRNA expression in various human cell lines
The representative agarose gel photographs demonstrate Gaf1 identification using Gaf1 gene specific detection/expression primers and cDNA-templates derived from Ea.hy926 (lanes 1,2), HUtAEC (lanes 3,4), ECV (lanes 5,6), ECA (lanes 7,8), HUVEC (lanes 9,10) and HeLa cells (lanes 11,12). The Gaf1 lacking the C2-domain sequence was amplified using the primers (Gaf1xC2 *for* and Gaf1c *rev*) resulting in the expected products of 1531 base pairs (Gaf1xC2, lanes 1, 3, 5, 7, 9). As another control the various cDNA were additionally tested using a different primer pair (Gaf1b *for* and Gaf1c *rev*) for the amplification of a 1316 base pair containing gene fragment (Gaf1h with Bam HI site, lanes 2, 4, 6, 8, 10, 11, 12).

4.2.2 Validation of siRNA against Gaf1

The efficiency of the siRNA (Table 4) to knock down Gaf1 was validated by RT-PCR experiments in comparison to cells, which were transfected with a Negative Control siRNA (Table 4) as described previously (3.2.11). Accordingly the mRNA level of Gaf1 was about 52 % decreased in Ea.hy926 cells and even 65 % downregulated in HeLa cells (Figure 48).

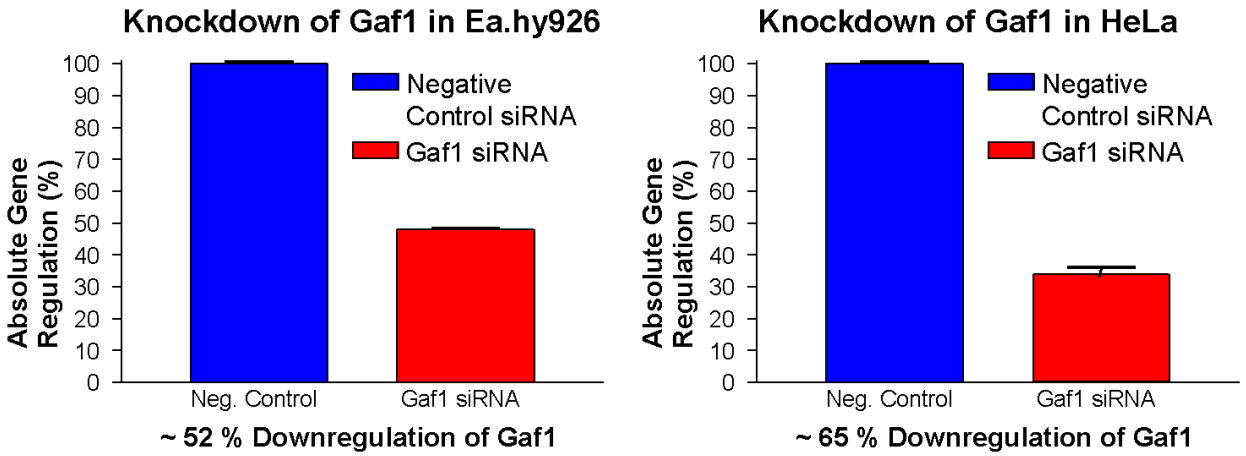

Figure 48: Validation of siRNA against Gaf1 in Ea.hy926 or Hela
Downregulation of Gaf1 in Ea.hy926 (n=5, P<0.005) or HeLa cells (n=4, P<0.05) 42 hours after transfection of siRNA against Gaf1 versus Negative Control siRNA

4.2.3 Cloning of Gaf1 and γ-SNAP expression vectors

The total coding sequence from the open reading frame (ORF) of Gaf1 has a length of 1961 base pairs. Several cloning strategies had been planned to clone this sequence or a part of it into the pBudCE 4.1 expression vector: On the one hand it was considered to construct a plasmid containing the full length Gaf1 sequence without its stop codon fused to a GFP at its C-terminal end to visualize expression of Gaf1; on the other hand to clone the full length Gaf1 without tag for overexpression studies regarding intracellular calcium measurements. Additionally, it was thought of creating a Gaf1 construct lacking in its C2 domain and either fused to the GFP or not to compare it with the full length Gaf1 expression patterns and calcium measurements in the overexpression studies. Due to the highly enrichment of GC bases in the N-terminal part of the Gaf1 coding sequence, it was neither possible to amplify the full length sequence nor the 662bp Gaf1a fragment (Gaf1a *for* containing overhang with HindIII restriction site, Gaf1a *rev*) from any cDNA template. According to that, the Gaf1a and the Gaf1h (Gaf1b *for*, Gaf1c *rev* containing overhang with a XbaI restriction site) fragments were amplified out of the Ultimate™ Human ORF Clone ID IOH27179 (Invitrogen Inc.) that contain the full length cds of Gaf1 in pENTR™221 vector (Figure 49A). In order to the BamHI restriction site of Gaf1 at position 651/655, the two fragments obtained were restricted and ligated in a three point ligation into the pBudCE 4.1 vector or in the pBudCE4.1 containing the citrine Sequence (Bam HI/Eco RI, Figure 44 and 45), respectively. Whereas the Gaf1 C2 domain lacking fragment (Gaf1XC2: Gaf1XC2 *for* containing an overhang with a HindIII restriction site and an ATG start codon, Gaf1c *rev*) was amplified out of a cDNA derived Ea.hy926 (Figure 49B) and cloned like the full

length Gaf1. Additionally the most prominent interaction partner of Gaf1, γ-SNAP, was amplified and fused with either citrine or CFP into the pBudCE4.1 vector (Figure 49C).

To sum up, 6 different plasmids were constructed (1-6 or Figure 49D and 49E):

1. Gaf1
2. Gaf1-citrine
3. Gaf1XC2
4. Gaf1XC2-citrine
5. γ-SNAP-CFP
6. γ-SNAP-citrine

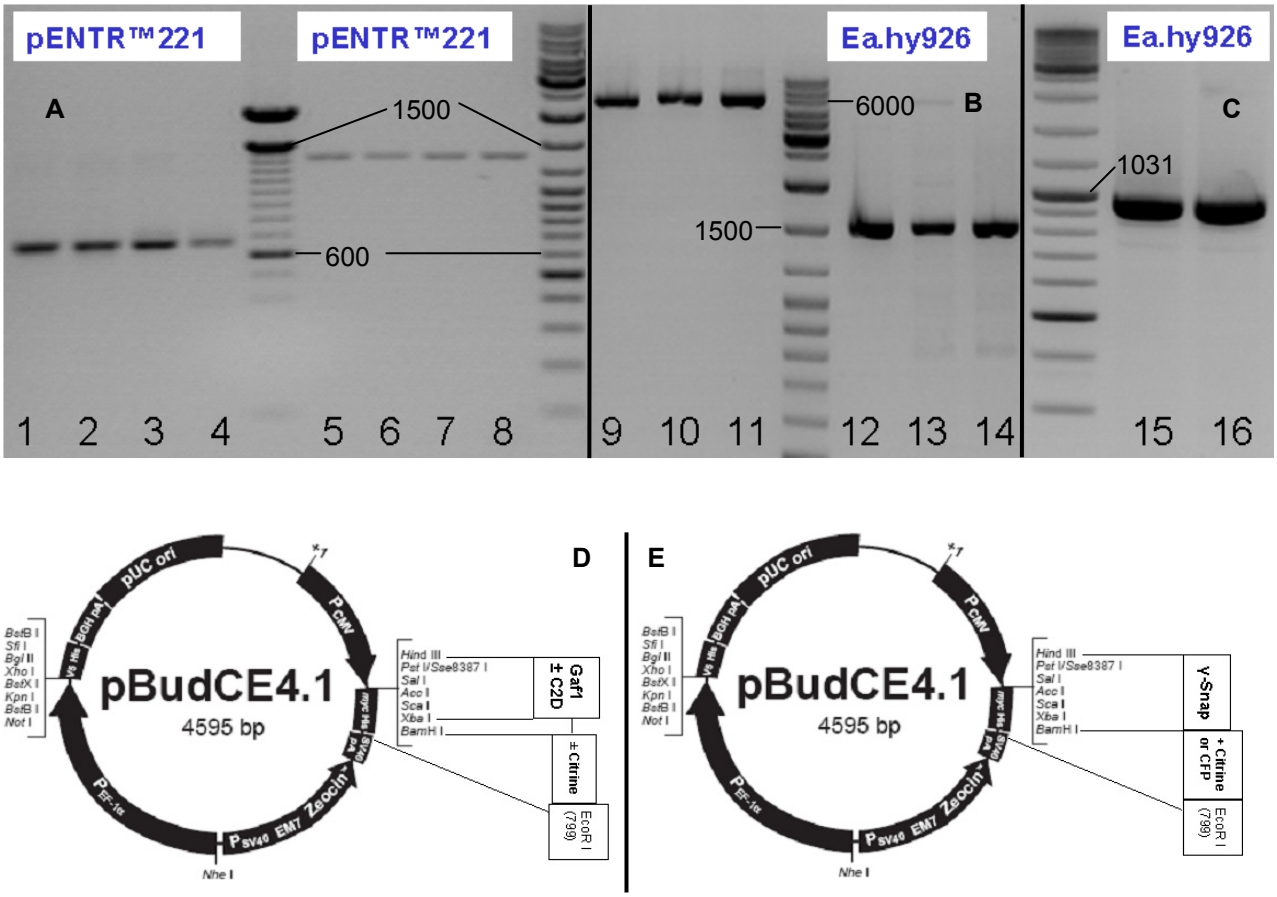

Figure 49: Cloning of Gaf1 and γ-SNAP
A-C: Representative agarose gel photographs demonstrating restricted gene fragments derived from cDNA templates highlighted above: **A:** Gaf1a restricted HindIII / BamHI (lanes 1-4: ~660 bp) and Gaf1h restricted BamHI / XbaI (lanes 5-8: ~ 1320 bp) **B:** pBudCE4.1 containing citrine HindIII / XbaI (lanes 9-11: ~ 5200 bp) and Gaf1XC2 HindIII / Eco RI (lanes 12-14: ~ 1500 bp) **C:** γ-SNAP restricted HindIII / BamHI (lanes 15,16: ~ 940 bp).
D,E: Gene maps of pBudCE4.1 containing either GFP-fused or non-fused genes at the CMV cloning site: **D:** Gaf1 overexpression vector, Gaf1XC2 overexpression vector, Gaf1-citrine fusion protein construct and Gaf1XC2 fusion protein construct. **E:** γ-SNAP-citrine and γ-SNAP-CFP fusion protein constructs.

4.2.4 Protein expression

In a first series of experiments, the expression and intracellular distribution of Gaf1 and γ-Snap were tested. Either Ea.hy926 or HeLa cells were transiently transfected with the Citine-tagged construct of Gaf1 or γ-SNAP and analyzed by digital imaging microscopy 48 hours after transfection. In order to observe any co-localization of Gaf1 or γ-SNAP

with mitochondria, these were either visualized by the co-transfection of mtDSRed or using the specific mitochondrial dye mito-tracker red® (Molecular Probes).

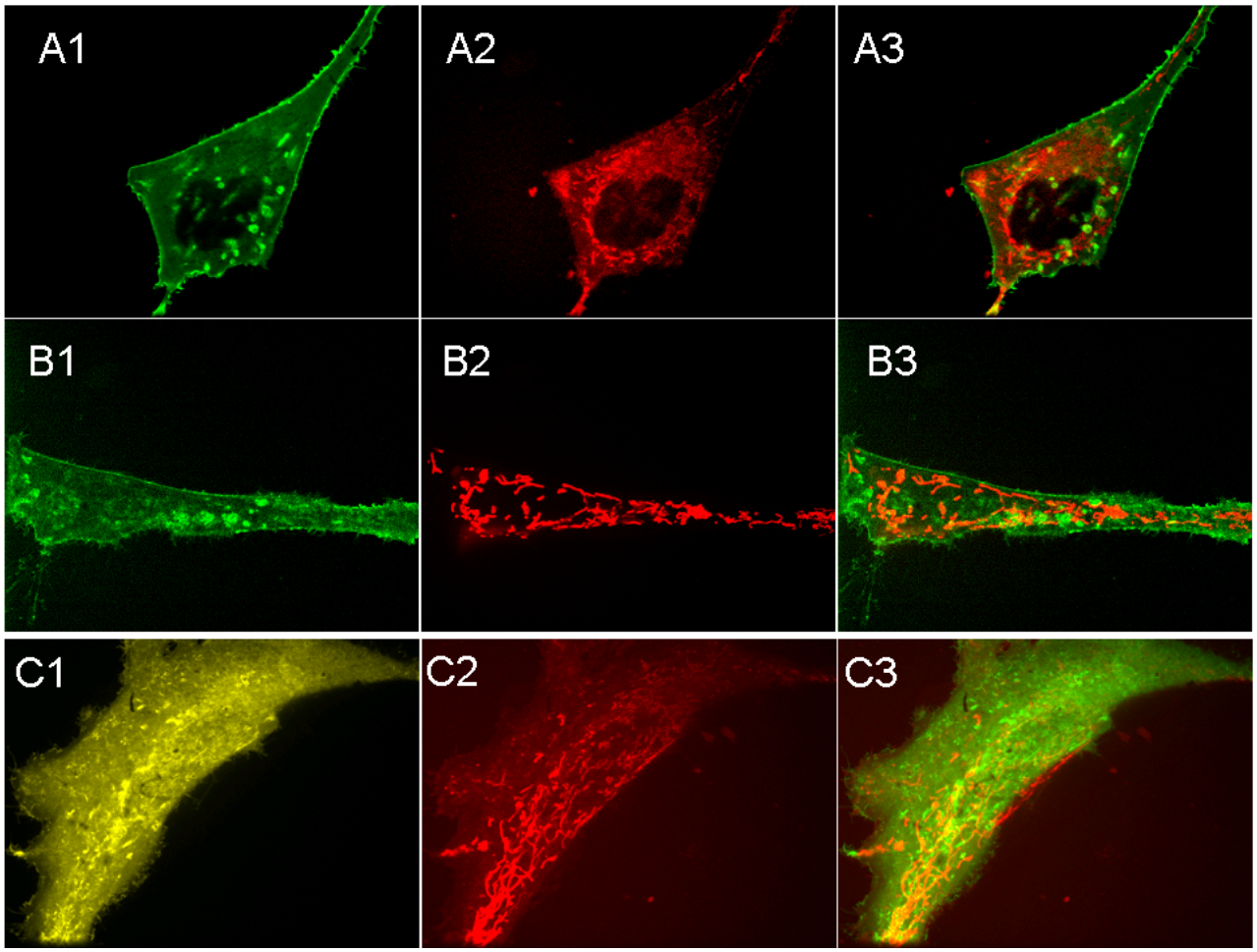

Figure 50: Targeting of citrine-fusion proteins and colocalization with mitochondria
A: Co-expression of Gaf1-citrine and mitoDSRed in Ea.hy926 cells
A1: Gaf1-citrine **A2:** mtDSRed **A3:** Overlay
B: Co-expression of Gaf1-citrine and mitoDSRed in HeLa **B1:** Gaf1-citrine **B2:** mtDSRed **B3:** Overlay
C: Expression of γ-SNAP-citrine, mitochondria stained with mito-tracker red® in Ea.hy926 cells
C1: γ-SNAP-citrine **C2:** mito-tracker red® visualized mitochondria **C3:** Overlay

The overexpression of the citrine-tagged Gaf1 or C2 domain lacking Gaf1 (not shown) resulted in similar protein expression patterns. Both were found out to be primarily localized in the plasma membrane of Ea.hy926 or HeLa cells, but secondary in intracellular compartments, which partially colocalized with mitochondria. However these data may also indicate that Gaf1 is part of a machinery linking mitochondria to the plasma membrane (1.3; 1.5).

In contrast, the protein expression of γ-SNAP was observed to be rather cytosolic but structurally shaped and partially colocolized with mitochondria, too.

4.2.5 Impact of Gaf1 on Mitochondrial Motility

In order that Gaf1 was described to interact with γ-tubulin like mitochondria were demonstrated to do we intended to test whether or not Gaf1 is involved in mitochondrial motility. Therefore HeLa cells were co-transfected with mtDSRed and siRNA against Gaf1 or Negative Control siRNA and monitored 42 hours after transfection. In response to 100 µM histamine mitochondrial motility was slightly influenced in cells that were Gaf1 downregulated, while mitochondria nearly stopped their activity in control cells. More precisely after analysis of the mitochondrial movements it was found out, that the minimal motility was about 80 % of the resting state in case of Gaf1 silenced cells, while it was about 40 % in case of control cells (Figure 51).

Additionally, for both conditions, this effect was reversible as mitochondria continued their movements like in the pre-treated state after histamine was washed out.

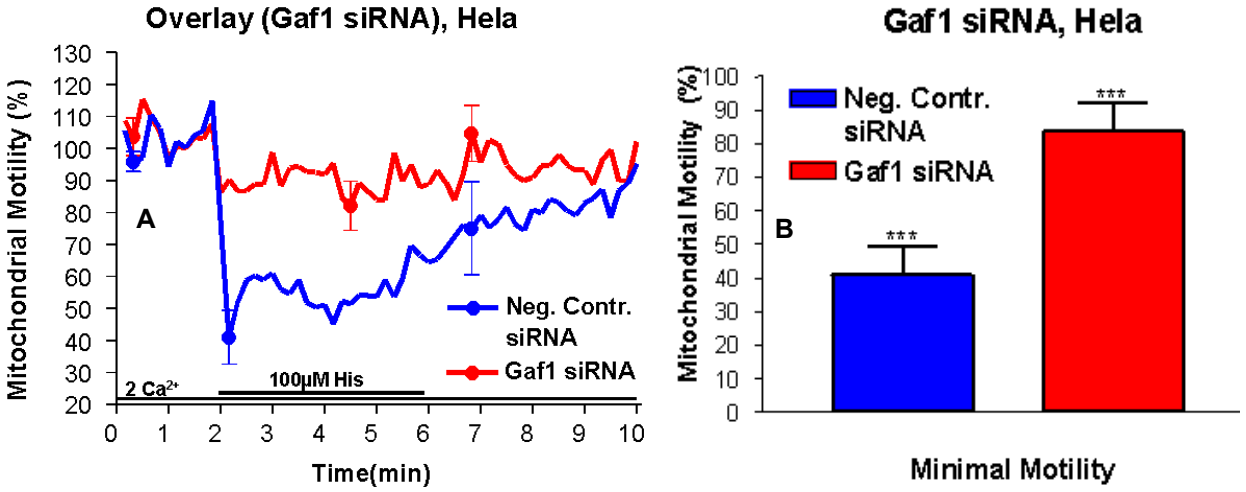

Figure 51: Mitochondrial Motility in response to histamine
A: Measurement of mitochondrial movements in HeLa cells transfected with the siRNA against Gaf1 (n=7) or Negative Control siRNA (n=7). Overlay of 60 individual two time-lapse confocal images (Δt=10 s) of mitoDSRed fluorescence in a live cell before and after stimulation by 100 µM Histamine.
B: In the average mitochondrial motility was decreased about 60 % compared to the resting state in control cells (blue bar), while it was just about 20 % decreased in Gaf1 downregulated cells

In order to verify the reason for this significant difference in mitochondrial motility in response to histamine, two models were established, that may cause this dramatic effect of increased motility in the absence of Gaf1:

1. The increased mitochondrial motility in Gaf1-silenced cells results in diminished Ca^{2+} entry (Figure 52).

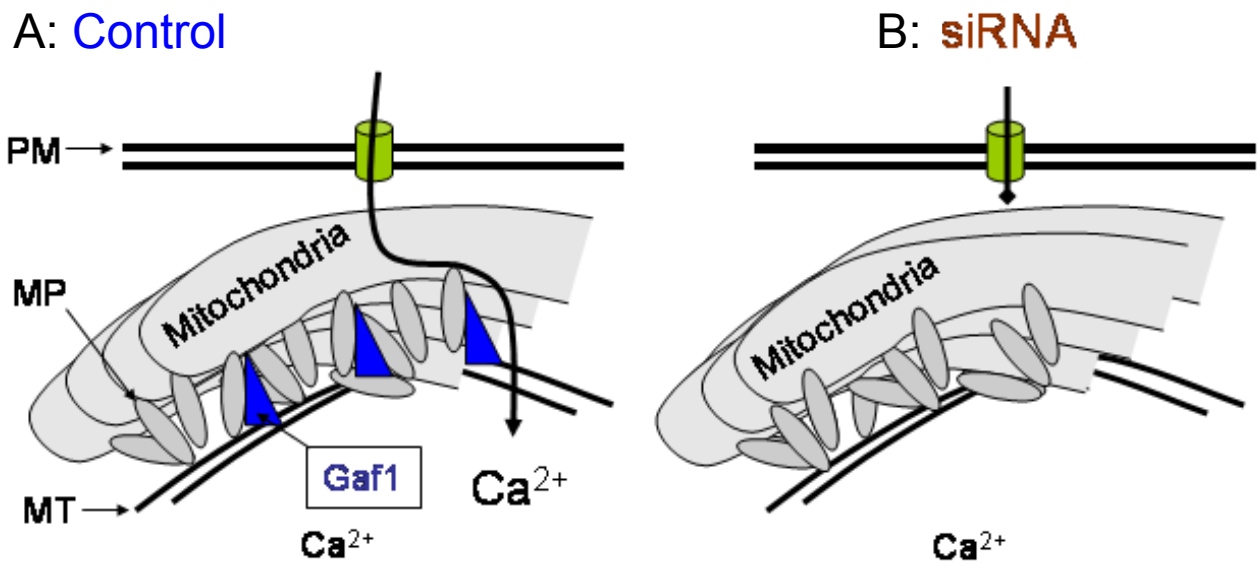

Figure 52: Scheme for Model 1
A: Gaf1 (blue triangles) acting as a linking protein between microtubles (MT) and motor proteins (MP) of mitochondria. Under this condition Gaf1 arrest mitochondria via its motor proteins (MP) and Ca^{2+} may enter easily through a plasma membrane Ca^{2+}-channel (yellow ton).
B: In the absence of Gaf1 mitochondria are able to continue their movements and therefore the probability of Ca^{2+} to enter is lower.

2. The diminished Ca^{2+} entry in Gaf1-silenced cells results in reduced mitochondrial deceleration (Figure 53).

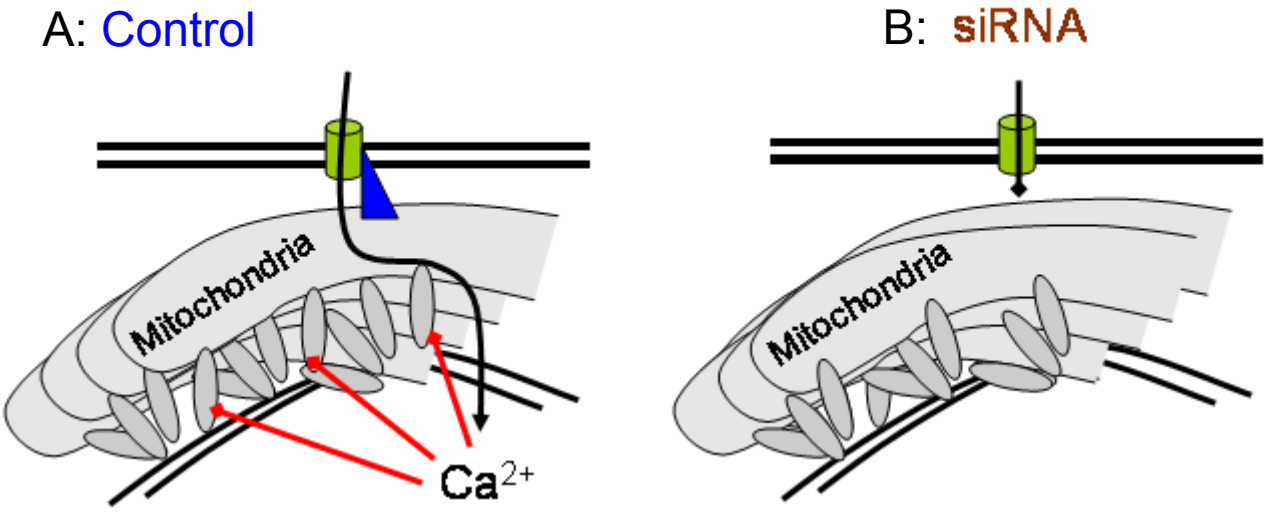

Figure 53: Scheme for Model 2
A: Gaf1 acting as a linking protein between mitochondria and a plasma membrane Ca^{2+}-channel. Under this condition Ca^{2+} may enter easily through the plasma membrane Ca^{2+}-channel and the increased Ca^{2+}-level might be responsible to arrest mitochondria.
B: In the absence of Gaf1 the probability for the Ca^{2+}-entry is lower and therefore mitochondria are rather able to fulfill their movements.

In order to exclude one of these models, it was considered to observe mitochondrial motility, while titrating calcium at various concentrations in the physiological range (0, 300, 500, 1000 nM). According to Yi M. et al., *The Journal of Cell Biology* **167(4)**: 661-

672, 2004, cells were treated with ionomycin (Iono), a Ca^{2+} ionophore that allows both Ca^{2+} release from intracellular stores and Ca^{2+} entry from the extracellular bathing medium to elevate $[Ca^{2+}]_c$. When EGTA and Iono were added together to nonstimulated cells the $[Ca^{2+}]_c$ was lowered to 0 and no change in mitochondrial movement activity was observed, suggesting that the motility was maximal at the resting level of under this condition. To adjust the desired calcium of any other concentrations in this buffer (5 mM EGTA, 138 mM NaCl, 1 mM $MgCl_2$, 5 mM KCl, 10 mM Hepes, 10 mM D-glucose, 3 µM Ionomycin), which is equivalent to 0 nM Ca^{2+}, different volumes of a 1 M $CaCl_2$ solution were added according to the volumes, that were calculated by the winmaxc software. Subsequently after readjusting the pH to 7.4 the buffers containing 300 nM, 500 nM and 1000 nM Ca^{2+} were obtained. These buffers ensured measurements of mitochondrial motility under conditions of clamped cytosolic Ca^{2+} with different concentrations.

Regarding the proposed model 1:
Under conditions of clamped cytosolic Ca^{2+} concentration, silencing of Gaf1 should still result in a reduced mitochondrial deceleration.
Thus, Gaf1 should attenuate the apparent Ca^{2+} sensitivity of moving mitochondria.

According to model 2:
Under conditions of clamped cytosolic Ca^{2+} concentration, silencing of Gaf1 should not have any impact on mitochondrial deceleration.
Thus, Gaf1 should not affect the apparent Ca^{2+} sensitivity of moving mitochondria.

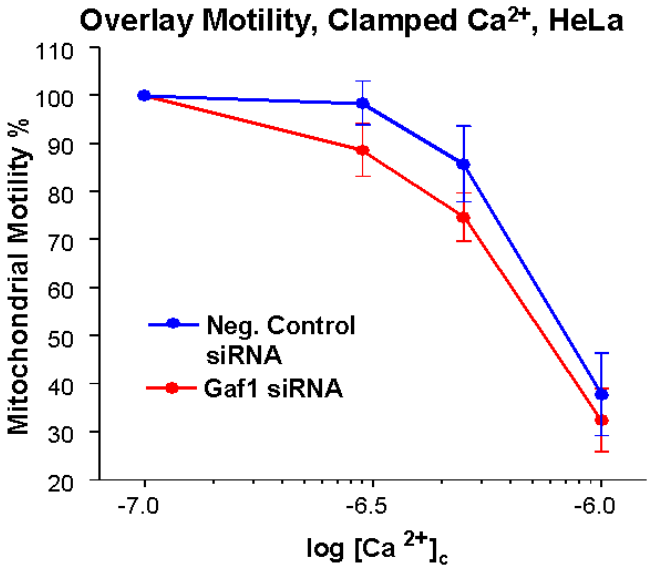

Figure 54: Relationship between $[Ca^{2+}]_c$ and mitochondrial motility
Stepwise increases in $[Ca^{2+}]_c$ induce stepped decreases in mitochondrial motility. MitoDSRed-expressed HeLa cells transfected with siRNA against Gaf1 or Negative Control siRNA were incubated in free extracellular medium supplemented with 5 mM EGTA and 3 µM Iono for 3 minutes. Simultaneous measurements of mitochondrial motility were performed in single cells exposed to stepped increases of extracellular Ca^{2+} from 0 – 1000 nM. After 1 minute incubation in the particular Ca^{2+}-concentration, mitochondrial motility was recorded in 3 minute mitochondria moving analyzes. The mean mitochondrial motility inhibition was plotted (n=6 cells for each Negative Control siRNA and Gaf1 siRNA).

As a result to the titration of Ca^{2+}, there was no significant difference in mitochondrial motility between Control and Gaf1-silenced cells under conditions of clamped cytosolic Ca^{2+}. According to that, it was concluded that the scheme for model 2, that was presented in Figure 53 rather confirm to the function of Gaf1 to be responsible for the reduced mitochondrial deceleration in response to histamine.

Thus, this result indicated, that Gaf1 elevates the concentration of intracellular Ca^{2+}. Accordingly Ca^{2+}-measurements were performed to verify the impact of Gaf1 on Ca^{2+} recycling in cells.

4.2.6 Impact of Gaf1 on Cytosolic Calcium

Measurements of Cytosolic Calcium ($[Ca^{2+}]_c$) were performed after Fura2-AM loading as described. To verify any changes in $[Ca^{2+}]_c$, Ea.hy926 or HeLa cells were transfected with either the siRNA against Gaf1 for knockdown experiments or with the Gaf1 plasmid for overexpression studies. For both conditions the effect of 100 µM histamine was measured once in a Ca^{2+} environment using the CB (Figure 55A) and once in a Ca^{2+} free environment using the EB (Figure 55B,C).

Additionally the Ca^{2+} influx was observed after the depletion of Ca^{2+} from intracellular stores upon histamine stimulation (Figure 55B,C).

$[Ca^{2+}]_c$-measurements revealed, that Ea.hy926 cells transfected with Gaf1 siRNA, significantly reduced cytosolic calcium concentration in the presence of 2 mM Ca^{2+}, when stimulated with 100 µM histamine, whereas in Gaf1-overexpressed cells it was elevated.

Moreover it was shown, that under nominal Ca^{2+}-free condition the intracellular Ca^{2+}-release upon histamine stimulation was not influenced, whereas $[Ca^{2+}]_c$ was either reduced about 41 % in Gaf1 silenced HeLa cells or elevated about 45 % after readdition of 2 mM Ca^{2+}, when Gaf1 was overexpressed (Figure 55D).

According to the predicted interaction partner of Gaf1, γ-SNAP, the described experiments were also performed for measuring $[Ca^{2+}]_c$ after the co-transfection of Gaf1 and γ-SNAP, but no differences were observed. Cells that were overexpressed with these two proteins showed a similar increase in $[Ca^{2+}]_c$ elevation as the overexpression of Gaf1 alone (graph not shown).

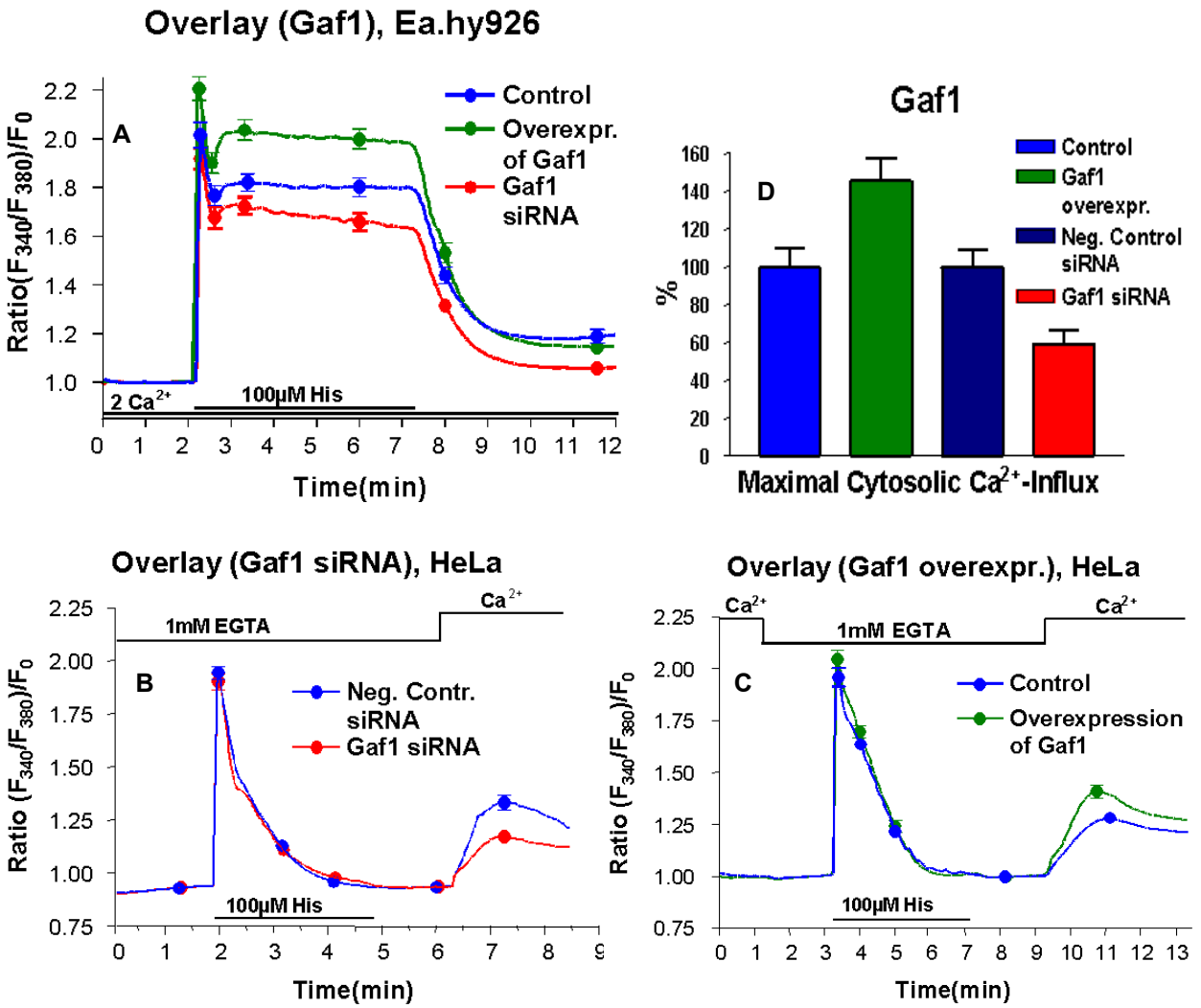

Figure 55: Effect of Gaf1 silencing and overexpression on $[Ca^{2+}]_c$
A: Impact of Gaf1, overexpressed (n=16) or silenced (n=10) in Ea.hy926 cells versus control (n=18), in the presence of 2 mM Ca^{2+} upon 100 µM Histamine stimulation; **B:** Downregulation (n=37) versus Control (n=44) or **C:** Overexpression (n=48) versus Control (n=49) of Gaf1 in HeLa cells. Under a nominal Ca^{2+}-free condition no changes in $[Ca^{2+}]_C$ were observed on intracellular Ca^{2+} depletion upon 100 µM histamine, but significant differences were obtained after the readdition of 2 mM Ca^{2+}. **D:** Overexpression of Gaf1 revealed ~ 145 % of max. $[Ca^{2+}]_C$-Influx, whereas silencing of Gaf1 reduced it to ~ 59 % in comparison to their controls.

4.2.7 Impact of Gaf1 on Mitochondrial Calcium

In order, that close associations between subdomains of the plasma membrane and mitochondria seem to be important for the control of Ca^{2+}-entry (1.5), mitochondrial calcium, $[Ca^{2+}]_{mito}$, was measured. Therefore the siRNA against Gaf1 or the overexpression plasmid of Gaf1 were either co-transfected with mtRP in Hela (Figure 56B,C) or transfected into C8 cells, which are mtRP stable transfected Ea.hy926 cells (Figure 56A). Changes in $[Ca^{2+}]_{mito}$ were monitored under the same conditions used for $[Ca^{2+}]_c$-measurements.

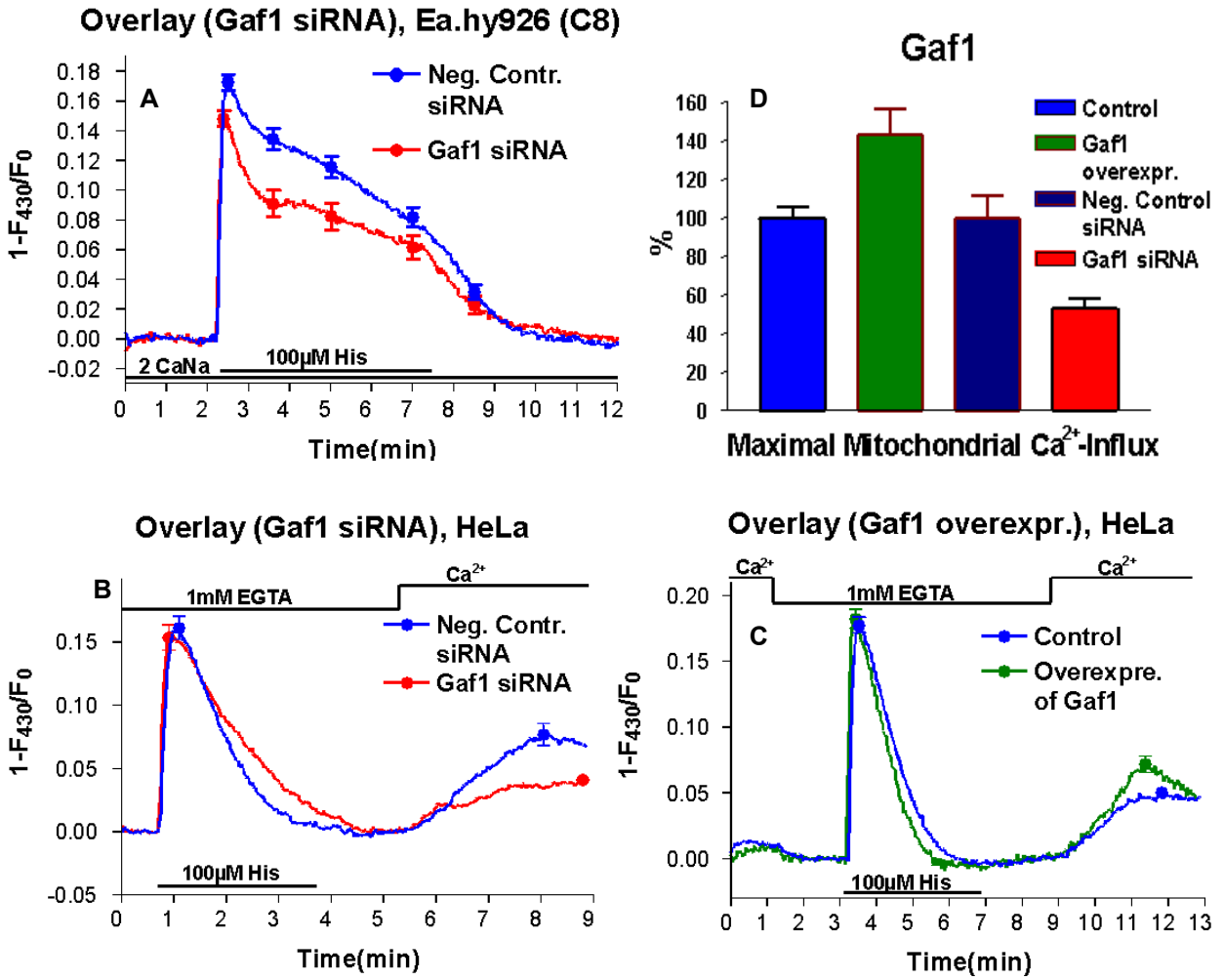

Figure 56: Effect of Gaf1 silencing and overexpression on $[Ca^{2+}]_{mito}$
A: In the presence of 2 mM Ca^{2+} C8 cells transfected with the siRNA against Gaf1 (n=66) showed a reduced elevation of $[Ca^{2+}]_{mito}$ in response to 100 µM histamine compared to control (n=52) **B,C:** Under nominal Ca^{2+} free condition neither Gaf1 silencing nor Gaf1 overexpression had an impact on the intracellular Ca^{2+} release to mitochondria upon histamine in HeLa cells. **B:** While after readdition of 2 mM Ca^{2+} $[Ca^{2+}]_{mito}$ was reduced in Gaf1 silenced cells (n=42) compared to Control (n=47); **C:** whereas it was increased, when Gaf1 was overexpressed (n=32) versus Control (n=67). **D:** Overexpression of Gaf1 revealed ~ 143 % of max. $[Ca^{2+}]_{Mito}$-Influx, whereas silencing of Gaf1 reduced it to ~ 53 % in comparison to their controls.

$[Ca^{2+}]_{mito}$-measurements revealed similar results to $[Ca^{2+}]_c$-measurements as the impact of Gaf1 was resulting in a change of the Ca^{2+}-Influx, but not in Ca^{2+}-release. Accordingly the maximal mitochondrial Ca^{2+}-accumulation in response of Ca^{2+}-influx was either decreased about 47 % in case of Gaf1 silencing or increased about 43 % in case of Gaf1 overexpression (Figure 56D).

4.2.8 Impact of Gaf1 downregulation on ER Calcium

A close association between subdomains of the ER and the mitochondrial surface appears to be necessary for the propagation of ER Ca^{2+} release to the mitochondria (1.6).

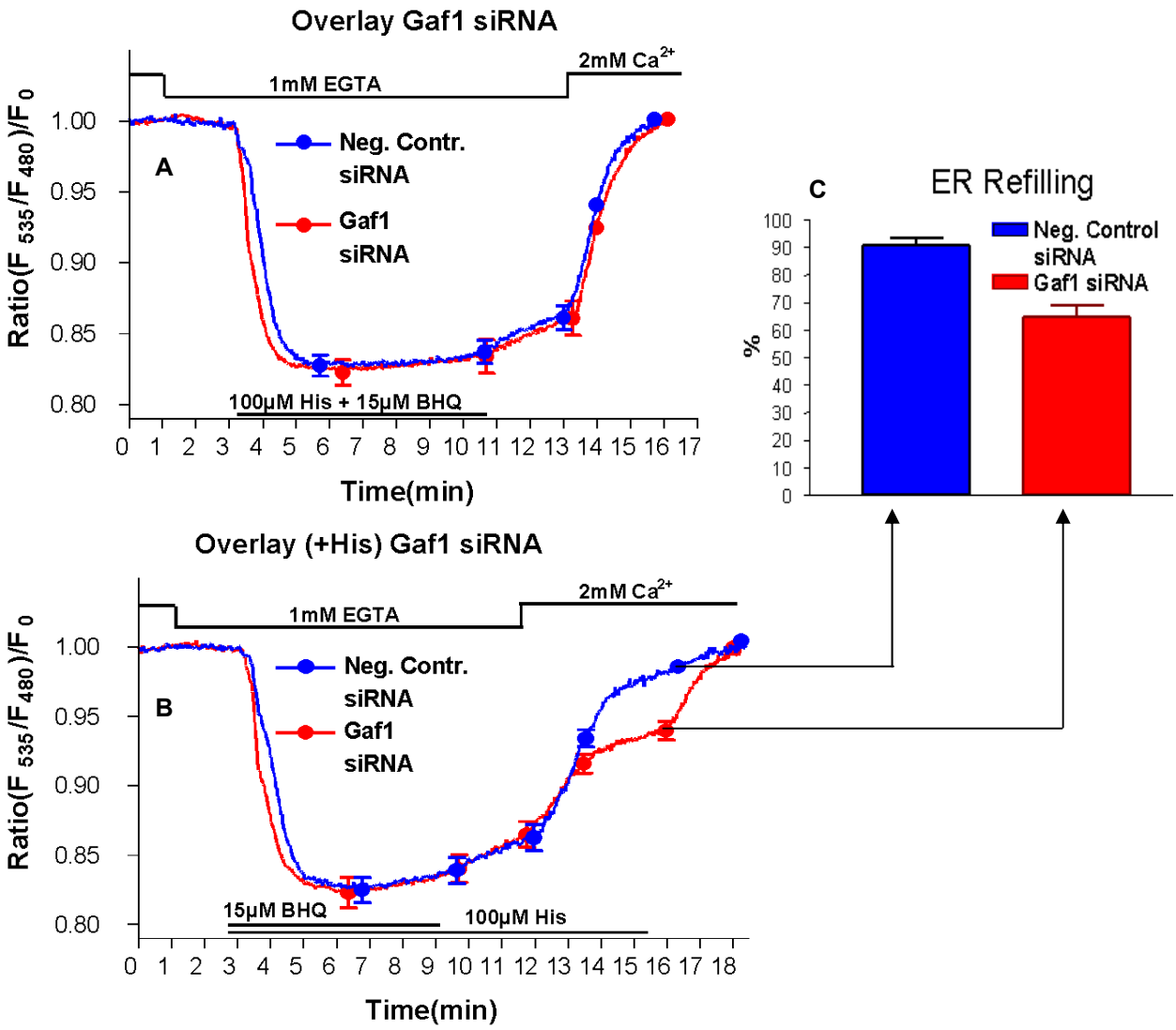

Figure 57: Effect of Gaf1 silencing on $[Ca^{2+}]_{ER}$
A: No differences in $[Ca^{2+}]_{ER}$ were observed in Ea.hy926 cells transfected with siRNA against Gaf1 (n=10) or Negative Control siRNA (n=9) upon ER-Refilling in the absence of histamine. **B:** ER-Refilling in the presence of histamine resulted in a reduced ER-refilling in Gaf1 downregulated cells (n=15) versus Control (n=13). **C:** At a particular point of time ER was just about 65 % refilled in case of Gaf1 silenced cells, while it was nearly fully refilled about 91 % in Control.

ER Ca^{2+} refilling requires trans-mitochondrial Ca^{2+} flux, whereas in the absence of the agonist, the ER refills independently of mitochondria (Malli R. et al., *The Journal of Biological Chemistry* **288(13)**: 12114-12122, 2005). Furthermore it was demonstrated that mitochondrial Ca^{2+} buffering is essential to maintain Ca^{2+} flux from the extracellular area and to ensure Ca^{2+} filling of the ER during cell stimulation (Malli R. et al., *Cell Calcium* **41**: 63-76, 2007).

Regarding the results, that knockdown of Gaf1 significantly reduced the mitochondrial uptake of entering Ca^{2+}, the impact of Gaf1 on $[Ca^{2+}]_{ER}$ was measured after co-transfecting Ea.hy926 cells with the siRNA against Gaf1and D1ER. $[Ca^{2+}]_{ER}$ was depleted in the absence of extracellular Ca^{2+} upon 100 µM histamine plus 15 µM BHQ.

Downregulation of Gaf1 had no effect on ER depletion concluding, that the transfer of Ca^{2+} from the ER towards the mitochondria was unaltered (Figure 57A,B). On the one hand ER was refilled in the absence of histamine (Figure 57A) and on the other hand in the presence of histamine (Figure 57B). Accordingly it was shown that exclusively the mitochondrial dependent ER Ca^{2+} refilling was about 26 % diminished in cells treated with siRNA against this Gaf1 (Figure 57C).

4.2.9 Gaf1 as a putative interaction partner of ORAI1

As a consequence of the obtained results it was suggested, that Gaf1 is an essential component of focal contact sites between a Ca^{2+} entry channel and mitochondria. To verify a possible interaction partner of Gaf1 on the plasma membrane site the recently identified Ca^{2+} entry channel ORAI1 (Zhang SL. et al., *PNAS* **103(24)**: 9357-9362, 2006) was considered. Accordingly, colocalization studies between these two proteins were performed. Therefore, the Gaf1-citrine construct was co-transfected in Ea.hy926 cells with an ORAI1-CFP plasmid obtained from the Institute of Biophysics, Linz. The overexpression patterns of these two C-terminal tagged GFP fused proteins were monitored using the ACLSM system. Accordingly Gaf1-citrine or ORAI1-CFP expression were visualized at $\lambda_{Em.}$= 535 nm after the excitation of $\lambda_{Exc.}$= 488 nm exposed to the YFP for 3.8 seconds or $\lambda_{Exc.}$= 457 nm exposed to the CFP for 9.8 seconds (Figure 58A-C).

The expression surface area of ORAI1 was shown to be a little bit larger compared to that of Gaf1. However, to resolve this difference, two colocalization studies had been performed; once to colocalize the expression pattern of ORAI1 in relation to that of Gaf1 and once to colocalize the Gaf1 area in relation to that of ORAI1 (Figure 58D-F).

These resulted in a 52.54 % coverage of pixels, when ORAI1 was colocalized with Gaf1, and in a 79.57 % coverage, when Gaf1 was colocalized with ORAI1. All colocalization studies were performed by Malli R.

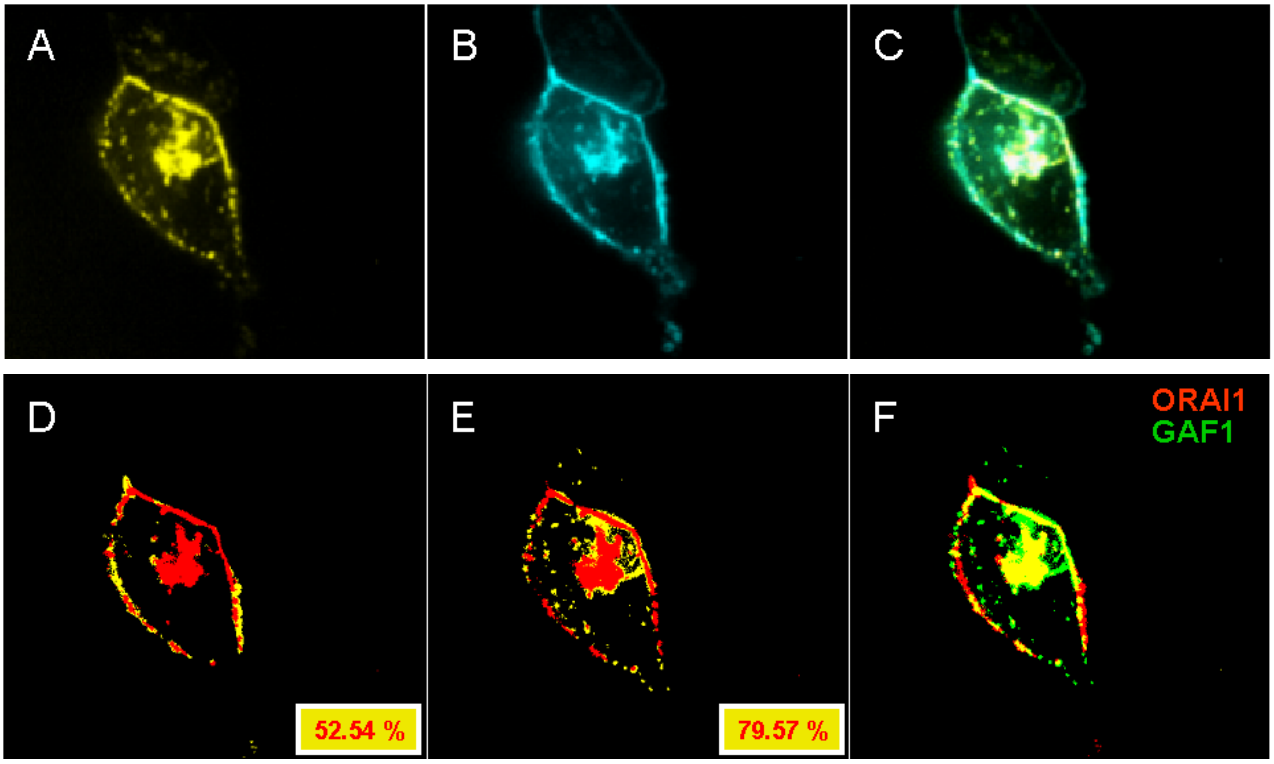

Figure 58: Colocalization of Gaf1 and ORAI1
A: Overexpression of Gaf1-citrine **B:** Overexpression of ORAI1 **C:** Merge
D: Colocalization of ORAI1 with Gaf1 **E:** Colocalization of Gaf1 with ORAI1 **F:** Merge

5 Discussion

The transmission of extracellular signals into the cell is induced by various agonists or antagonists that bind to specific transmembrane receptors and trigger a controlled signal transduction, that selectively regulates cell growth, cell division, migration or adhesion, as a prerequisit for the maintenance of cell viability or cellular response to stimuli. Accordingly, the intracellular signal transduction is accomplished by the formation of protein associations or multiprotein complexes that need to be controlled by so called scaffold proteins. Although the functional principles of scaffolds has been well characterized so far, there are just a few identified to date. Despite their importance to regulate or facilitate signaling events in cells is indisputable, their structures and the presence of functional domains are manifold. Nevertheless, they all have in common to bring single interactors (client proteins) together to establish the desired effect for the cell: (A) Scaffolds can regulate the combination of single interactors to force a directed protein-protein-interaction. (B) The allosteric activation of client proteins can result in an amplified effect upon their binding to a scaffold. (C) The local effect of a signal can be limited to a distinct cell compartment upon the interaction of a scaffold with a membrane adaptor protein.
Accordingly, scaffold proteins serve as interaction platforms for protein-protein-interactions and as anchors for the localization of large signaling protein complexes.

In the present study, the identification of new putative Ca^{2+}-dependent scaffold proteins or their clients was performed using two approaches, a proteomic and a bioinformatic approach. Several strategies have been applied for these, including:

Proteomic approach:
1. Identification of putative plasma membrane scaffolds
2. Identification of putative membrane scaffolds
3. Identification of putative nuclear scaffolds

Bioinformatic approach:
1. Selection of Gaf1 as a putative scaffold protein
2. Overexpression of Gaf1
3. Overexpression of Gaf1 lacking C2 domain
4. Knockdown of Gaf1 expression by siRNA techniques

5.1 Proteomic approach

In the proteomic approach Ea.hy926 cells were activated with the IP_3-generating agonist histamine that may initiate the formation of Ca^{2+}-dependent multiprotein complexes. The recruitment of proteins to form these signalplexes results in their translocation to distinct organelles. In our studies it was investigated to identify such translocated proteins (or protein complexes) to their cellular target regions. Therefore Ea.hy926 cells were stimulated with 100 µM histamine or remained unstimulated and protein extracts were subsequenly isolated from either plasma membrane, total membrane or nuclear fractions. The samples of treated or untreated protein extracts, derived from the respective cell compartment were labeled with two different fluorophores (CyDyes) and separated by 2D-gel electrophoresis. Accordingly it was investigated to detect proteins that significantly varied in their abundance within these cell compartments upon 100 µM histamine stimulation in comparison to untreated cells.

5.1.1 Assets and drawbacks

The Proteomic Approach consists of several procedures (Figure 14, 15). The major problems concerning the visualization of cell compartment protein extracts lie in the sample preparation, which has to be adapted and further optimized for the individual cell type used, in this case Ea.hy926 cells. Therefore an ideal protease inhibitor, an appropriate buffer for setting the stimulus as well as an adequate homogenization buffer were found to be best-known for these endothelial cells. Cell disruption had to be optimized in order to break up the cells without breaking open their nuclei to avoid any release of nucleic acids. This was experimentally observed to be optimal in homogenizing the cells by sonication (4.1.2.1). Furthermore the fractionation steps for the various compartments of Ea.hy926 cells were adjusted to their individual flotation properties. Plasma membrane fractions were verified by western blot analysis using an antibody for the PM specific marker protein Caveolin 1 (4.1.2.2). As the compartmentalized isolation procedures implicated the generation of very diluted protein contents as well as the presence of a number of disturbing compounds, several methods were investigated to concentrate the protein sample and to remove or inactivate the substances, that may interfere in the 2D-electrophoresis (4.1.2.3, 4.1.3, 4.1.4). Moreover, to solubilize even high hydrophobic proteins, a modified Laemmli buffer was used, that consists of several detergents (4.1.2.4).

Procedure		Assets / Troubleshooting	Drawbacks
Harvesting (un)stimulated cells			Protein complexes that may be formed upon histamine stimulation can be disassembled during this procedure, even at temperatures below 4°C.
Homogenization		Optimized for Ea.hy926 cells (4.1.2.1)	Organelles may remain associated with cytoskeletal elements.
Fractio -nation	High speed sedimentation	Good amount of protein	Isolation of whole and crude membrane fraction
	Sucrose gradient centrifug.	Isolation of pure plasma membrane fraction	Less protein amount; high sucrose concentration, PM fractions are overlapping with membrane fractions
Western Blot Analysis		Caveolin1 Ab specifically detects PM fractions	
Removal or in-activation of inter-fering compounds	Salts	Removal upon Precipitation or dialysis	Disturb in the SDS-PAGE
	Nucleic Acids	Inactivation with RNase/DNase mixture	Interferes in the IEF because of negatively charged DNA; Inactiv. → Smear
	Sucrose	Removal upon dialysis	Increase viscosity of protein sample, Clog the pores of polyacrylamide gel
	Polysacch.	Removal upon Precipitation	Interact with carrier ampholytes and proteins resulting in a loss of protein
	Preteolyt Enz.	Inactivation with Protease Inhibitor Mix (Sigma)	Loss of proteins
	Lipids	Removal upon Precipitation	Interact with membrane proteins and consume detergents; loss of protein
Precipitation of proteins		Removal of interfering compounds; Concentrating of protein extracts	Loss of proteins; if protein pellet gets to dry, it remains unsoluble.
Solubilization of proteins			Hydrophobic proteins are hardly soluble, even in the modified Laemmli buffer.
Labeling of proteins		Minimal Labeling does hardly dilute a protein sample and the Cy DIGE fluors have nearly no effect on a proteins´ isoelectric point or mass.	The dyes are very cost-intensive
Isoelectric Focusing		IPG-strips are well designed for separation of proteins according to their isoelectric point.	Highly hydrophobic proteins may precipitate on the IPG-strip. Time consuming procedure (2 days for Reswelling and IEF)
SDS-PAGE		Proper method for mass separation of proteins	Time consuming (16 hours running time)
Scanning		The Typhoon 9400 scanner is well equipped for detecting Cy DIGE Fluors	Scanner is producing heat that may result in gel shrinking. Therefore it is necessary to place the gel in a Hoefer Easy Breeze Drying Frame.
DeCyder Differential Analysis (DIA) Software		The DIA module algorithms allows co-detection of up to three individual images from one gel and precisely quantifies each protein spot.	
Spot Picking		The Ettan Spot Picker works in picking exactly the highest protein amount of a spot.	The gel piece picked by the Spot is very small compared to the whole protein spot. Manual picking is often necessary to increase the amount of protein.
Tryptic in Gel digestion & Peptide Extraction		Easy protocols and easy handling.	Not useful for highly hydrophobic proteins in order that these proteins are less soluble in the trypsin and/or peptide extraction buffers and possess less tryptic cleavage sites.
Mass spectrometry		The ProteoMass™ Peptide & Protein MALDI-MS Calibration Kit (Sigma: MS-CAL1) is properly designed for MALDI-TOF analyses.	Identification of a protein using the MALDI-TOF is limited to the quantity of applied peptide extract; that means that MALDI-TOF has less sensitivity than other mass spectrometer like e.g. nano LC-ESI-MS.
General Aspects		All proteins that vary in their abundunce upon one distinct stimulus can be identified in one experiment.	Time- and cost-consuming procedures; high sources of error especially in the sample preparation procedures; low output of MALDI-TOF analysis especially for the identification of low abundant proteins.

Table 21: Assets and drawbacks in the Proteomic Approach

In addition to these optimization procedures to prepare the protein sample, there are several advantages and disadvantages existing in the following methods including labeling, 2D-electrophoresis, tryptic in-gel digestion and protein identification. Assets and drawbacks of these as well as a troubleshooting for the removal or inactivation of interfering compounds are summarized in Table 21.

5.1.2 Valosin containing protein

After 2D gel electrophoresis of the nuclear protein extract the valosin containing protein (VCP) was found to be about 50 % decreased upon 100 µM histamine stimulation compared to unstimulated Ea.hy 926 cells. Additionally, in overexpression studies of the citrine tagged VCP, it was mainly visualized in the nucleus of this cell line, but did not clearly translocate during stimulation with histamine.

However, as VCP is a member of the AAA superfamily (ATPases associated with diverse cellular activities) it contains an ATP-binding region. Accordingly, AAA proteins have been implicated in a widely diverse biological processes, including protein degradation, vesicle/membrane fusion, and cell cycle events, these diverse functions are mediated by different sets of adaptor proteins (for review see Ogura T. et al., *Genes Cells* **6**: 575-597, 2001; Patel S. et al., *Trends Cell Biol.* **8**: 67-71, 1998). Therefore VCP was shown to interact with at least 30 different cellular proteins and its localization was studied in several mammalian cell culture lines, where it was present in the cytoplasm and nucleus (Partridge JJ. et al., *Mol. Biol. Cell* **14**: 4221-4229, 2003; Greenberg SA. et al., *Muscle Nerve* **36** :447–454, 2007). In order to that, an N-terminal domain in VCP was shown to be essential for nuclear binding, but this domain was not sufficient for proper nuclear localization indication that more than one domain is involved regulating VCP localization in the cytoplasm and nucleus. Accordingly it was shown that VCP interacts with the nuclear Werner syndrome helicase, WRNp, in an ATP dependent way (Indig FE. et al., *J. Struct. Biol.* **146**: 251-259, 2004). In another study it was reported that VCP translocates from the nucleus to the cytoplasm after stimulation with epidermal growth factor and to participate to DNA repair by its ATP transport function (Zhang H. et al., *DNA and Cell Biology* **19.5**: 253-263, 2000). In line with these findings, VCP translocation from the nucleus into the cytosol was found in EC in this study. It seems plausible that the histamine induced VCP translocation shifts the ATP transport function to that compartment, in which the highest demand of ATP upon histamine-induced Ca^{2+} elevation occurs.

5.1.3 Peroxiredoxin 1

2D-electrophroresis of the membrane extract revealed a 31 % elevated abundance of Peroxiredoxin 1 (Prdx1) within the histamine treated sample in comparison to the untreated control. Furthermore, imaging the overexpressed Prdx1 fused to citrine showed that this protein is mainly localized in various subcellular organelles and few in the cytosol of Ea.hy926 cells. Interestingly, the membrane localization of Prdx1 seems to be limited to endothelial cells. In bovine aortic endothelial cells (BAEC) Prdx1 was co-localized with the Golgi apparatus (Mowbray AL. et al., *J. Biol. Chem.* **283.3**: 1622–1627, 2008) and with mitochondria (Yang Y. et al., *PNAS* **102.1**: 117-122, 2005). In contrast, in other cells Prdx1 was predominantly found in the cytosol and nucleus (Wen S.-T. et al., *Genes and Development* **11.19**: 2456-2467, 1997; Andersen JS. et al., *Nature* **433.7021**: 77-83, 2005). Notably, endothelial cells are physiologically exposed to the mechanical forces associated with the blood flow (shear stress) and a multitude of paracrines and hormones to which they exhibit multiple functions. Accordingly, they have the ability to react to a changing flow via mechanosensors that leads to a modulation of protein expression and cellular functions (for review see Chien S. *Am. J. Physiol. Heart. Circ. Physiol.* **292**: H1209–H1224, 2007). It was reported that laminar shear stress induces ROS production and therefore many genes protective against oxidative stress are induced by its exposure (Chen XL. et al., *J. Biol. Chem.* **278.2**: 703-711, 2003; for review see Paravicini TM. et al., *Cardiovascular Res.* **71.2**: 247-258, 2006).

Moreover, Mowbray and co-workers demonstrated that peroxiredoxins, were up-regulated in BAECs upon laminar shear stress and in particular Prdx1 acts as a mechanosensitive antioxidant in response to shear stress induced ROS generation (Mowbray AL. et al., *J. Biol. Chem.* **283.3**: 1622–1627, 2008). In regard to ROS production especially mitochondria are a major source of superoxide as a result of electron leakage from electron transfer chain (Patwari P. et al., *Am. J. Path.* **170.3**: 805-808, 2007). In order to that Prdx1 may act as a part of the extra antioxidant system and gets activated by the mitochondria-derived superoxide (mROS) production to protect them from ROS damage. However, in other studies it was reported that shear stress stimulates a rapid increase in intracellular calcium (Hutcheston IR. et al., *Br. J. Pharm.* **122**: 117-125, 1997). Thus, these observations offer the possibility of a direct activation of Prdx1 via Ca^{2+} that is independent from ROS generation. Furthermore shear stress has also been shown to activate the Ca^{2+}-dependent c-Src, a highly phosphorylated protein that is localized to focal adhesions and acts as an adaptor protein that mediates

tyrosine phosphorylation of p130 Crk-associated substrate (Cas) (Okuda M. et al., *J. Biol. Chem.* **274.28**: 26803-26809, 1999). Moreover it was reported, that ROS mediates an activation of c-Src tyrosine kinases serving as a scaffold for interaction of proteins (Schaefer G. et al., *Diabetologia* **46**: 773-783, 2003; for rewiev see Otani H., *Antioxid. Redox Signal.* **6.2**: 449-469, 2004). Thus, this let suggest that Prdx1 may get recruited by c-Scr in a Ca^{2+}-dependent way or via c-Scr activation upon mROS production independently of Ca^{2+}.

In the contrary, an IP_3-generating agonist like histamine induces Ca^{2+} mobilization and subsequent uptake by mitochondria, which is also correlated with an increase in mROS production (Hawkins BJ. et al., *Mol. Cell Biol.* **27.21**: 7582-7593, 2007). As Prdx1 was increased in the membrane fraction upon histamine stimulation in our studies, it may get recruited by a scaffold protein from the cytosol to the mitochondria to protect them from mROS generation. Hence, we investigated in further studies whether or not a translocation of the citrine fused Prdx1 can be visualized in single cells. Since no translocation of Prdx1 was observed upon histamine stimulation, which indicates that Prdx1 does not get activated by Ca^{2+}. But then these data suggest that Prdx1 seems more likely to get activated upon mROS production. In this case, the overexpression of Prdx1 that also mean a greater content in the mitochondria will yield sufficient protection of mitochondria from the histamine induced mROS generation and no additional Prdx1 recruitment from the cytosol will be necessary to accomplish this function. Alternatively, it is also possible that the FP (citrine) inhibits an activation of Prdx1 towards the mitochondria. Although additional experiments are necessary, these data point to a recruitment of Prdx1 into the mitcohondria as a phenomenon to protect this organelle against radical damage.

5.2 γ-SNAP associated factor 1

The γ-SNAP associated factor 1 (Gaf1), also named Rab11FIP5, Rip11 or pp75, was chosen from the sequence and structure annotation of a bioinformatic approach. Gaf1 was selected in order there were some evidence that it is a scaffold protein and therefore acts in a Ca^{2+}-dependent manner:

First, it possesses a C2-domain, which was found in many proteins that are involved in cell signaling (e.g. phosphoinositide-3 kinase) and membrane trafficking (rabphillin, synaptotagmin). They are approximately 130 amino acid motifs, which serve as protein-phospholipid and protein-protein binding modules. Their phospholipid binding is mostly

Ca^{2+}-dependent and results in the translocation of the protein to specific regions (for review see Lemmon M., *Nature Rev. Mol. Cell Biol.* **9**: 99-111, 2008). Second, Gaf1 was found to be ubiquitously expressed in all mammalian tissues detected by Northern blotting (Wang D. et al., *J. Clin. Invest.* **104.9**: 1265-1275, 1999) or Western blotting (Chen D. et al., *J. Biol. Chem.* **276.16**: 13127-13135, 2001), which let suggest that this protein is of high importance for human cells. Accordingly, in our PCR experiments Gaf1 was also detected in all cDNAs tested, which either derived from a number of different endothelial cell lines or form HeLa cells. Third, it was demonstrated that γ-SNAP/Gaf1 complexes are able to transiently interact with γ-tubulin (Chen D. et al., *J. Biol. Chem.* **276.16**: 13127-13135, 2001), which is part of the microtubule organizing center (Schiebel E., *Curr. Opin. Cell Biol.* **12.1**: 113-118, 2000). Finally fourth, Gaf1 was found to be localized to recycling endosomes as well as to the plasma membrane (Prekeris R. et al., *Mol. Cell* **6**: 1437-1448, 2000). Moreover, there is evidence that Gaf1 is also able to associate with the outer mitochondrial membrane (Chen D. et al., *J. Biol. Chem.* **276.16**: 13127-13135, 2001), that indicates that Gaf1 serves as a high dynamic protein during cell signaling events. Accordingly, in our localization studies in Ea.hy926 and HeLa cells, the overexpression of Gaf1 fused to citrine at its C-terminal end reveals that it is mainly localized at sites of the plasma membrane, while the intracellular distribution is sparely punctate or tubular and just partially overlaps with mitochondria.

However, based on a hypothesis described by Chen and co-workers, Gaf1 serves as the mitochondrial attachment site for the Gaf1/γ-SNAP complex and herein γ-SNAP might act as an adaptor connecting Gaf1 on mitochondria to the γ-tubulin-containing microtubles (Chen D. et al., *J. Biol. Chem.* **276.16**: 13127-13135, 2001). In order that mitochondria use the microtubular network for their Ca^{2+}-dependent movements, this work indicates, that Gaf1 is likely involved in mitochondrial motility by sensing the Ca^{2+} concentration and connecting mitochondria to the microtubles. For that purpose, we did some studies regarding mitochondrial movements using a validated siRNA against Gaf1 in HeLa cells. In accordance to the hypothesis of Chen and co-workers, our data demonstrate that knockdown of Gaf1 results in an elevated mitochondrial motility during histamine stimulation in comparison to wild type cells. However, since we found Gaf1 predominantly localized close to the plasma membrane, it was unclear how Gaf1 is able to effect mitochondrial motility. For that reason, we observed their movements in permeabilized cells under various Ca^{2+} concentrations. In contrast to our previous observation, downregulation of Gaf1 has no influence on mitochondrial motility under these conditions, suggesting that Gaf1 is not directly involved in the regulation of Ca^{2+}-

dependent mitochondrial movements at microtubular sites. Nevertheless, further investigations concerning Ca^{2+}-measurements confirmed that Gaf1 acts in a Ca^{2+}-dependent way. Silencing of Gaf1 results in a decreased intracellular Ca^{2+}-elevation, whereas its overexpression increases $[Ca^{2+}]_{cyto}$, indicating that the effect of Gaf1 downregulation on mitochondrial motility is indirectly caused by a lowered intracellular Ca^{2+} concentration. Interestingly, neither silencing nor overexpression of Gaf1 results in a changed cytosolic Ca^{2+}-release from intracellular stores during histamine stimulation in a nominal Ca^{2+}-free environment. In contrast readdition of Ca^{2+} leads to an attenuated Ca^{2+}-influx in case of Gaf1 silencing or an increased Ca^{2+}-influx in case of Gaf1 overexpression. Accordingly, mitochondrial Ca^{2+}-measurements goes in line with the results observed in $[Ca^{2+}]_{cyto}$ and effects a changed mitochondrial Ca^{2+}-influx depending on the expression of Gaf1. Moreover, we demonstrated in $[Ca^{2+}]_{ER}$ -measurements that downregulation of Gaf1 does not influence the Ca^{2+}-release from the ER as expected and does not effect Ca^{2+}-refilling in the absence of histamine. In contrast, in the presence of histamine ER cannot completely refill in Gaf1 silenced cells, which goes in line with our previous data that exclusively the mitochondrial dependent ER Ca^{2+} refilling gets diminished as mitochondrial Ca^{2+}-influx is also decreased upon downregulation of Gaf1.

Concerning Ca^{2+}-entry it has been reported, that there are several different Ca^{2+}-influx channels existing in non excitable cells (for rewievs see Quintana A. et al., *Pflugers Arch. – Eur. J. Physiol.* **450**: 1-12, 2005; Grafton G. et al., *Immunology* **104**: 119-126, 2001). Bases on this knowledge our data indicate that Gaf1 plays a crucial role in maintaining the direct Ca^{2+}-entry from a selective plasma membrane Ca^{2+}-channel through the mitochondrial Ca^{2+} uniporter into the mitochondrial matrix and therefore it may serve as a linker protein connecting mitochondria to the plasma membrane.

Due to this hypothesis Gaf1 is colocalizing with ORAI1, a selective plasma membrane Ca^{2+}-channel, which was thoroughly shown to interact with STIM1 (stromal interaction molecule 1), that is localized at the ER site, maintaining a store-operated Ca^{2+}-entry into the ER (Muik M. et al., *J. Biol. Chem.* **283.12**: 8014-8022, 2008; for review see Smyth JT. et al. *Biochim. Biophys. Acta* **1763.11**: 1147-1160, 2006).

Based on our Ca^{2+}-measurements it is shown that Gaf1 may link mitochondria to a selective plasma membrane Ca^{2+}-channel maintaining a direct Ca^{2+}-influx into mitochondria.

Additionally, we could not confirm the studies of Lindsay AJ. and co-workers, that Gaf1 lacking in its C2 domain is not able to localize at the plasma membrane as

overexpressing Gaf1 lacking in its C2 domain fused to citrine at its C-terminal end shows a similar expression pattern as full length Gaf1. This discrepancy may possibly appear in order that they used an N-terminal GFP-tag that might due to protein missfolding.

Due to our colocalization studies, it is likely that also Gaf1 may interact with ORAI1 and/or other plasma membrane ion channels. In such a model, Gaf1 would serve as the plasma membrane attachment site for mitochondria and/or to the γ-tubulin-containing microtuble. Future studies are aimed to test this hypothesis, further.

6 Literature

AIRD WC.: Phenotypic Heterogeneity of the Endothelium. *Circulation Research* **100**: 158-173, 2007.

ALTO NM., SODERLING J., SCOTT JD.: Rab32 is an A-kinase anchoring protein and participates in mitochondrial dynamics. *J. Cell Biol.* **158**: 659-668, 2002.

ANDERSEN JS., LAM YW., LEUNG AKL., ONG S-E., LYON CE., LAMOND AI., MANN M.: Nucleolar proteome dynamics. *Nature* **433.7021**: 77-83, 2005.

ARCARO AND WYMANN: Wortmannin is a potent phosphatidylinositol 3-kinase inhibitor: the role of phosphatidylinositol 3,4,5-trisphosphate in neutrophil responses. *Biochem. J.* **296**: 297, 1993.

ARMSTRONG JS.: The role of the mitochondrial transition in cell death. *Mitochondrion* **6**: 225-234, 2006.

ARONSON NN., TOUSTER O.: Isolation of Rat Liver Plasma Membrane Fragments in Isotonic Sucrose. *Methods Enzymol.* **31(Pt.A)**: 90-102, 1974.

BALDASSARE, JJ., HENDERSON PA., BURNS D., LOOMIS C., FISHER GJ.: Translocation of protein kinase C isozymes in thrombin-stimulated human platelets. Correlation with 1,2-diacylglycerol levels. *J. Biol. Chem.* **267.22**: 15585-15590, 1992.

BALL EH., SINGER SJ.: Mitochondria are associated with microtubles and not with intermediate filaments in cultured fibroblasts. *PNAS* **79**: 123-126, 1982.

BERGER L.: Crystallization of the sodium salt of adenosine triphosphate. *Biochim. Biophys. Acta* **20**: 23, 1956.

BERRIDGE MJ., IRVINE RF.: Inositol triphosphate, a novel second messenger in cellular signal transduction. *Nature* **312**: 315-321, 1984.

BERRIDGE MJ., LIPP P., BOOTMAN MD.: The versatility and universality of calcium signalling. *Nat. Rev. Mol. Cell Biol.* **1**: 11-21, 2000.

BERRIDGE MJ., BOOTMAN MD., RODERICK, HL.: Calcium signalling: dynamics, homeostasis and remodelling. *Nat. Rev. Mol. Cell Biol.* **4**: 517-529, 2003.

BEZPROZVANNY I., WATRAS J., EHRLICH BE.: Bell-shaped calcium-response curves of Ins(1,4,5)P3- and calcium-gated channels from endoplasmic reticulum of cerebellum. *Nature* **351**: 751-754, 1991.

BLEASDALE JE., THAKUR NR., GREMBAN RS. BUNDY GL., FITZPATRICK FA., SMITH RJ., BUNTING S.: Selective inhibition of receptor-coupled phospholipase C-dependent processes in human platelets and polymorphonuclear neutrophils. *J. Pharmacol. Exp. Ther.* **255**: 756, 1990.

BOLDOGH IR., PON LA.: Mitochondria on the move. *Trends in Cell Biol.* **17.10**: 502-510, 2007.

BOONE CW., FORD LE., BOND HE., STUART DC., LORENZ D.: Isolation of Plasma Membrane Fragments from HeLa cells. *The J. of Cell Biology* **41**: 378-392, 1969.

BOOTMAN MD., LIPP P., BERRIDGE M.: The organisation and functions of local Ca^{2+} signals. *J. Cell Sci.* **114**: 2213-2222, 2001.

BOOTMAN MD., COLLINS TJ., PEPPIATT CM., PROTHERO LS., MACKENZIE L., DE SMET P., TRAVERS M., TOVEY SC., SEO JT., BERRIDGE MJ., CICCOLINI F., LIPP P.: Calcium signaling - an overview. *Semin. Cell Dev. Biol.* **12**: 3-10, 2001.

BRADFORD MM.: A rapid and sensitive method for the quantitation of microgram quantities of protein utilizing the principle of protein-dye binding. *Anal. Biochem.*, **72**: 248, 1976.

BRUMMELKAMP T.R, BERNARDS R., AGAMI R.: A System for Stable Expression of Short Interfering RNAs in Mammalian Cells. *Science* **296.5567**: 550-553, 2002.

Burack WR., Shaw AS.: Signal transduction: hanging on a scaffold. *Curr. Opin. Cell Biol*. **12**: 211-216, 2000.

BURACK WR., CHENG AM., SHAW AS.: Scaffolds, adaptors and linkers of TCR signaling: theory and practice. *Current Opinion in Immunology* **14**: 312–316, 2002.

BURNSTOCK G.: Purine and pyrimidine receptors. *Cell. Mol. Sci.* **64.12**:1471-1483, 2007.

CAÑAS B., PIÑEIRO C., CALVO E., LÓPEZ-FERRER D., GALLARDO JM.: Trends in sample preparation for classical and second generation proteomics. *Journal of Chromatography A* **1153**: 235–258, 2007.

CANCELA JM., VAN COPPENOLLE F., GALIONE A., TEPIKIN AV., PETERSEN OH.: Transformation of local Ca^{2+} spikes to global Ca^{2+} transients: the combinatorial roles of multiple Ca^{2+} releasing messengers. *EMBO J.* **21**: 909-919, 2002.

CAO TT., CHANG W., MASTERS SE., MOOSEKER MS.: Myosin-Va binds to and mechanochemically couples microtubles to actin filaments. *Mol. Biol. Cell.* **15**: 151-161, 2004.

CAO YQ.: Voltage-gated calcium channels and pain. *Pain* **126**: 5-9, 2006.

CHAE HZ., ROBINSON K., POOLE LB., CHURCH G., STORZ G., RHEE SG.: Cloning and sequencing of thiol-specific antioxidant from mammalian brain: alkyl hydroperoxide reductase and thiol-specific antioxidant define a large family of antioxidant enzymes. *PNAS* **91.15**: 7017-7021, 1994.

CHALFIE M., TU Y., EUSKIRCHEN G., WARD WW., PRASHER DC.: Green fluorescent protein as a marker for gene expression. *Science* **263**: 802–805, 1994.

CHAN DC.: Mitochondria: dynamic organelles in disease, aging, and development. *Cell* **125**: 1241-1252, 2006.

CHEN D., XU W., HE P., MEDRANO EE., WHITEHEART SW.: Gaf-1, a gamma -SNAP-binding protein associated with the mitochondria. *J. Biol. Chem.* **276.16**: 13127-13135, 2001.

CHEN XL., VARNER SE., RAO AS., GREY JY., THOMAS S., COOL CK., WASERMAN MA., MEDFORD RM., JAISWAL AK., KUNSCH C.: Laminar flow induction of antioxidant response element-mediated genes in endothelial cells. *J. Biol. Chem.* **278.2**: 703-711, 2003.

CHIEN S.: Mechanotransduction and endothelial cell homeostasis: the wisdom of the cell. *Am. J. Physiol. Heart. Circ. Physiol.* **292**: H1209–H1224, 2007.

COLÓN-GONZÁLEZ F., KAZANIETZ MG.: C1 domains exposed: From diacylglycerol binding to protein–protein interactions. *Biochim. Biophys. Acta* **1761.8**: 827-837, 2006.

COTRAN RS.: New roles for the endothelium in inflammatory and immunity. *Am. J. Pathol.* **129**: 407-413, 1987.

COX D., LEE DJ., DALE BM., CALAFAT J., GREENBERG S.: A Rab11-containing rapidly recycling compartment in macrophages that promotes phagocytosis. *PNAS* **97.2**: 680-685, 2000.

COX DA., CONFORTI L., SPERELAKIS N., MATLIB MA.: Selectivity of inhibition of Na^+/Ca^{2+} exchange of Heart mitochondria by benzothiazepine CGP-37157. *J. Cardiovasc. Pharmacol.* **21**: 595, 1993.

DA SILVA CP., GUSE AH.: Intracellular Ca^{2+} release mechanisms: multiple pathways having multiple functions within the same cell type? *Biochim. Biophys. Acta* **1498**: 122-133, 2000.

DEACON SW., SERPINSKAYA AS., VAUGHAN PS., LEPEZ FANARRAGA M., VERNOS I., VAUGHAN KT., GELFAND VI.: Dynactin is required for bidirectional organelle transport.
J. Cell Biol. **160**: 297-301, 2003.

DEMAUREX N., DISTELHORST C.: Apoptosis – the calcium connection.
Science **300**: 65-67, 2003.

DESJARDINS M. CELIS JE., GERRIT VAN MEER, DIEPLINGER H., JAHRAUS A., GRIFFITHS G., HUBER LA.: Molecular Characterization of Phagosomes.
The Journal of Biological Chemistry **269.51**: 32194-32200, 1994.

DHALLA NS.: Excitation-contraction coupling in heart. I. Caomparison of calcium uptake by sarcoplasmic reticulum and mitochondria in the rat heart.
Arch. Int. Physiol. Biochim. **77**: 916-934, 1969.

DOLMETSCH RE., PAJVANI U., FIFE K., SPOTTS JM., GREENBERG ME.: Signaling to the nucleus by an L-type calcium channel-calmodulin complex through the MAP kinase pathway.
Science **294**: 333-339, 2001.

DRUBIN DG., JONES HC., WERTMAN KF.: Actin structure and function: roles in mitochondrial organization and morphogenesis in budding yeast and identification of the phalloidin-binding site. *Mol. Biol. Cell.* **4**: 1277-1294, 1993.

DUBIEL W., FERRELL K., PRATT G., RECHSTEINER M.: Subunit 4 of the 26 S protease is a member of a novel eukaryotic ATPase family. *J. Biol Chem.* **267.32**: 22699-22702, 1992.

DUCHEN MR.: Mitochondria and Ca^{2+} in cell physiology and pathophysiology.
Cell Calcium **28**: 339-348, 2000.

DUTTA D.: Mechanism of store-operated calcium entry. *J. Biosci*. **25**: 397-404, 2000.

EBASHI S., ENDO M.: Calcium ion and muscle contraction.
Prog. Biophys. Mol. Biol. **18**: 123-183, 1968.

EDGELL CJ., MC DONALD CC., GRAHAM JB.: Permanent cell line expressing human factor VIII-related antigen established by hybridization. *PNAS* **80**: 3734-3737, 1983.

EMMELOT P., BOS CJ., VAN HOEVEN RP., VAN BLITTERSWIJK WJ.: Isolation of Plasma Membranes from Rat and Mouse Liver and Hepatomes. *Methods enzymol*. **31(Pt.A)**: 75-90,1974.

ENDEMANN DH., SCHIFFRIN EL.: FRONTIERS IN NEPHROLOGY: Endothelial Dysfunction.
Am. Soc. Nephrol. **15**:1983-1992, 2004.

ER E., OLIVER L., CARTOON PF., JUIN P., MANON S., VALETTE FM.: Mitochondria as the target of pro-apoptotic protein Bax. *Biochim. Biophys. Acta* **1757**: 1301-1311, 2006.

ERDMANN R., WIEBEL FF., FLESSAU A., RYTKA J., BEYER A., FRÖHLICH KU., KUNAU WH.: PAS1, a yeast gene required for peroxisome biogenesis, encodes a member of a novel family of putative ATPases. *Cell* **64.3**: 499-510, 1991.

FELDER CC., BRILEY EM., AXELROD J., SIMPSON JT., MACKIE K., DEVANE WA.: Anandamide, an endogenous cannabimimetic eicosanoid binds to the cloned human cannabinoid receptor and stimulates receptor mediated signal transduction. *PNAS* **90**:7656-7660, 1993.

FERRELL JE. JR.: What do scaffold proteins really do? *Sci. STKE* **52**: PE1, 2000.

FINKEL T.: Oxygen radicals and signaling. *Curr. Opin. Cell Biol.* **10.2**: 248-253,1998.

FINKEL T., HOLBROOK NJ.: Oxidants, oxidative stress and the biology of ageing. *Nature* **408.6809**: 239-247, 2000.

FOSKETT JK., WHITE C., CHEUNG KH., MAK DOD.: Inositol Trisphosphate Receptor Ca^{2+} Release Channels. *Physiol. Rev.* **87**: 593-658, 2007.

FOWLER CJ., JONSSON KO., ANDERSSON A., JUNTUNEN J., JÄRVINEN T., VANDERVOORDE S., LAMBERT DM., JERMAN JC., SMART D.: Inhibition of C6 glioma cell proliferation by anandamide, 1-arachidonoylglycerol, and by a water soluble phosphate ester of anandamide: variability in response and involvement of arachidonic acid. *Biochemical Pharmacology* **66**: 757-767, 2003.

FRANSSON A., RUUSALA A., ASPENSTRÖM P.: Atypical Rho GTPases have roles in mitochondrial homeostasis and apoptosis. *J. Biol. Chem.* **278**: 6495-6502, 2003.

FREDERICK RL., SHAW JM.: Moving Mitochondria: Establishing distribution of an essential Organelle. *Traffic* **8**: 1668-1675, 2007.

FRIEDEN M., GRAIER WF.: Subplasmalemmal ryanodine-sensitive Ca^{2+}-release contributes to Ca^{2+}-dependent K^+ channel activation in a human umbilical vein endothelial cell line. *J. Physio.* **524**: 715-724, 2000.

FRIEDEN M., MALLI R., SAMARDZIJA M., DEMAUREX N., GRAIER WF.: Subplasmalemmal endoplasmic reticulum controls K(Ca) channel activity upon stimulation with a moderate histamine concentration in a human umbilical vein endothelial cell line. *J. Physio.* **540**: 73-84, 2002.

FRÖHLICH KU., FRIES HW., RÜDIGER M., ERDMANN R., BOTSTEIN D., MECKE D.: Yeast cell cycle protein CDC48p shows full-length homology to the mammalian protein VCP and is a member of a protein family involved in secretion, peroxisome formation, and gene expression. *J. Cell Biol.* **114.3**: 443-453, 1991.

FU LW., PAN HL., LONGHURST JC.: Endogenous histamine stimulates ischemically sensitive abdominal visceral afferents through H_1 receptors. *Am. J. Physiol.* **273.6 (Pt.2)**: H2726-H2737, 1997.

FUKAMI J.I. YAMAMOTO I., CASIDA JE.: Metabolism of Rotenone in vitro by Tissue Homogenates from Mammals and Insects. *Science* **155**: 713, 1967.

FURCHTGOTT RF., ZAVADSKI JV.: The obligatory role of endothelial cells in the relaxation of arterial smooth muscle by acetylcholin. *Nature* **288**: 373-376,1980.

GALLANT EM., HART J., EAGER K., CURTIS S., DULHUNTY AF.: Caffeine sensitivity of native RyR channels from normal and malignant hyperthermic pigs: effects of a DHPR II-III loop peptide. *Am. J. Physiol. Cell Physiol.* **286**: C821-830, 2004.

GALLEY HF., WEBSTER NR.: Physiology of the endothelium. *British Journal of Anaesthesia* **93.1**: 105-113, 2004.

GILABERT JA., PAREKH AB.: Respiring mitochondria determine the pattern of activation and inactivation of the store-operated Ca^{2+} current I_{crac}. *EMBO J.* **19**: 6401-6407, 2000.

GILABERT JA., BAKOWSKI D., PAREKH AB.: Energized mitochondria increase the dynamic range over which inositol 1,4,5-triphosphate activates store-operated calcium influx. *EMBO J*. **20**: 2672-2679, 2001.

GÖRG, A., POSTEL W., WESER J., GÜNTHER S., STRAHLER JR., HANASH SM., SOMERLOT L.: Elimination of point streaking on silver stained two-dimensional gels by addition of iodoacetamide to the equilibration buffer: *Electrophoresis* **8**, 122-124, 1987.

GÖRG A., POSTEL W., GÜNTHER S.: Two-dimensional electrophoresis. The current state of two-dimensional electrophoresis with immbilized pH gradients. *Electrophoresis* **9**: 531-546,1988.

GÖRG A., POSTEL W., FRIEDRICH C., KUICK R., STRAHLER JR., HANASH SM.: Temperature dependent spot positional variability in two-dimensional polypeptide patterns. *Electrophoresis* **12**: 653-658, 1991.

GÖRG A., BOGUTH G., OBERMAIER C., POSCH A., WEISS W.: Two-dimensional polyacryl-amide gel electrophoresis with immobilized pH gradients in the first dimensin (IPG-Dalt): The state of the art and the controversy of vertical versus horizontal systems. *Electrophoresis* **16**: 1079-1086, 1995.

GÖRG A., OBERMAIER C., BOGUTH G., HARDER A., SCHEIBE B., WILDGRUBER R., WEISS W.: The current state of two-dimensional electrophoresis with immobilized pH gradients. *Electrophoresis* **21**, 1037-1053, 2000.

GÖRG A., Two-Dimensional Electrophoresis with Immobilized pH Gradients for Proteome Analysis, **A laboratory Manual**: 1-77, 2003.

GÖRG A., WEISS W., DUNN MJ.: Current two-dimensional electrophoresis technology for Proteomics. *Proteomics* **4**, 3665–3685, 2004.

GRAFTON G., THWAITE L.: Calcium channels in lymphocytes. *Immunology* **104**: 119-126, 2001.

GRAIER WF., SIMECEK S., STUREK M.: Cytochrome P450 mono-oxygenase-regulated signalling of Ca^{2+} entry in human and bovine endothelial cells. *Journal of Physiology* **482.2**: 259-274, 1995.

GRAIER WF., PALTAUF-DOBURZYNSKA J., HILL BJ., FLEISCHHACKER E., HOEBEL BG., KOSTNER GM., STUREK M.: Submaximal stimulation of porcine endothelial cells causes focal Ca^{2+} elevation beneath the cell membrane. *The Journal of Physiology* **506.1**: 109-125, 1998.

GRAIER WF.:Integration and Organization of Intracellular Pathways in the Regulation of Endothelial Function. *Proposal for a FWF Spezialforschungsbereich: Endothelial Signaling Networks*, 2005.

GRAIER WF., FRIEDEN M., MALLI R.: Mitochondria and Ca^{2+} signaling: old guests, new functions. *Pflugers Arch. Eur. J. Phys.* **455.3**: 375-396, 2007.

GREENBERG SA., WATTS GD., KIMONIS VE., AMATO AA., PINKUS JL.: Nuclear Localization of valosin-containing protein in normal muscle and muscle affected by inclusion-body myositis. *Muscle Nerve* **36** :447–454, 2007.

GRIESBECK O., BAIRD GS., CAMPBELL RE., ZACHARIAS DA., TSIEN RY.: Reducing the Environmental Sensitivity of Yellow Fluorescent Protein. *J. Biol. Chem.* **276**: 29188–29194, 2001.

GRYNKIEWICZ G., POENIE M., TSIEN RY.: A new generation of Ca^{2+} indicators with greatly improved fluorescence properties. *J. Biol. Chem.* **260**: 3440, 1985.

GUINTO JB., RITSON GP., TAYLOR JP., FORMAN MS.: Valosin-containing protein and the pathogenesis of frontotemporal dementia associated with inclusion body myopathy. *Acta Neuropathol.* **114**: 55-61, 2007.

HABERMANN A., SCHROER TA., GRIFFITHS G., BURKHARST JK.: Immunolocalization of cytoplasmic dynein and dynactin subunits in cultured macrophages: enrichment on early endocytic organelles. *J. Cell Sci.* **114**: 229-240, 2001.

HAJNOCZKY G., CSORDAS G., DAS S., GARCIA-PEREZ C., SAOTOME M., SINHA ROY S., YI M.: Mitochondrial calcium signaling and cell death: approaches for assessing the role of mitochondrial Ca^{2+}uptake in apoptosis. *Cell Calcium* **40**: 553-560, 2006.

HALAWANI D., LATTERICH M.: p97: The Cell's Molecular Purgatory? *Mol. Cell* **22**: 713-717, 2006.

HALES CM., GRINER R., HOBDY-HENDERSON KC., DORN MC., HARDY D., KUMAR R., NAVARRE J., CHAN EKL., LAPIERRE LA., GOLDENRING JR.: Identification and Characterization of a family of Rab11-interacting proteins. *J. Biol. Chem.* **276.42**: 39067-39075, 2001.

HAMMOND S.M., BOETTCHER S., SCOTT M., CAUSY AA., KOBAYASHI R., HANNON GJ.: Argonaute2, a Link Between Genetic and Biochemical Analyses of RNAi. *Science* **293**: 1146-50, 2001.

HANKE JH., GARDNER JP., DOW RL., CHANGELIAN PS., BRISETTE WH., WERINGER EJ., POLLOK BA., CONNELLY PA.: Discovery of a novel, potent, and Src family-selective tyrosine kinase inhibitor. Study of Lck- and FynT-dependent T cell activation. *J. Biol. Chem.* **271**: 695, 1996.

HASSESSIAN H., VACA L.,KUNZE DL.: Blockade of the inward rectifier potassium current by the Ca(2+)-ATPase inhibitor 2',5'-di(tert-butyl)-1,4-benzohydroquinone (BHQ). *Br. J. Pharmacol.* **112**: 1118, 1994.

HAWKINS BJ., SOLT LA., CHOWDHURY I., KAZI AS., ABID MR., AIRD WC., MAY MJ., FOSKETT JK., MADESH M.: G protein-coupled receptor Ca2+-linked mitochondrial reactive oxygen species are essential for endothelial/leukocyte adherence. *Mol. Cell Biol.* **27.21**: 7582-7593, 2007.

HEILBRUNN LV., WIERCINSKY FJ.: Action of various cations on muscle protoplasm. *J. Cell Comp. Physiol.* **19**: 15–32, 1947.

HEIM R., CUBITT AB., TSIEN RY.: Improved green fluorescence. *Nature* **373**: 663-664 Scientific Correspondance, 1995.

HEYTLER PG., PRITCHARD WW.: A new class of uncoupling agents - carbonyl cyanide phenylhydrazones. *Biochem. Biophys. Res. Comm.* **7**: 272, 1962.

HILLARD CJ., MANNA S., GREENBERG MJ., DICAMELLI R., ROSS RA., STEVENSON LA., MURPHY V., PERTWEE RG., CAMPBELL WB.: Synthesis and characterization of potent and selective agonists of the neuronal cannabinoid receptor (CB1). *J. Pharmacol. Exp. Ther.* **289**: 1427, 1999.

HOFER AM., FASOLATO C., POZZAN T.: Capacitative Ca^{2+} entry is closely linked to the filling state of internal Ca^{2+}-stores: a study using simultaneous measurements of I_{crac} and intraluminal [Ca^{2+}]. *J. Cell Biol.* **140**: 325-334, 1998.

HOTH M., FANGER CM., LEWIS RS.: Mitochondrial regulation of store-operated calcium signaling in T lymphocytes. *J. Cell Biol.* **137.3**: 633-648, 1997.

HOTH M., BUTTON DC., LEWIS RS.: Mitochondrial control of calcium-channel gating: a mechanism sustained signaling and transcriptional activation in T lymphocytes. *PNAS* **97**: 10607-10612, 2000.

HU B., SUN SG., TONG ET.: NMDA and AMPA receptors mediate intracellular calcium increase in rat cortical astrocytes. *Acta Pharmacol. Sin.* **25**: 714-720, 2004.

HU CD., KERPPOLA TK.: Simultaneous visualization of multiple protein interactions in living cells using multicolor fluorescence complementation analysis. *Nature Biotechnology* **21**: 539–545, 2003.

HUANG KP.: The mechanism of protein kinase C activation. *Trends Neurosci.* **12**: 425-432, 1989.

HUBER LA., PFALLER K., VIETOR I.: Organelle proteomics: implications for subcellular fractionation in proteomics. *Circ. Res*. **92:** 962-968,2003.

HUTCHESTON IR., GRIFFITH TM.: Central role of intracellular calcium stores in acute flow- and agonist-evoked endothelial nitric oxide release. *Br. J. Pharm.* **122**: 117-125, 1997.

INDIG FE., PARTRIDGE JJ., VON KOBBE C., ALADJEM MI., LATTERICH M., BOHR VA.: Werner syndrome protein directly binds to the AAA ATPase p97/VCP in an ATP-dependent fashion. *J. Struct. Biol.* **146**: 251-259, 2004.

ISLAM R., KO C., LANDERS T.: A new approach to rapid immobilised pH gradient IEF for 2-D electrophoresis. *Science Tools* **3**: 14-15, 1998.

IZZO G., GUERRIERI F., PAPA S.: On the mechanism of inhibition of the respiratory chain by 2-heptyl-4-hydroxyquinoline-N-oxide. *FEBS Lett.* **93**: 320, 1978.

JAFFE EA., NACHMANN RL., BECKER CG., MINICK CR.: Culture of humanendothelial cells derived from umbilical veins, Identification by morphologic and immunologic criteria. *J. Clin. Invest.* **52**: 2745-2756, 1973.

JAFFE EA.: Physiologic functions of normal endothelial cells. *Ann. NY Acad. Sci.* **454**: 279-291, 1985.

JÁRAI Z., WAGNER JA., VARGA K., LAKE KD., COMPTON DR., MARTIN BR., ZIMMER AM., BONNER TI., BUCKLEY NE., MEZEY E., RAZDAN RK., ZIMMER A., KUNOS G.: Cannabinoid-induced mesenteric vasodilation through an endothelial site distinct from CB1 or CB2 receptors. *PNAS* **96.24**: 14136-14141, 1999.

JOUSSET H., MALLI R., GIRARDIN N., GRAIER WF., DEMAUREX N., FRIEDEN M.: Evidence for a receptor-activated Ca^{2+} entry pathway independent from Ca^{2+} store depletion in endothelial cells. *Cell Calcium* **43**: 83-94, 2008.

JUST H.: Structure and Function of the Endothelium in Cardiovascular Disease. *Biotechnology in Drug Research* **44**: 382-384, 1994.

KATZ B., MILEDI R.: The timing of calcium action during neuromuscular transmission. *J. Physiol.* **189**: 535-544, 1967.

KAWASE K., SHIBATA M., KAWASHIMA H., HATSUZAWA K., NAGAHAMA M., TAGAYA M., TANI K.: Gaf-1b is an alternative splice variant of Gaf-1/Rip11. *Biochem. Biophys. Res. Commun.* **303.4**: 1042-1046, 2003.

KESSLER A., TOMAS E., IMMLER D., MEYER HE., ZORZANO A., ECKEL J.: Rab11 is associated with GLUT4-containing vesicles and redistributes in response to insulin. *Diabetologia* **43.12**: 1518-1527, 2000.

KIM K., RHEE SG., STADTMAN ER.: Nonenzymatic cleavage of proteins by reactive oxygen species generated by dithiothreitol and iron. *J. Biol. Chem.* **260.29**: 15394-15397, 1985.

KIRISCHUK, S., KETTENMANN, H., AND VERKHRATSKY, A.: Na^{+}/Ca^{2+} exchanger modulates kainate-triggered Ca^{2+} signaling in Bergmann glial cells in situ. *FASEB J.* **11.7**: 566-572, 1997.

KNOT HJ., LAHER I., SOBIE EA., GUATIMOSIM S., GOMEZ-VIQUEZ L., HARTMANN H., SONG L-S., LEDERER WJ., GRAIER WF., MALLI R., FRIEDEN M., PETERSEN OH.: Twenty years of Calcium Imaging: Cell Physiology to Dye for. *Molecular Interventions* **5.2**: 112-127, 2005.

KOLLER JK., BROWNSTEIN MJ.: Use of a cDNA clone to identify a supposed precursor protein containing valosin. *Nature* **325**: 542-545, 1987.

KREMENTSOV DN., KREMENTSOVA EB., TRYBUS KM.: Myosin V: regulation by calcium, calmodulin, and the tail domain. *J. Cell Biol.* **164**: 877-886, 2004.

LAEMMLI, UK.: Cleavage of Structural Proteins during the Assembly of the Head of Bacteriophage T4. *Nature* **227**: 680-685, 1970.

LAWRIE AM., RIZZUTO R., POZZAN T., SIMPSON AWM.: A role for calcium in the regulation of mitochondrial calcium in endothelial cells. *J. of Biol. Chem.* **271.18**: 10753-10759, 1996.

LEE, NS., DOHJIMA T., BAUER G., LI H., LI MJ., EHSANI A., SALVATERRA P., ROSSI J.: Expression of small interfering RNAs targeted against HIV-1 *rev* transcripts in human cells. *Nature Biotechnology* **20**: 500-505, 2002.

LEIPE DD., WOLF YI., KOONIN EV., ARAVIND L.: Classification and evolution of P-loop GTPases and related ATPases. *J. Mol. Biol.* **317.1**:41-72, 2002.

LEMMON M.: Membrane recognition by phospholipid-binding domains. *Nature Rev. Mol. Cell Biol.* **9**: 99-111, 2008.

LENZ T., KLEINEKE JW.: Hormone-induced rise in cytosolic Ca^{2+} in axolotl hepatocytes: properties of the Ca^{2+} influx channel. *Am. J. Physiol. Cell Physiol.* **273**: C1526-C1532, 1997.

LESTER LB., SCOTT JD.: Anchoring and scaffold proteins for kinases and phosphatases. *Recent. Prog. Horm. Res.* **52**: 409-429, 1997.

LEWIS, M.R., LEWIS, W.H.: Mitochondria (and othercytoplasmic structures) in tissue cultures. *Am. J. Anat.* **17**: 339–401, 1915.

LINDSAY AJ., HENDRICK AG., CANTALUPO G., SENIC-MATUGLIA F., GOUD B., BUCCI C., MCCAFFREY MW.: Rab coupling protein (RCP), a novel Rab4 and Rab11 effector protein. *J. Biol. Chem.* **277**: 12190-12199, 2002.

LINDSAY AJ., MCCAFFREY MW.: The C2 domains of the class I Rab11 family of interacting proteins target recycling vesicles to the plasma membrane. *J. Cell Sci.* **117**: 4365-4375, 2004.

LIU J., XIAO N., DEFRANCO DB.: Use of digitonin-permeabilized cells in studies of steroid receptor subnuclear trafficking. *Methods* **19**: 403, 1999.

MAHAJAN S., GOSH S., SUDBECK EA., ZHENG Y., DOWNS S., HUPKE M., UCKUN FM.: Rational design and synthesis of a novel anti-leukemic agent targeting Bruton's tyrosine kinase (BTK), LFM-A13 [alpha-cyano-beta-hydroxy-beta-methyl-N-(2, 5-dibromophenyl) propenamide]. *J. Biol. Chem.* **274:** 9587-9599, 1999.

MALLI R., FRIEDEN M., OSIBOW K., GRAIER WF.: Mitochondria efficiently buffer subplasmalemmal Ca^{2+} elevation during agonist stimulation. *J. Biol. Chem.* **278**: 10807-10815, 2003.

MALLI R., FRIEDEN M., OSIBOW K., ZORATTI C., MAYER M., DEMAUREX N., GRAIER WF.: Sustained Ca^{2+} transfer across mitochondria is essential for mitochondrial Ca^{2+} buffering, sore-operated Ca^{2+} entry, and Ca^{2+} store refilling. *J. Biol. Chem.* **278.45**: 44769-79, 2003.

MALLI R., FRIEDEN M., TRENKER M., GRAIER WF.: The Role of Mitochondria for Ca^{2+} refilling of the Endoplasmic Reticulum. *Journal of Biological Chemistry* **288.13**: 12114-12122, 2005.

MALLI R., FRIEDEN M., HUNKOVA M., TRENKER M., GRAIER WF.: Ca^{2+} refilling of the endoplasmic reticulum is largely preserved albeit reduced Ca^{2+} entry in endothelial cells. *Cell Calcium* **41**: 63-76, 2007.

MALOLANARASIMHAN K., KEDEI N., SIGANO DM., KELLEY JA., LAI CC., LEWIN NE., SURAWSKI RJ., PAVLYUKOVETS VA., GARFIELD SH., WINCOVICH S., BLUMBERG PM., MARQUEZ VE.: Conformationally constrained analogues of diacylglycerol (DAG). Modulation of membrane translocation of protein kinase C (PKC) isozymes alpha and delta by diacylglycerol lactones (DAG-lactones) containing rigid-rod acyl groups. *J. Med. Chem.* **50.5**: 962-978, 2007.

MAROUGA R., KJELLEBERG S.: Synthesis of Immediate Upshift (Iup) Proteins during Recovery of Marine *Vibrio* sp. Strain S14 Subjected to Long-Term Carbon Starvation. *Journal of Bacteriology* **178.3**: 817-822, 1996.

MATZ MV., FRADKOV AF., LABAS YA., SAVITSKY AP., ZARAISKY AG., MARKELOV ML., LUKYANOV SA.: Fluorescent proteins from nonbioluminescent Anthozoa species. *Nature Biotechnology* **17**: 969-973, 1999.

MEYERS JM., PREKERIS R.: Formation of mutually exclusive Rab11 complexes with members of the Rab11-interacting proteins regulates Rab11 endocytic targeting and function. *J. Biol. Chem.* **277.50**: 49003-49010, 2002.

MIYAWAKI A., LLOPIS J., HEIM R., MCCAFFERY JM., ADAMS JA., IKURA M., TSIEN RY.: Fluorescent indicators for Ca2+ based on green fluorescent proteins and calmodulin. *Nature* **388**: 882-887, 1997.

MORRIS RL., HOLLENBECK PJ.: Axonal transport of mitochondria along microtubles and F-actin in living vertebrate neurons. *J. Cell Biol.* **131**: 1315-1326, 1995.

MIYAGISHI, M., TAIRA, K.: U6 promoter−driven siRNAs with four uridine 3' overhangs efficiently suppress targeted gene expression in mammalian cells. *Nature Biotechnology* **20**: 497-500, 2002.

MONTERO M., ALONSO MT., CARNICERO E., CUCHILLO-IBÁÑEZ I., ALBILLOS A., GARCIA AG., GARCIA-SANCHO J., ALVAREZ J.: Chromaffin-cell stimulation triggers fast millimolar mitochondrial Ca^{2+} transients that modulate secretion. *Nat. Cell Biology* **2**: 57-61, 2000.

MOWBRAY AL., KANG D-H., RHEE SG., KANG SW., JO H.: Laminar Shear Stress Up-regulates Peroxiredoxins (PRX) in Endothelial Cells PRX 1 AS A MECHANO-SENSITIVE ANTIOXIDANT *J. Biol. Chem.* **283.3**:1622–1627, 2008.

MUIK M., FRISCHAUF I., DERLER I., FAHRNER M., BERGSMANN J., EDER P., SCHINDL R., HESCH C., POLZINGER B., FRITSCH R., KAHR H., MADL J., FRUBER H., GROSCHNER K., ROMANIN C.: Dynamic coupling of the putative coiled-coil domain of ORAI1 with STIM1 mediates ORAI1 channel activation. *J. Biol. Chem.* **283.12**: 8014-8022, 2008.

MYSLINSKI E., AMÉ JC., KROL A., CARBON P.: An unusually compact external promoter for RNA polymerase III transcription of the human H1RNA gene. *Nuc. Acid Res.* **29**: 2502-2509, 2001.

NAGAI T., SAWANO A., PARK ES., MIYAWAKI A.: Circularly permuted green fluorescent proteins engineered to sense Ca^{2+}. *PNAS* **98.6**: 3197-3202, 2001.

NAGAI T., IBATA K., PARK ES., KUBOTA M., MIKOSHIBA K., MIYAWAKI A.: A variant of yellow fluorescent protein with fast and efficient maturation for cell-biological applications. *Nature Biotechnology* **20**: 87–90, 2002.

NAGAMUNE H.,FUKUSHIMA Y., TAKADA J., YOSHIDA K., UNAMI A., SHIMOOKA T., TERADA H.: The lipophilic weak base (Z)-5-methyl-2-[2-(1-naphthyl)ethenyl]-4-piperidinopyridine (AU-1421) is a potent protonophore type cationic uncoupler of oxidative phosphorylation in mitochondria. *Biochim. Biophys. Acta* **1141**: 231-237, 1993.

NAWROTH P., KISIEL W., STERN D.: The role of endothelium in the homeostatic balance of haemostasis. *Clin. Haematol.* **14.2**: 531-546, 1985.

NEHER E., SAKMANN B.: Single-channel currents recorded from membrane of denerved frog muscle fibres. *Nature* **260**: 799-802, 1976.

NEUMANN CA., KRAUSE DS., CARMAN CV., DAS S., DUBEY DP., ABRAHAM JL., BRONSON RT., FUJIWARA Y., ORKIN SH., VAN ETTEN RA.: Essential role for the peroxiredoxin Prdx1 in erythrocyte antioxidant defence and tumour suppression. *Nature* **424**: 561-565, 2003.

NEUPERT W.: Protein import into mitochondria. *Annu. Rev. Biochem.* **66**: 863-917, 1997.

NILIUS B., DROOGMANS G.: Ion channels and their functional role in vascular endothelium. *Physiol. Rev.* **81**: 1415-1459, 2001.

OANCEA E., MEYER T.: Protein kinase C as a molecular machine for decoding calcium and diacylglycerol signals. *Cell* **95.3**: 307-318, 1998.

O'FARRELL, PH.: High resolution two-dimensional electrophoresis of proteins. *J. Biol. Chem* **250**: 4007-4021, 1975.

OGURA T., WILKINSON AJ.: AAA+ superfamily ATPases: common structure-diverse function. *Genes Cells* **6**: 575-597, 2001.

OKA S., NAKAJIMA K., YAMASHITA A., KISHIMOTO S., SUGIURA T.: Identification of GPR55 as a lysophosphatidylinositol receptor. *Biochem. Biophys. Res. Comm.* **362**: 928–934, 2007.

OKUDA M., TAKAHASHI M., SUERO J., MURRY CE., TRAUB O., KAWAKATSU H., BERK BC.: Shear stress stimulation of p130^{cas} tyrosine phosphorylation requires calcium-dependent c-Scr activation. *J. Biol. Chem.* **274.28**: 26803-26809, 1999.

OSIBOW K., MALLI R., KOSTNER GM., GRAIER WF.: A new type of non-Ca^{2+}-buffering Apo(a)-based fluorescent indicator for intraluminal Ca^{2+} in the endoplasmic reticulum. *J. Biol. Chem.* **281**: 5017-5025, 2006.

OTANI H.: Reactive oxygen species as mediators of signal transduction in ischemic preconditioning. *Antioxid. Redox Signal.* **6.2**: 449-469, 2004.

OWENS GP., BURFOON MP., DEVLIN ME., GILDEN DH.: Extraction and purification of active IgG from SSPE and MS brain. *Journal of Virological Methods* **68**: 119-125, 1997.

PADDISON PJ., CAUDY AA., BERNSTEIN E., HANNON GJ., CONKLIN DS.: Short hairpin RNAs (shRNAs) induce sequence-specific silencing in mammalian cells. *Genes Dev.* **16.8**: 948-958, 2002.

PALMER AE., JIN C., REED JC., TSIEN RY.: Bcl-2-mediated alterations in endoplasmic reticulum Ca^{2+} analyzed with an improved genetically encoded fluorescent sensor. *PNAS* **101.50**: 17404–17409, 2004.

PALTAUF-DOBURZYNSKA J., POSCH K., PALTAUF G., GRAIER WF.: Stealth ryanodine-sensitive Ca^{2+} release contributes to activity of capacitative Ca^{2+} entry and nitric oxide synthase in bovine endothelial cells. *The Journal of Physiology* **513.2**: 369-379, 1998.

PALTAUF-DOBURZYNSKA J., FRIEDEN M., SPITALER M., GRAIER WF.: Histamine-induced Ca^{2+} oscillations in a human endothelial cell line depend on transmembrane ion flux, ryanodine receptors and endoplasmic reticulum Ca^{2+}-ATPase. *The Journal of Physiology* **524.3**: 701-713, 2000.

PARAVICINI TM., TOUYZ RM.: Redox signaling in hypertension. *Cardiovascular Res.* **71.2**:247-258, 2006.

PAREKH AB., PENNER R.: Store Depletion and Calcium Influx. *Physio. Rev.* **77**: 901-930, 1997.

PAREKH AB.: Slow Feedback inhibition of calcium release-activated calcium current by calcium entry. *J. Biol. Chem.* **273**: 14925-14932*,* 1998.

PAREKH AB. AND PUTNEY JW.JR.: Store-Operated Calcium Channels. *Physiol. Rev.* **85**: 757–810, 2005.

PASQUALI C., FIALKA I., HUBER LA.: Subcellular fractionation, electromigration analysis and mapping of organelles. *Journal of Chromatography B* **722**: 89–102, 1999.

PARTRIDGE JJ., LOPREIATO JO. JR., LATTERICH M., INDIG FE.: DNA damage modulates nucleolar interaction of the Werner protein with the AAA ATPase p97/VCP. *Mol. Biol. Cell* **14**: 4221-4229, 2003.

PATEL S., LATTERICH M.: The AAA team: related ATPases with diverse functions. *Trends Cell Biol.* **8**: 67-71, 1998.

PATWARI P., LEE RT.: Thioredoxins, mitochondria and hypertension. *Am. J. Path.* **170.3**: 805-808, 2007.

PETERSON OH., MICHALAK M., VERKHRATSKY A.: Calcium signaling: Past, present and future. *Cell Calcium* **38**: 161-169, 2005.

PFEFFER SR.: Rab GTPases: specifying and deciphering organelle identity and function. *Trends in Cell Biol.* **11.12**: 487-491, 2001.

PAUL, CP., GOOD PD., WINER I., ENGELKE DR.: Effective expression of small interfering RNA in human cells. *Nature Biotechnology* **20**: 505-508, 2002.

PAWSON T., SCOTT JD.: Signaling through Scaffold, Anchoring, and Adaptor proteins. *Science* **278**: 2075-2080, 1997.

PEDEN AA., SCHONTEICH E., CHUN J., JUNUTULA JR., SCHELLER RH., PREKERIS R.: The RCP-Rab11 complex regulates endocytic protein sorting. *Mol. Biol. Cell.* **15.8**: 3530-3541, 2004.

PODOLSKY DK., WEISER MM., LA MONT JT., ISSELBACHER KJ.: Galactosyltransferase and Concanavalin A Agglutination of Cells. *PNAS* **71.3**: 904–908, 1974.

PREKERIS R., KLUMPERMAN J., SCHNELLER RH.: A Rab11/Rip11 protein complex regulates apical membrane trafficking via recycling endosomes. *Mol. Cell.* **6.6**: 1437-1448, 2000.

PREKERIS R., DAVIES JM., SCHELLER RH.: Identification of a novel Rab11/25 binding domain present in Eferin and Rip proteins. *J. Biol. Chem.* **276.42**: 38966-38970, 2001.

PRLIC A., DOMINGUES FS., LACKNER P., SIPPL MJ.: WILMA-automated annotation of Protein sequences. *Bioinformatics* **20**: 127-128, 2004.

PULLIKUTH AK., CATLING AD.: Scaffold mediated regulation of MAPK signaling and cytoskeletal dynamics: A perspective. *Cellular Signalling* **19**: 1621–1632, 2007.

PUTNEY, JW. JR.: Muscarinic, α-adrenergic and peptide receptors regulate the same calcium influx sites in the parotid gland. *J. Physiol.* **268**: 139-149, 1977.

PUTNEY JW. JR.: A model for receptor-regulated calcium entry. *Cell Calcium* **7**: 1-12, 1986.

PUTNEY JW. JR., BROAD LM., BRAUN FJ., LIEVREMONT JP., BIRD GS.: Mechanisms of capacitative calcium entry. *J. Cell Sci.* **114**: 2223-2229, 2001.

QUINTANA A., GRIESEMER D., SCHWAR EC., HOTH M.: Calcium-dependent activation of T-lymphocytes. *Pflugers Arch. – Eur. J. Physiol.* **450**: 1-12, 2005.

RABILLOUD T., VALETTE C., LAWRENCE JJ.: Sample application by in-gel rehydration improves the resolution of two-dimensional electrophoresis with immobilized pH gradients in the first dimension. *Electrophoresis* **15**: 1552-1558, 1994.

RABILLOUD T., ADESSI C., GIRAUDEL A., LUNARDI J.: Improvement of the solubilization of proteins in two-dimensional electrophoresis with immobilized pH gradients. *Electrophoresis* **18**: 307-316, 1997.

RABILLOUD T.: Use of Thiourea to Increase the Solubility of Membrane Proteins in Two-Dimensional Electrophoresis. *Electrophoresis* **19**: 758–760, 1998.

RABILLOUD T., CHEVALLET M.: Solubilization of proteins in 2D electrophoresis. In: *Proteome Research: Two-Dimensional Gel Techniques and Identification Methods*. (T. Rabilloud, Ed.), **Springer**: 9-29, 2000.

RECK-PETERSON SL., PROVANCE DW. JR., MOOSEKER MS., MERCER JA.: Class V myosins. *Biochim. Biophys. Acta* **1496**: 36-51, 2000.

REMOLD-O´DONELL E.: Purification of plasma membrane of guinea pig peritoneal macrophages. *Preparative Biochemistry* **7.6**: 441-455, 1977.

RHEE SG., CHAE HZ., KIM K.: PEROXIREDOXINS: A historical overview and speculative preview of novel mechanisms and emerging concepts in cell signaling. *Free Radical Biology & Medicine* **38**: 1543– 1552, 2005.

RINALDI-CARMONA M., BARTH F., HÉAULME M., SHIRE D., CALANDRA B., CONGY C., MARTINEZ S., MARUANI J., NÉLIAT G., CAPUT D., FERRARA P., SOUBRIÉ P., BRELIÈRE JC., LE FUR G.: SR141716A, a potent and selective antagonist of the brain cannabinoid receptor. *FEBS Lett* **350**: 240-244, 1994.

RINGER, S.: A further contribution regarding the influence of the different constituents of the blood on the contraction of the heart. *J. Physiol.* **4**: 29-42, 1883.

RINTOUL GL., FILIANO AJ., BROCARD JB., KRESS GJ., REYNOLDS IJ.: Glutamate decreases mitochondrial size and movement in primary forebrain neurons. *The Journal of Neuroscience* **23.21:** 7881-7888, 2003.

RIZO J., SÜDHOF TC.: C_2-domains, Structure and Function of a Universal Ca^{2+}-binding Domain. *J. Biol. Chem.* **273.26**: 15879-15882, 1998.

RIZZUTO R., BRINI M., MURGIA M., POZZAN T.: Microdomains with high Ca^{2+} close to IP_3-sensitive channels that are sensed by neighbouring mitochondria. *Science* **262**: 744-747, 1993.

RIZZUTO R., PINTON P., CARRINGTON W., FAY FS., FOGARTY KE., LIFSHITZ LM., TUFT RA., POZZAN T.: Close contacts with the endoplasmic reticulum as determinants of the mitochondrial Ca^{2+} responses. *Science* **280**: 1763-1766, 1998.

RIZZUTO R., PINTON P., BRINI M., CHIESA A., FILIPPIN L., POZZAN T.: Mitochondria as biosensors of calcium microdomains. *Cell Calcium* **26.5**: 193-199, 1999.

RIZZUTO, R.; BERNARDI, P.; POZZAN, T.: Mitochondria as all-round players of the calcium game. *J. Physiol.* **529.1**: 37-47, 2000.

ROGERS M., COLQUHOUN LM., PATRICK JW., DANI JA.: Calcium flux through predominantly independent purinergic ATP and nicotinic acetylcholine receptors. *J. Neurophysiol.* **77**: 1407-1417, 1997.

SANCHEZ JC., ROUGE V., PISTEUR M., RAVIER F., TONELLA L., MOOSMAYER M., WILKINS MR., HOCHSTRASSER DF.: Improved and simplified in-gel sample application using reswelling of dry immobilized pH gradients. *Electrophoresis* **18**: 324-327, 1997.

SCHAEFFER G., LEVAK-FRANK S., SPITALER MM., FLEISCHHACKER E., ESENABHALU VE., WAGNER AH., HECKER M. GRAIER WF.: Intercellular signaling within vascular cells under high d-glucose involves free radical-triggered tyrosine kinase activation. *Diabetologia* **46**: 773-783, 2003.

SCHIEBEL E.: gamma-tubulin complexes: binding to the centrosome, regulation and microtubule nucleation. *Curr. Opin. Cell Biol.* **12.1**: 113-118, 2000.

SCHWARZ M., ANDRADE-NAVARRO MA., GROSS A.: Mitochondrial carriers and pores: Key regulators of the mitochondrial apoptotic program ?. *Apoptosis* **12**: 869-876, 2007.

SCORRANO L., OAKES SA., OPFERMAN JT., CHENG EH., SORCINELLI MD., POZZAN T., KORSMEYER SJ.: BAX and BAK regulation of endoplasmic reticulum Ca^{2+}: a control point for apoptosis. *Science* **300**: 135-139, 2003.

SEO MS., KANG SW., KIM K., BAINES IC., LEE TH., RHEE SG.: Identification of a new type of mammalian peroxiredoxin that forms an intramolecular disulfide as a reaction intermediate. *J. Biol. Chem.* **275.27**: 20346-20354, 2000.

SHEVCHENKO A., WILM M., VORM O., MANN M.: Mass spectrometric sequencing of proteins silver-stained polyacrylamide gels. *Anal. Chem.* **68**: 850-858, 1996.

SHIBUYA H., IRIE K., NINOMIYA-TSUJI J., GOEBL M., TANIFUCHI T., MATSUMOTO K.: New human gene encoding a positive modulator of HIV Tat-mediated transactivation. *Nature* **357**: 700-702, 1992.

SHIMOMURA O., JOHNSON FH., SAIGA Y.: Extraction, purification and properties of aequorin, a bioluminescent protein from the luminous hydromedusan, Aequorea. *J. Cell. Comp. Physiol.* **59**: 223–39, 1962.

SIPPL MJ., HENDLICH M., LACKNER P.: Assembly of polypeptide and protein backbone conformatics from low energy ensembles of short fragments:development of stretegies and construction of models for myoglobin, lysozyme, and thymosin β4. *Protein Science* **1**: 625-640, 1992.

SMYTH JT., DEHAVEN WI., JONES BF., MERCER JC., TREBAK M., VAZQUEZ G., PUTNEY JW. JR.: Emerging perspectives in store-operated Ca2+ entry: roles of Orai, Stim and TRP. *Biochim. Biophys. Acta* **1763.11**: 1147-1160, 2006.

SPARAGNA GC., GUNTER KK., SHEU SS., GUNTER TE.: Mitochondrial calcium uptake from physiological-type pulses of calcium. A discription of rapid uptake mode. *J. Biol.Chem.* **270**: 27510-27515, 1995.

STROMER MH., BENDAYAN M.: Immunocytochemical identification of cytoskeletal linkages to smooth muscle cell nuclei and mitochondria. *Cell Motil. Cytoskeleton* **17**: 11-18, 1990.

SUMMERHAYES IC., WONG D., CHEN LB.: Effect of microtubles and intermediate filaments on mitochondrial distribution. *J. Cell Sci.* **61**: 87-105, 1983.

SUPATTAPONE S., WORLEY PF., BARABANT JM., SNYDER SH.: Solubilization, purification and characterization of an inositol trisphosphate receptor. *J. Biol. Chem.* **263**: 1530-1534, 1988.

SZABADKAI G., SIMONI AM., BIANCHI K., DE STEFANI D., LEO S., WIECKOWSKI MR., RIZZUTO R.: Mitochondrial dynamics and Ca^{2+} signaling. *Biochim. Biophys. Acta* **1763**: 442-449, 2006.

TAKAHASHI A., CAMACHO P., LECHLEITER JD., HERMAN B.: Measurement of intracellular calcium. *Physiol. Rev.* **79.4**: 1089-1125, 1999.

TALBOT K., ANSORGE O.: Recent advances in the genetics of amyotrophic lateral sclerosis and frontotemporal dementia: common pathways in neurodegenerative disease. *Hum. Mol. Genet.* **15.2**: R182-R187, 2006.

TANAKA Y., KANAI Y., OKADA Y., NONAKA S., TAKEDA S., HARADA A., HIROKAWA N.: Targeted disruption of mouse conventional kinesin heavy chain, Kif5B, results in abnormal perinuclear clustering of mitochondria. *Cell* **93**: 1147-1158, 1998.

TANI K., SHIBATA M., KAWASE K., KAWASHIMA H., HATSUZAWA K., NAGAHAMA M., TAGAYA M.: Mapping of functional domains of gamma-SNAP. *J. Biol. Chem.* **278.15**: 13531-13538, 2003.

TAUHATA SB., DOS SANTOS DV., TAYLOR EW., MOOSEKER MS., LARSON RE.: High affinity binding of brain myosin-Va to F-actin induced by calcium in the presence of ATP. *J. Biol. Chem.* **276**: 39812-39818, 2001.

TAYLOR CW., LAUDE AJ.: IP_3-receptors and their regulation by calmodulin andcytosolic Ca^{2+}. *Cell Calcium* **32**: 321-334, 2002.

TRENKER M., MALLI R., FERTSCHAI I., LEVAK-FRANK S., GRAIER WF.: Uncoupling-proteins 2 and 3 are elementary for mitochondrial Ca^{2+} uniport. *Nat. Cell Biol.* **9**: 445-452, 2007.

TSIEN RY.: A non-disruptive technique for loading calcium buffers and indicators. *Nature* **290**: 527-528, 1981.

TSIEN RY.: The green fluorescent protein. *Annu. Rev. Biochem.* **67**: 509-544, 1998.

TUSCHL T.: Expanding small RNA interference. *Nature Biotechnology* **20.5**:446-8, 2002.

ULLRICH O., REINSCH S., URBÉ S., ZERIAL M., PARTON RG.: Rab11 regulates recycling through the pericentriolar recycling endosome. *J. Cell Biol.* **135.4**: 913-924, 1996.

VALE RD.: The molecular motor toolbox for intracellular transport. *Cell* **112**: 467-480, 2003.

VAN DER STELT M., DI MARZO V.: Endovanilloids: Putative endogenous ligands of transient receptor potential vanilloid 1 channels. *Eur. J. Biochem.* **271**: 1827-1834, 2004.

VARADI A., JOHNSON-CADWELL LI., CIRULLI V., YOON Y., ALLAN VJ., RUTTER GA.: Cytoplasmic dynein regulates the subcellular distribution of mitochondria by controlling the recruitment of the fission factor dynamin-related protein. *J. Cell Sci.* **117**: 4389-4400, 2004.

VAZQUEZ G., WEDEL BJ., AZIZ O., TREBAK M., PUTNEY JW. JR.: The mammalian TRPC cation channels. *Biochim. Biophys. Acta* **1742**: 21-36, 2004.

VEITH D., VEITH M.: Ein Regenbogen aus dem Ozean: Biologie fluoreszierender Proteine. *Biologie Unserer Zeit* **6.35**: 394-404, 2005.

VERKHRATSKY A., SHMIGOL A.: Calcium-induced calcium release in neurones. *Cell Calcium* **19**: 1-14, 1996.

VONDRISKA TM., PASS JM., PING P.: Scaffold proteins and assembly of multiprotein complexes. *Journal of Molecular and Cellular Cardiology* **37**: 391-397, 2004.

WALLACE DM., LINDSAY AJ., HENDRICK AG., MCCAFFREY MW.: The novel Rab11-FIP/Rip/RCP family of proteins displays extensive homo- and hetero-interacting abilities. *Biochem. Biophys Res. Commun.* **292**: 909-915, 2002.

WANG D., BUYTON JP., ZHO W., CHAN EKL.: Defining a novel 75-kDa phosphoprotein associated with SS-A/Ro and identification of distinct human autoantibodies. *J. Clin. Invest.* **104.9**: 1265-1275, 1999.

WANG Q., SONG C., LI CC.: Molecular perspectives on p97-VCP: progress in understanding its structure and diverse biological functions. *J. Struct. Biol.* **146**: 44-57, 2004.

WANG X., KUMAR R., NAVARRE J., CASANOVA JE., GOLDENRING JR.: Regulation of vesicle trafficking in madin-darby canine kidney cells by Rab11a and Rab25. *J. Biol. Chem.* **275**: 29138-29146, 2000.

WEN S.-T., VAN ETTEN RA.: The *PAG* gene product, a stress-induced protein with antioxidant properties, is an Abl SH3-binding protein and a physiological inhibitor of c-Abl tyrosine kinase activity. *Genes and Development* **11.19**: 2456-2467, 1997.

WESSEL D., FLUEGGE U.I.: A method for the quantitative recovery of protein in dilute solution in the presence of detergents and lipids. *Analytical Biochemistry* **138**: 141-143, 1984.

WESTON CR., DAVIS RJ.: SIGNAL TRANSDUCTION: Signaling Specificity – a complex Affair. *Science* **292.5526**: 2439-2440, 2001.

WILCKE M., JOHANNES L., GALLI T., MAYAU V., GOUD B., SALAMERO J.: Rab11 regulates the compartmentalization of early endosomes required for efficient transport from early endosomes to the trans-golgi network. *J. Cell Biol.* **151.6**: 1207-1220, 2000.

WILSON DW., WILCOX CA., FLYNN GC., CHEN E., KUANG WJ., HENZEL WJ., BLOCK MR., ULLRICH A., ROTHMAN JE.: A fusion protein required for vesicle-mediated transport in both mammalian cells and yeast. *Nature* **339**: 355-359, 1989.

WÓJCIK C., ROWICKA M., KUDLICKI A., NOWIS D., MCCONNELL E., KUJAWA M., DEMARTIONO GN.: Valosin-containing Protein (p97) Is a Regulator of Endoplasmic Reticulum Stress and of the Degradation of N-End Rule and Ubiquitin-Fusion Degradation Pathway Substrates in Mammalian Cells. *Mol. Biol. Cell* **17**: 4606-4618, 2006.

WOOD ZA., SCHRÖDER E., HARRIS JR., POOLE LB.: Structure, mechanism and regulation of peroxiredoxins *Trends Biochem. Sci.* **28.1**: 32-40, 2003.

WOODMAN PG.: p97, a protein coping with multiple identities. *J. Cell Sci.* **116**: 4283–4290, 2003.

WU P., BRAND L.: Resonance Energy Transfer: Methods and Applications. *Analytical Biochemistry* **218**: 1-13, 1994.

YAFFE MP.: Dynamic mitochondria. *Nat. Cell Biol.* **1**: E149-E150, 1999.

YANG Y., LOSCALZO J.: S-nitrosoprotein formation and localization in endothelial cells. *PNAS* **102.1**: 117-122, 2005.

YI M., WEAVER D., HAJNÓCZKY G.: Control of mitochondrial motility and distribution by the calcium signal: a homeostatic circuit. *J. Cell Biol.* **167.4**: 661-672, 2004.

YOSHIDA Y., IMAI S.: Structure and function of inositol 1,4,5-trisphosphate receptor. *Jpn. J. Pharmacol.* **74**: 125-137, 1997.

ZHANG H., WANG Q., KAJINO K., GREENE MI.: VCP, a weak ATPase Involved in Multiple Cellular events, Interacts Physically with BRCA1 in the Nucleus of Living Cells. *DNA and Cell Biology* **19.5**: 253-263, 2000.

ZHANG SL., YEROMIN AV., ZHANG XHF., YU Y., SAFRINA O., PENNA A., ROOS J., STAUDERMAN KA., CAHALAN MD.: Genome-wide RNAi screen of Ca^{2+} influx identifies genes that regulate Ca^{2+} release activated Ca^{2+} channel activity. *PNAS* **103.24**: 9357-9362, 2006.